

POLITECNICO DI TORINO

**Corso di Laurea Magistrale  
in Ingegneria Civile - Geotecnica**

Master's Degree Thesis

**Design and Test of a Prototype of Soil Sampler  
Equipped on a Rover for Mars Exploration**



**Politecnico  
di Torino**

**Supervisor:**

Prof. Maria Migliazza, Ph.D.

**Co-supervisors:**

Prof. Daniele Costanzo, Ph.D.

Ing. Gianluca Bella. Ph.D.

**Candidate:**

Sara Sacco

March 2022



*Dedicated to those who love me,  
thanks for patience.*

*"The real test is not whether you avoid this failure, because you won't. It's whether you let it harden or shame you into inaction, or whether you learn from it; whether you choose to persevere."*

*Barack Obama*



## **Abstract**

This study deals with the design and the experimental test of a prototype of soil sampler to be equipped on team DIANA's rover ARDITO, a vehicle designed for competitions related to human assistance during Mars exploration. The project was carried out in collaboration with team DIANA, a student team from Politecnico di Torino involved in the design and production of rovers, with the purpose of joining the Rover Challenge series. A brief analysis of the main systems available for Earth and Mars soil sampling was first carried out to quantify the parameters mainly affecting the quality of the sampling and the effective feasibility on Mars soil. Then, the design of the soil sampler prototype was described in its four main components: sampler, percussion system, lifting system and control system. Afterwards, the development and results of an extensive experimental campaigns was analysed. All test campaigns were performed at MastrLAB of Department of Structural, Building and Geotechnical Engineering (DISEG) of Politecnico di Torino. The aim of the different tests concerned a preliminary evaluation of the performances and operational limits of the prototype. Some tests were also performed on two parts of the sampler sub-system: the holder and the catcher, to study the influence of the type of tested soil by changing the diameter of the holder and the stiffness of the catcher. Basing on these outcomes, the soil sampler prototype was tested, evaluating the correlation between the soil penetration and the number of blows required. All the experimental investigations were performed on a test bench specifically built for the soil sampler prototype, and different soils grading and mixtures were employed, in loose and compacted conditions. A compaction procedure for each soil was also proposed together with some safety aspects concerning the use and maintenance of the prototype. The results of the tests campaign on the soil sampler prototype revealed that the soil sampling was not performed due to the undersized internal diameter of the advanced shoe. The preliminary results concerning the soil penetration provided positive outcomes on the possibility of correlating the number of blows with the compaction degree of different soils.



# Table of contents

1	Introduction.....	1
1.1	Team DIANA .....	1
1.2	Soil sampling system for DIANA’s rovers.....	3
2	Earth and Mars soil sampling .....	7
2.1	Mars soil simulants.....	7
2.1.1	ALTEC S.p.A. simulant .....	7
2.1.2	Thales Alenia Space S.p.A. simulant.....	9
2.2	Soil sampling techniques on Earth .....	11
2.2.1	Core-Barrel Denison sampler .....	13
2.2.2	Cable Percussion Drilling.....	14
2.2.3	Standard Penetration Test Equipment .....	16
2.3	Soil sampling techniques on Mars.....	18
2.3.1	Mars sample return mission.....	18
2.3.2	Perseverance sample handling.....	19
3	DIANA’s soil sampling system .....	22
3.1	Project requirements and main challenges .....	22
3.2	Prototype design .....	22
3.2.1	Lifting system .....	22
3.2.2	Sampler.....	26
3.2.3	Percussion system.....	36
3.2.4	Control system.....	42
4	Laboratory tests.....	44
4.1	Test bench.....	44
4.2	Soils employed .....	45
4.3	Preparation technique .....	49
4.3.1	Loose soil.....	49
4.3.2	Compacted soil .....	50
4.4	Holder tests on loose soils .....	53
4.5	Catcher tests on loose soils.....	57
4.6	Sampler prototype test.....	67
4.6.1	Uniform sand at loose condition.....	68
4.6.2	Mars regolith simulant at loose condition .....	70
4.6.3	Uniform sand at compacted condition.....	72
4.6.4	Mars regolith simulant at compacted condition.....	73
4.6.5	Uniform sand at compacted condition, without equipping the catcher .....	74
4.6.6	Comparison of results about soil penetration with the sampler prototype .....	75
4.7	Safety aspects .....	76
4.7.1	Prototype manual of operation and maintenance.....	76

4.8	Synthesis of the results .....	77
4.9	Considerations on future prototype updates .....	78
4.9.1	Prototype updates .....	78
4.9.2	Future test campaigns .....	78
5	Conclusions.....	80
6	Annex.....	83
6.1	Annex 1: sampling system control code.....	83
6.2	Annex 2: prototype manual of operation and maintenance .....	85
7	List of figures.....	92
8	List of tables .....	95
9	List of equations.....	96
10	References.....	97
11	Acknowledgments	

# 1 Chapter 1: introduction

This introduction chapter describes the student team DIANA, its main projects and the origins of the soil sampling system project.

## 1.1 Team DIANA

Team DIANA was born in 2008 in Politecnico di Torino, with the purpose of taking part to the Google Lunar X-Prize. DIANA stands for Ducti Ingenio Accipimus Naturam Astrorum, which means “Driven by Intellect we Understand the Nature of Stars”. The student team is involved in space robotic, focused on designing and testing engineering models of rovers for astronauts’ support in future human missions on other planets. A rover is a robotic vehicle able to perform, in a teleoperated and autonomous way, various kinds of tasks on harsh terrains. As part of Team ITALIA, a collaboration between Italian universities and companies, team DIANA was in charge of the design and production of rover AMALIA (Figure 1.1), that was developed and realised until 2015. This rover was completely space-grade and could be folded up for entering the lander. Solar panels installed on the chassis could provide the rover enough energy independence to perform autonomous operations for the whole length of the itinerary preliminary defined.

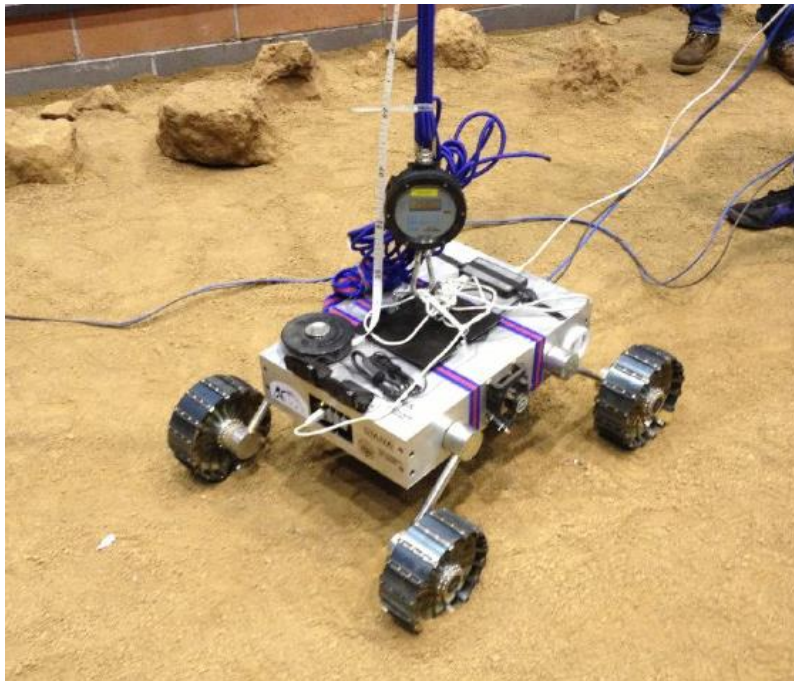


*Figure 1.1 Team DIANA's lunar rover AMALIA*

Once Google Lunar X-Prize was closed, team DIANA started the project of a new rover for Mars environment aiming to attend the University Rover Challenge and more in general the Rover Challenge series. For this purpose, T0-R0 was created with a completely new architecture for locomotion. It was based on a rocker-bogie system, and it was equipped with a new 6-Degree of Freedom arm for manipulation. After a 3-year development T0-R0 was finally presented at the European Rover Challenge (ERC) in Starachowice, Poland in September 2018 (Figure 1.2).



Figure 1.2 Team DIANA's Martian rover TO-RO at European Rover Challenge 2018

The following year, based on the experience acquired, Project Trinity started. The Rover concept was similar to TO-R0, but integrated with some improvement to the locomotion mobility terrain system, consisting in four steering wheels, and to the arm and wrist. This model was then presented just one year later to the ERC 2019 edition in Kielce, Poland (Figure 1.3).



Figure 1.3 Team DIANA's Martian rover Trinity at European Rover Challenge 2019

On the basis of the experience and feedbacks gained from the previous years, DIANA team started working on an improved version of Trinity, but very soon understood it was a major upgrade and named the project ARDITO (Figure 1.4). ARDITO is currently on its third year of development and with more focus on modularity and expansion capabilities for payloads, it integrates new systems such as a new mobility system with higher thrust, a lighter arm with a sensed robotic hand, and a new *soil sampling system*. ARDITO was presented during the ERC 2021 edition in Kielce, Poland.



Figure 1.4 Team DIANA's Martian rover ARDITO at European Rover Challenge 2021

## 1.2 Soil sampling system for DIANA's rovers

The soil sampling system was designed and developed for the Science Task of European Rover Challenge since October 2019. The design was initially entrusted to a research group composed by Sara Sacco (Civil Geotechnical Engineering student) and Alessandro Dell'Atti (Mechanical Engineering student).

A list of preliminary design requirements was defined:

- simplicity and modularity;
- materials as much compatible as possible with space exploration (space-grade), so preferring metallic materials;
- overall height in compact condition lower than 100 cm due to space limitations: the robotic arm of the rover must pass over the sampling system that at the same time must be anchored to the chassis of the rover avoiding the risk of scraping the soil during rover's movements;
- total weight lower than 10 kg owing to ERC requirements on the overall weight of the rover;
- low power consumption because the total amount of energy that rover can employ is limited;
- operativity on Martian regolith, initially simplified as a dusty sand;
- continuous sampling until a depth of 30 cm below soil surface with identification of the soil profile crossed (ERC requirement);
- real time information gathering about the soil sample collected (type of material, temperature, humidity, weight);
- automatization of operations with no human intervention during sampling process;
- repeatability of sampling procedures (capability of providing more soil samples);
- real time feedbacks on operational conditions;
- possibility of immediate suspension of operations due to safety requirements.

Following this requirements, the standalone unit of sampling system was designed to be attached to the chassis of ARDITO rover and employed during the Science Task of European Rover Challenge 2020.

The design reached can be described as a core-driller compact prototype, driven into the soil by means of vertical pressure and a rotative system. A critical aspect faced was the separation of reaction forces transmitted from the sampling process to the rover body. In order to provide enough contrast to rotation, it was planned to perform the sampling operations positioning ARDITO's wheels in opposite direction from the rotation one,

but in this condition it was impossible to separate torque reaction forces. Relating vertical forces, those were partially balanced inserting a few nail-shaped parts in the terrain during the positioning of the sampler close to the soil.

The lifting system was made out of two telescopic linear guides made of carbon fiber tubes, reducing the weight of the system. Sampling forces were provided by three different motors placed on the top of the two linear guides: one dedicated to the rotation to the sampler, one for approaching the sampler to the terrain with the descent of the system along the first stage of linear guides, and a last motor provided the vertical pressure necessary to penetrate the soil.

The sampling part was constituted by a non-rotating inner tube equipped with a spring catcher. Finally a series of electronic End Stops were positioned in order to provide feedbacks about sampling operations. An example of an important feedback needed is related to the sampler contact with the soil before starting sampling operations. This was checked with an End Stop positioned on the lower plate and information provided were coupled with the ones from a distance ranging sensor. A scheme of the prototype can be observed in Figure 1.5.

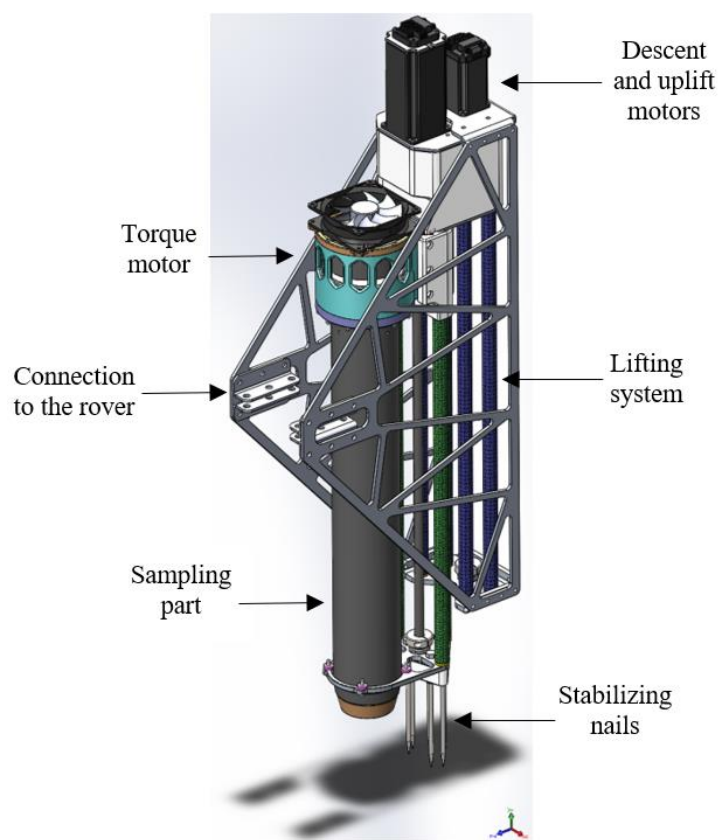
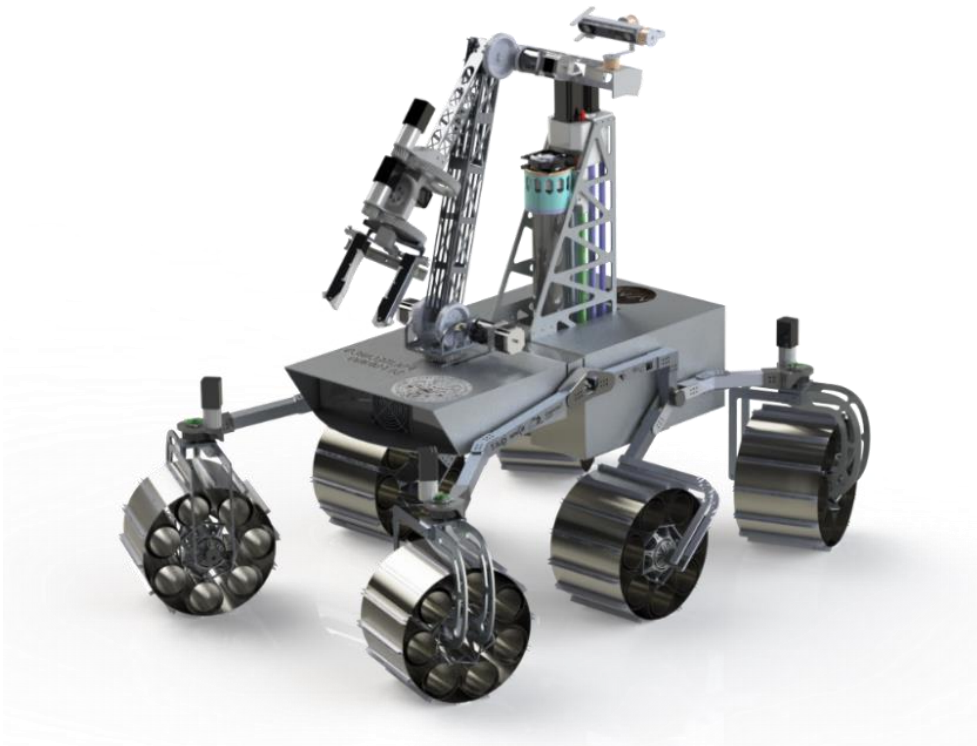


Figure 1.5 First design of DIANA's soil sampling system for ARDITO rover

The resulting version of ARDITO (Figure 1.6) was presented to the Indian Design Rover Challenge 2020 and ARDITO rover placed 9th gaining an Innovation Award for Scientific research, thanks to Life Detection and Soil Sampling systems.



*Figure 1.6 Team DIANA's Martian rover ARDITO (design version presented at Indian Design Rover Challenge 2020)*

In October 2020 Sara Sacco became coordinator of a sub-group of team DIANA completely dedicated to the design of a sampling system, called Core Drill Group. The Core Drill Group of team DIANA was composed by: Sara Sacco (coordinator), Lorenzo Caraccio (Mechanical Engineering student), Tommaso Colamartino (Mechatronics Engineering student) and Carlo Tiozzo (Environmental Engineering student). The design development work of this group is presented in Chapter 3. Since October 2021 the Core Drill Group is dedicated to the test campaign (described in Chapter 4) and design optimization of the soil sampling prototype for ERC 2022 edition.

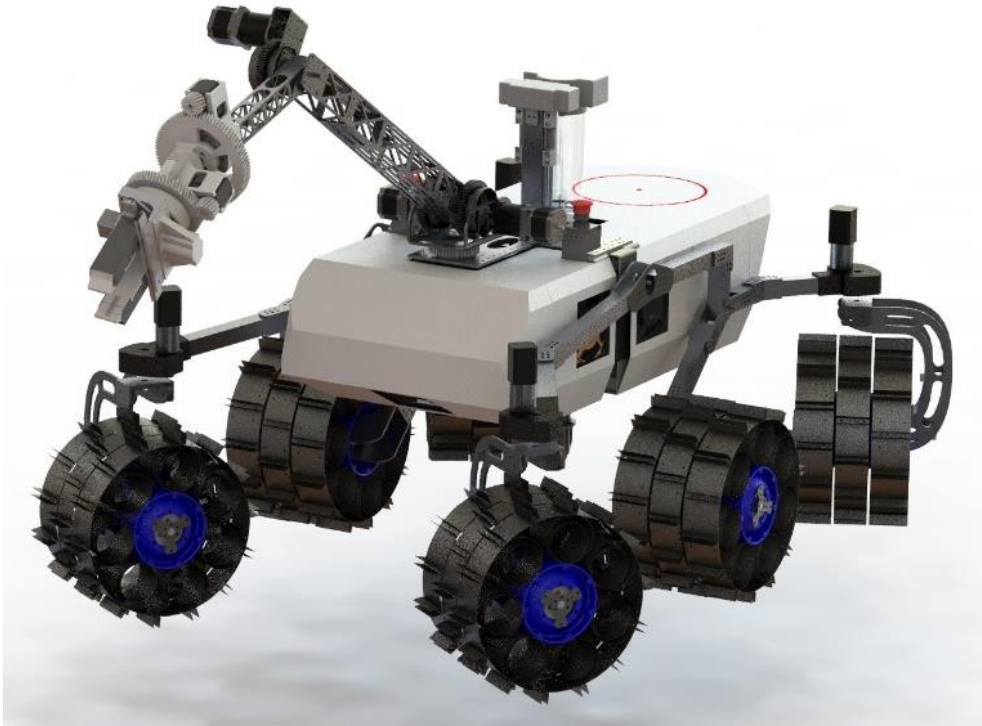


*Figure 1.7 Team DIANA's Martian rover ARDITO (ERC 2021)*

## 2 Chapter 2: Earth and Mars soil sampling

In this chapter soil sampling operations on Earth and Mars are studied in order to define the key parameters for the design of a new sampler prototype for Mars sub-surface exploration. Soil sampling on Earth is generally applied in support of geotechnical investigations for engineering design. Sampling operations on Mars, at present, are mainly related to understanding the formation processes and the evolution of the planet.

Soil sampling can be defined as a procedure that allows obtaining a portion of material from the original mass. Referring to the sample quality, Hvorslev (Hvorslev, 1949) defined samples as representative and non-representative. Representative samples are those materials that were not chemically altered or contaminated by particles from other layers, while non-representative samples are mixtures of soil and rock from different layers. Undisturbed samples are usually subjected to little disturbance, with no alteration of structure, water content and chemical composition; resulting useful for the determination of strength, compressibility and permeability parameters. On the other hand, disturbed samples are used for moisture content, Atterberg limits and grain size distribution (ASCE, 1999).

Regarding Mars soil, it is generally defined as the fine regolith found on the surface which simulants grain distribution will be further described as a gravelly sand with a small silt fraction (Pizzamiglio, et al., 2018). A detailed definition of the granulometric distribution of Mars regolith is provided starting from two different simulants: one provided by ALTEC S.p.A. and one by Thales Alenia Space S.p.A.

Starting from the assumption that Mars soil can be described as a sand-likely material, a limited number of samplers available on Earth can be effectively employed. At the same time, several geometrical and mechanical parameters are imposed for a sampler prototype equipped on a rover for Mars exploration. For this reason, only a few samplers employed on Earth can provide indications for the design of a new sampler prototype and the more relevant are described.

Finally, an overview of sampling techniques that have recently been applied during NASA Mars exploration is provided.

### 2.1 Mars soil simulants

At present, any samples of Mars soil have been returned to Earth, as explained in paragraph 2.3. For this reason, different kinds of simulants have been created starting from data obtained from Mars surface exploration. In the following paragraphs two different simulants of Mars regolith are analysed, provided by ALTEC S.p.A. and Thales Alenia Space S.p.A.

The simulant provided by ALTEC S.p.A. will be then assumed as reference for creating a granulometric simulant of Mars regolith to be used for tests on the sampler prototype described in Chapter 4.

#### 2.1.1 ALTEC S.p.A. simulant

Aerospace Logistics Technology Engineering Company (ALTEC S.p.A.) is the Italian center for the provision of engineering and logistics services to support operations and utilization of the International Space Station and the development and implementation of planetary exploration missions. The headquarter is based in Turin and the company provided a sample of Mars soil simulant that was tested in order to define its physical properties at the International Research School of Planetary Sciences (Pescara, Italy) (Pizzamiglio, et al., 2018). The obtained results can be observed in Figures 2.1 and 2.2.

Regarding the grain size distribution (Figure 2.1), the percentual fractions are 16% of gravel ( $>2$  mm), 74% of sand ( $0.06 \div 2$  mm) and 10% of the clay/silt component ( $0.002 \div 0.06$  mm). It is so possible to define the regolith simulant as a gravelly sand with a small silt fraction.

It is possible to define the *effective particle size* of the distribution,  $D_{10}$ , that means that 10% percent of the particles are finer than  $D_{10}$  and 90% of the particles are coarser. This parameter can be obtained (blue lines of Figure 2.1) drawing a line on the semilogarithmic grain size distribution plot, that starts from percentage passing equal to 10% and crosses the grain size distribution curve, the value that is read on the particle size axis is equal to 0,05 mm. In the same way is possible to obtain  $D_{60}$ , the particle size at which 60% of the particles are finer and 40% are coarser than  $D_{60}$  size. The value that is found in this case (green lines of Figure

2.1) is approximately 0.74. Finally, the uniformity coefficient  $C_u$  is given by the ratio between  $D_{60}$  and  $D_{10}$  and, in this case, the result is 14,8, that describes a well graded soil ( $C_u > 6$ ).

The Mohr-Coulomb failure line (Figure 2.2) was obtained from direct shear tests carried out at three different normal: 100 , 200 and 300 kPa. Direct shear tests, consolidated triaxial tests and drained triaxial tests allowed to evaluate the cohesion ( $c'$ ), the friction angle ( $\phi'$ ) and the elasticity modulus (E). The Mohr-Coulomb failure envelope was obtained processing the direct shear test results. The intercept equal to zero describes the cohesionless nature of the soil, while the slope of the line is the angle of internal friction equal to  $42.6^\circ$ . The pycnometer test was performed with the intention of estimating the particle density. All the physical properties acquired are resumed in Table 2.1.

The sample provided can be observed in Figure 2.3.

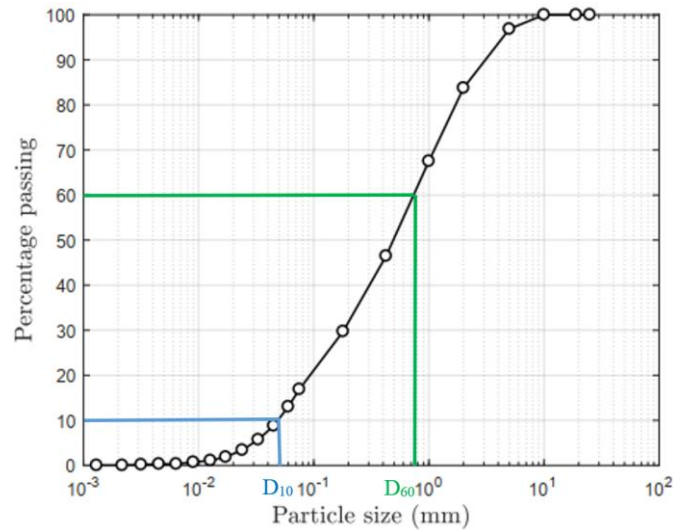


Figure 2.1 ALTEC S.p.A. Mars soil simulant: grain size distribution with detail of D10 and D60 (Pizzamiglio, et al., 2018)

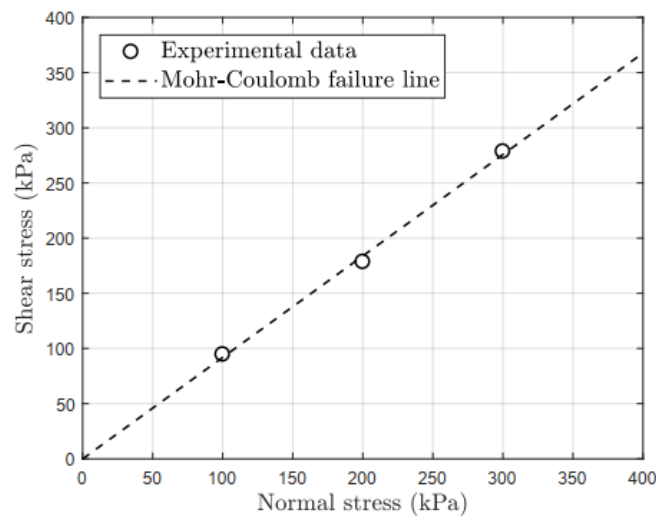


Figure 2.2 ALTEC S.p.A. Mars soil simulant: Mohr Coulomb failure line (Pizzamiglio, et al., 2018)



Figure 2.3 Sample of Mars soil simulant from ALTEC S.p.A.

Table 2.1 Physical properties of ALTEC S.p.A. Mars soil simulant (modified from Pizzamiglio, et al., 2018)

Parameter	Value	Unit
Cohesion, $c'$	$\cong 0$	kPa
Friction angle, $\phi'$	42.6	$^\circ$
Young's modulus, E	21.8	MPa
Poisson ratio, $\nu$	0.25	-
Particle density, $\gamma$	2659	$\text{kg m}^{-3}$

## 2.1.2 Thales Alenia Space S.p.A. simulant

Thales Alenia Space ROXY facility will be described in paragraph 3.2.3. It was developed taking reference on the soil categorization made by (Golombek, et al., 2003) and aimed to reproduce one of the possible critical scenario for Mars terrain. From the mentioned study is possible to visualise the plot reported in Figure 2.4, describing the cumulative number of rocks at the Pathfinder (rover mission landed on Mars' Ares Vallis on 4<sup>th</sup> July 1997) site.

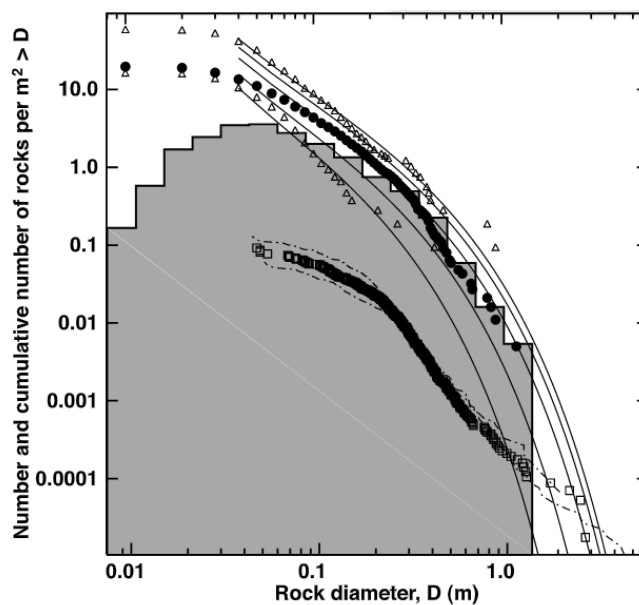


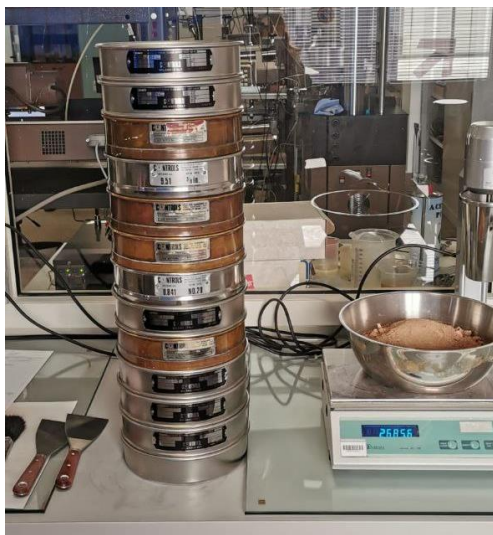
Figure 2.4 Cumulative number of rocks/ $\text{m}^2$  greater than diameter  $D$  at the Pathfinder landing site (Golombek, et al., 2003)

During test performed at ROXY Facility (paragraph 3.2.3), Thales Group provided to team DIANA a sample of Mars regolith simulant. Afterwards, a laboratory screening procedure was performed at the Geotechnical Laboratory of the Department of Structural, Building and Geotechnical Engineering (DISEG) of Polytechnic of Turin, in order to obtain the granulometric distribution of the sample.

The following pictures represent: the sample provided by Thales Group (Figure 2.5); the mechanical screening equipment (Figure 2.6 left) and the biggest soil grains individuated during the screening procedure (Figure 2.6 right), with maximum particle dimension equal to 30 mm and finally the granulometric curve obtained (Figure 2.7).



Figure 2.5 Sample of Mars soil simulant from Thales Alenia Space



a)



b)

Figure 2.6 a) Mechanical screening equipment, b) detail of biggest soil particles from Thales Alenia Space Mars soil simulant

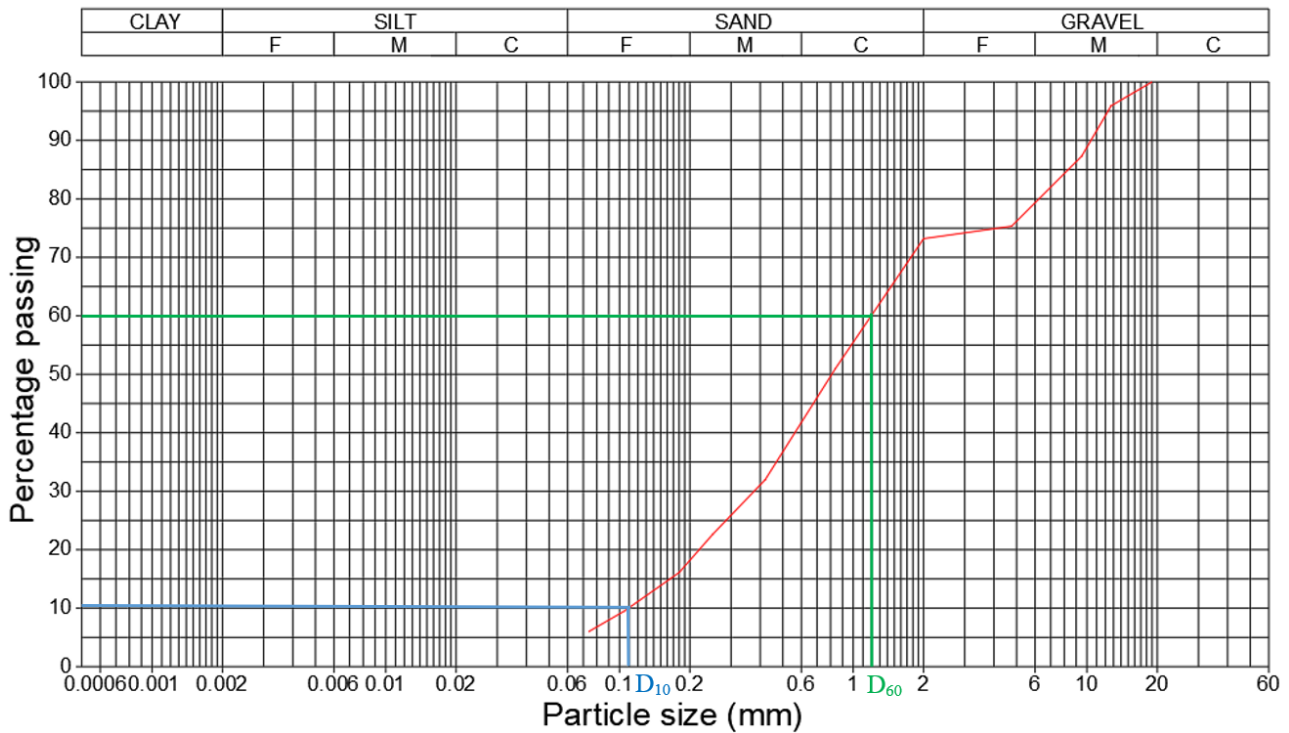


Figure 2.7 Thales Alenia Space Mars soil simulant: grain size distribution with detail of  $D_{10}$  and  $D_{60}$

The percentual fractions are 26.8% for gravel ( $>2$  mm), 67.2% for sand ( $0.06 \div 2$  mm) and 6% for the clay/silt component ( $0.002 \div 0.06$  mm). Like for the ALTEC S.p.A. simulant, it is possible to describe the regolith simulant as a gravelly sand with a small silt fraction. The effective particle size of the distribution,  $D_{10}$ , is equal to 0,11 mm, while  $D_{60}$  is equal to 0.12. The resulting uniformity coefficient is 1.09, that describes a uniformly graded soil ( $C_u \cong 1$ ).

## 2.2 Soil sampling techniques on Earth

A wide variety of soil samplers is available on Earth, depending on the expected conditions of the soil and also on the faced circumstances. Starting from the direct observation, expected geology, and depending on the requested sample quality, the most suitable soil sampling equipment can be employed.

From soil samples obtained in situ is possible to derive samples to be employed during laboratory tests. These samples are classified by Eurocode 7 (Bond, et al., 2013), considering the soil properties that are assumed to remain unchanged during sampling and handling, transport and storage. The result is a classification with five classes resumed in the following table (Table 2.2), in combination with the sampling category according to EN ISO 22475-1.

Table 2.2 Quality Classes of soil samples (after EN 1997-2)

Soil properties / quality class	1	2	3	4	5
<b>Unchanged soil properties</b>					
particle size	*	*	*	*	
water content	*	*	*		
density, density index, permeability	*	*			
compressibility, shear strength	*				
<b>Properties that can be determined</b>					
sequence of layers	*	*	*	*	*
boundaries of strata - broad	*	*	*	*	
boundaries of strata - fine	*	*	*	*	
Atterberg limits, particle density, organic content	*	*	*		
water content	*	*			
density, density index, porosity, permeability	*	*			
compressibility, shear strength	*				
Sampling category according to EN ISO 22475-1	A				
					B
				C	

Different types of sampling techniques provide different qualities of samples. In this chapter, only some systems are described, starting from some assumptions that determine the more probable conditions encountered during Mars surface exploration.

The main requirements for the sampler prototype to be developed are described in Chapter 3. As anticipation is possible to assume that the sample obtained should allow identifying the soil profile, the granulometric distribution, and other additional information as the temperature, humidity, and the unit weight. In these terms, a quality 4 (sampling category B) sample should be provided. An example of class quality that can be obtained from different samplers is provided by Associazione Geotecnica Italiana (AGI) in the following table (Table 2.3).

Table 2.3 Quality classes of samples from different samplers (modified from AGI recommendations, 1977)

Type of sampler	Type of soil				
	Finer material			Coarser material	
	Poorly consolidated	Moderately consolidated	Over consolidated	Above water level	Below water level
Thick-walled hammered	-	Q3 (4)	Q2 (3)	Q2	Q1
Thin-walled hammered	Q3	Q4	Q3 (4)	Q3	Q2
Thin-walled pushed	Q4	Q5	Q5 *	Q3	Q2
Piston pushed	Q5	Q5	-	Q3 (4)	Q2 (3)
Double rotation with advanced shoe	-	-	Q5 *	-	-

Following these prescriptions, undisturbed sampling techniques should be analysed, but a huge limitation in the application of this type of technology is provided by the dimensions of the rover ARDITO and so the forces that can be involved during operations. For this reason, also equipment's employed in disturbed sampling and in-situ tests are considered.

Samplers for undisturbed sampling in borings can be mainly divided into *Push-Tube* samplers and *Core-Barrel* samplers. Many other types have been specifically designed to cross different kinds of natural formations but can still be described as a variation from the main two types.

The *Push-Tube* sampler is excluded a priori because it can be employed to obtain samples only of soft-to-medium clays and fine sands with high cohesion. Sampling on Mars surface, in completely dry conditions, would lead to an almost total loss of material during recovery, due to the absence of cohesion in the sample.

The *Core-Barrel* samplers could be suitable for sampling Mars regolith, because can perform the penetration even into soils containing gravel. For this purpose, some types of Core-Barrel samplers are equipped with a spring catcher allowing to increase the percentage of recovered material. The Denison sampler is considered for this study and described because of its high recovery percentage and the very limited degree of disturbance.

If the requirement of undisturbed sampling is removed, it is possible to consider the systems available for hammering drill, where the borehole is formed using percussion systems and different types of tools, depending on the crossed material. The Cable Percussion drilling is analysed as it can be employed with non-cohesive soils and the percussive technology can be easily reproduced also at small scale.

Finally, a wide variety of in-situ tests have been developed to provide information on the geotechnical properties of the soil. Some, like the Standard Penetration Test (SPT), allow at the same time to collect disturbed samples. For this reason, also the SPT apparatus is described and evaluated for designing a final prototype for sampling on Mars soil.

### **2.2.1 Core-Barrel Denison sampler**

The Denison sampler is a type of rotary core-barrel sampler. The rotary drilling allows crossing any kind of soil. Depth and hole diameter are function only of the power of the engines employed (Tanzini, 2011). The system consists of pushing a steel tube into the soil, equipped at the bottom with a cutting edge (crown) and connected to the surface by a system of hollow rods. The advancement is performed by the rotation and pressure transmitted by the rods.

The available solutions for the core barrel sampler are single, double and triple tube. In triple tube the inner tube is stationary and holds the sample liners.

The Denison sampler is a double tube (or triple tube if a liner is equipped) specifically designed to provide reliable undisturbed samples from a wide variety of materials (from coarse sands to gravel and consolidated clays). The sampler consists of a steel outer barrel, an inner barrel with an advanced smooth cutting shoe and a liner equipped with a “basket” type spring core catcher that receives and holds the soil sample. This catcher is constituted by a number of curved and thin springs fixed to a steel base by welding or rivets. The shoe can have a sharpened or saw-toothed edge and different lengths available allow to sample different levels of hardness of the formation material. The inner barrel remains stationary while the outer barrel is rotated, this by means of an upper and lower bearing placed into the outer barrel head (ASCE, 1999).

A schematic view of the Denison sampler is provided in Figure 2.8. Figure 2.8 left describes the Denison triple-tube core barrel on the Johnson design of 1940, while Figure 2.8 right shows the FHWA version of the Denison sampler developed in 1997.

The advancement of the Denison sampler is performed with a continuous circulation of drilling fluids, that allow to cool and clean the bit, transport the cuttings to the surface, increase the stability of the borehole and control the pressures of the natural formation. The sampler is set at the bottom of the hole with the continuous circulation of drilling fluid, then it is pushed downward at a steady rate helped by a slow rotation. The core sample passes through the core retainer and the thin-wall liners of the inner barrel as the sampler is pushed downward. For this reason, a rotation velocity of 100 r/min should not be exceeded, because a fast rotation would develop vibrations that could destroy the integrity of the sample pushed into the inner liner.

The drilling fluid remaining on top of the sample is automatically vented on the outside of the core barrel through a disc valve (Shuter, et al., 1989).

After the whole sampling length is covered the downward push and rotation are stopped and the Denison sampler is slowly recovered from the borehole. Dismantling operations mainly consist in recovering the inner lining, capping, and waxing it in order to maintain intact the water content.

During the design stage of a new soil sampler for Mars exploration with rovers, it must be highlighted that is not possible to provide drilling fluids to the excavation due to the impossibility of carrying a sufficient quantity on the rover and the absence of water resources at least from the surface of the planet. At the same time, if sampling operations are performed with a rotative system and in dry conditions, it is possible to observe a great development of high temperatures and wear of the advanced bit, so the rotative system should not be employed for sampling for more than a few minutes, alternating pauses for reducing the temperature.

Field and laboratory sampling tests on Martian regolith simulants revealed the impossibility of driving the sampler with a rotative system because the operation required very high power to perform the rotation and high contrast at the surface to penetrate the material.

Considering the previous reasons, the Denison sampler is inadequate for Mars exploration, but the indications provided for the inner stationary barrel and catcher will be kept during the design of the part of the prototype called “sampler”. With a new design of the catcher, providing an overlap of the fingers, it could be possible to store the looser and dusty part of the soil sample inside the inner tube.

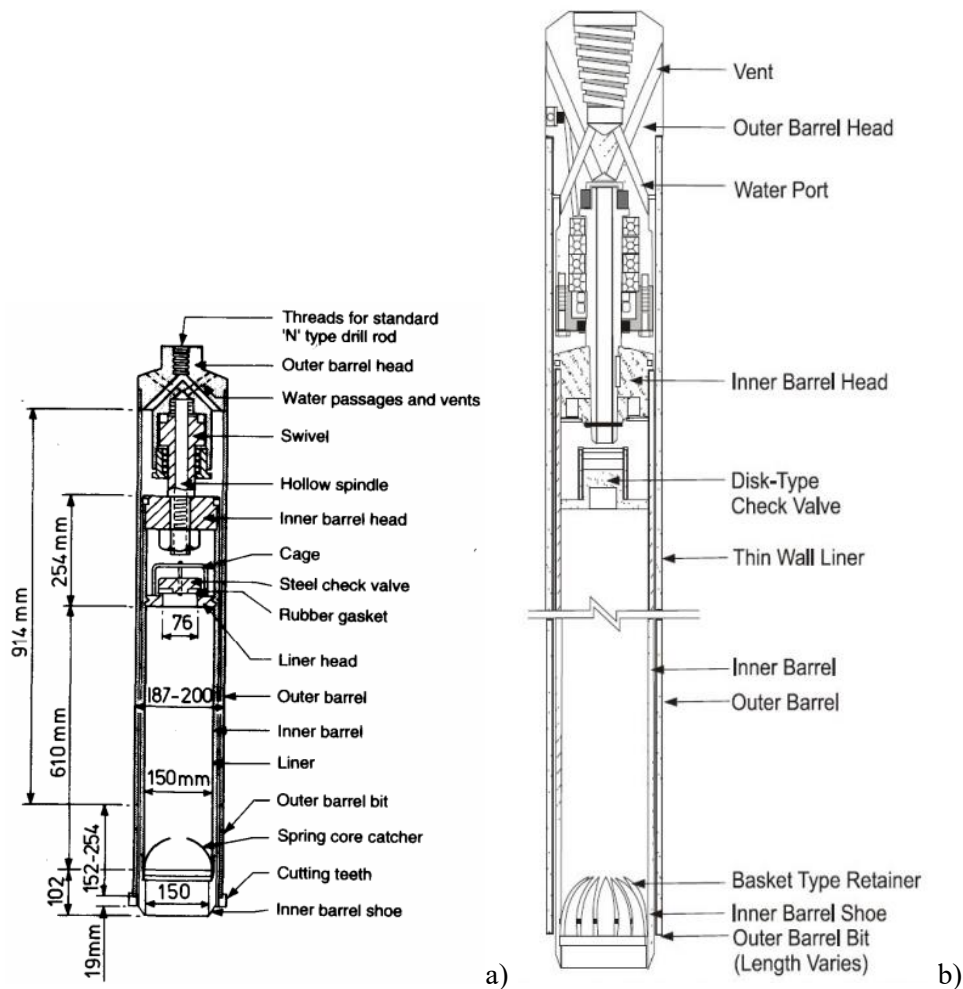


Figure 2.8 a) Denison triple-tube core barrel (Johnson design 1940), b) Denison sampler (FHWA, 1997)

## 2.2.2 Cable Percussion Drilling

Cable percussion is a drilling method that can provide disturbed and undisturbed samples, depending on the type of material crossed, and allows to perform different types of in-situ tests such as the Standard Penetration Test. The simplicity of the system, combined with the overall quality of results, allowed its large employment

in drilling operations. The percussion drilling method was adopted to build wells by Chinese and Persians as early as 2000 B.C.

The modern drilling rig is constituted by a mobile tripod that can be easily dismantled and transported by a wheeled vehicle. The tripod setup is characterized by a reduced impact on the environment and the rig is usually sizable, in this way the system can be employed also in conditions of restricted space.

The borehole is advanced using a cutter that is lifted up and then dropped down, inside a borehole casing. The cutter is attached to a cable that is used to lower and lift downward the cutter itself through the borehole. This operation is repeated until the required or maximum drilling depth (up to 60 m) is reached. A scheme of the overall system is provided in Figure 2.9.

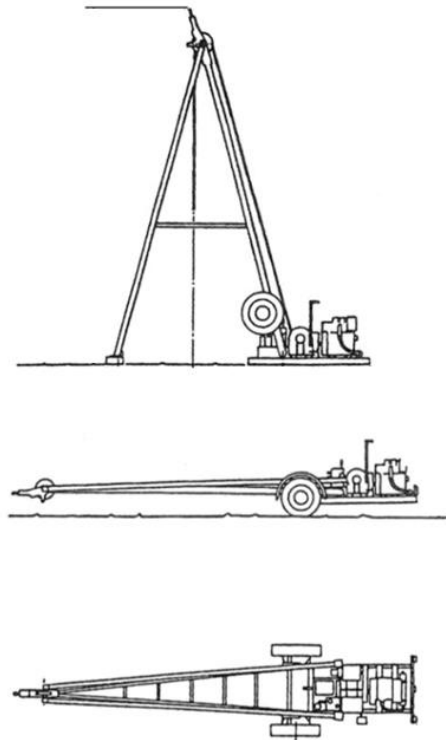


Figure 2.9 Cable percussion drilling, view from different sides (image from Sub Surface Ltd)

A series of tools are available to optimize the drilling operations: the “clay cutter” is used for plastic clays and similar cohesive soils, the “shell” or “bailer” is employed for soft non-cohesive formations like sands and gravels and finally a chiselling tool can be employed for very hard soils (Figure 2.10). The sinker bar is a weight that allows the advancement of the hole and is equipped behind the chosen drilling tool. Extra weight can be provided to the drilling tools equipping an intermediate sinker bar.

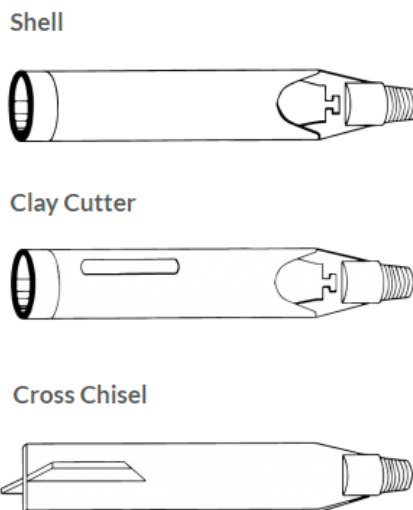


Figure 2.10 Cable percussion drilling tools (image from DANDO company website)

In non-cohesive or weak collapsing formations it is possible to employ casing as temporary support. Casing diameters of 150 mm or 200 mm are generally used.

The problem of retaining the material during sampling operations with non-cohesive soils is fixed with a clack valve made of steel or leather (Figure 2.11).



Figure 2.11 Cable percussion drilling clack valve (image from DANDO company website)

The percussive technology can be easily employed on granular soils like Martian regolith, but it must be pointed out that the available energy depends on mass  $m$ , gravity  $g$  and height of drop  $h$ , following the gravitational potential energy law:

$$E_g = mgh$$

Considering that the surface gravity on Mars is only about 38% of the surface gravity on Earth, and so  $3.721 \text{ m/s}^2$  compared to  $9.807 \text{ m/s}^2$  on Earth, the impact energy and so the drilling work will be significantly reduced. At the same time the available space and power of a rover leads to a reduced percussive mass and dropping height.

Considering the application of this equipment on the soil sampler prototype design, the simplicity of the technology and of its tool could allow a possible application, adapting it at small scale.

### 2.2.3 Standard Penetration Test Equipment

The Standard Penetration is an in-situ dynamic penetration test that can perform direct investigations in soils and rocks. The execution is very simple and low cost, for this reason this test is largely employed and a huge number of empirical correlations is available for the characterization of the natural material crossed. With the results obtained it is possible to estimate the relative density, the friction angle of cohesionless soils and strength parameters of stiff cohesive soils. In any case the test cannot be considered repeatable, because for example, two competent drillers testing next to each other would not produce the same resistance to penetration ( $N_{\text{value}}$ ) (Look, 2007).

The test apparatus and procedure is described in ISO 22476-3:2005 and consists of driving a thick-walled sample tube into the ground, at the bottom of a borehole. This is performed repeatedly dropping a standard

mass (63.5 kg) from a slide hammer, through a distance of 760 mm. First the sample tube is driven into the soil for 150 mm (seating drive), then the number of blows necessary to penetrate 150 mm is recorded, until a total distance of 450 mm. The Standard Penetration Resistance ( $N_{values}$ ) is the sum of the number of blows required for the second and third penetration of 150 mm.

The full equipment is composed by: drilling equipment, sampler, drive rods, drive weight assembly and eventually a blow counter and a penetration length measuring device. A scheme of the system is provided in Figure 2.12.

The drive weight assembly must not overcome a total weight of 115 kg and shall comprise the steel hammer of 63,5 kg  $\pm$  0,5 kg, an adequate guide to ensure minimal resistance during the drop, an automatic release mechanism with no induced parasitic movements in the drive rods and a steel drive head or anvil rigidly connected to the top of the drive rods.

The blow counter can measure mechanically or with electric impulses, in order to count the number of blows of the hammer.

The penetration length can be measured by counting on a scale on the rods or by recording sensors with a resolution less than 1/100 the measured length.

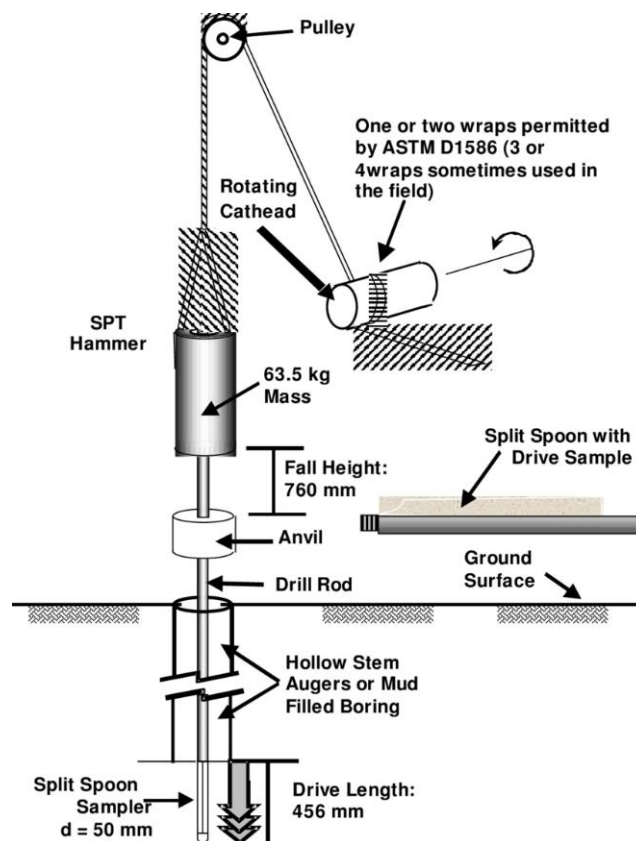
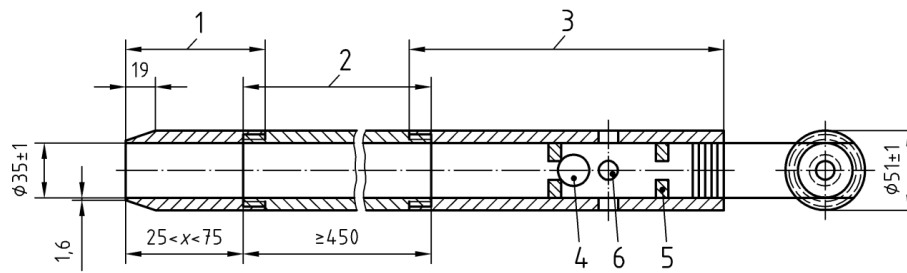


Figure 2.12 Standard Penetration Test equipment (Schneider, et al., October 1999)

The drilling equipment should provide a hole sufficiently clean, this to ensure that the penetration test is performed in undisturbed soil. The sampler is composed by a drive shoe that can be substituted with a 60° cone if sampling operations are performed in gravelly sands, connected with the split barrel that holds the sampler and finally with the coupling. It shall be provided with a non-return valve with sufficient clearance to permit the free flow of water or mud during driving (British Standard, 2007). A cross-section of a sampler without a provision for a liner is provided in Figure 2.13.



**Key**

- 1 Drive shoe
- 2 Split barrel
- 3 Coupling
- 4 Non return valve (ball diameter: recommended 25 mm; ball seating: recommended 22 mm)
- 5 Ball retaining pins
- 6 Four vent holes (min diameter 12 mm)
- x Length of the drive shoe

Figure 2.13 Longitudinal cross-section of a Standard Penetration Test sampler without a provision for a liner, dimensions in mm (British Standard, 2007)

The drive rods should be straight rods and the straightness should be periodically checked through different possible procedures. At certain depths appropriate stabilizers should be installed in order to provide the appropriate vertical alignment.

Several empirical formulas are available to correlate the number of blows to the density of the ground. One of the most traditional was obtained by Meyerhof (Meyerhof, 1956) and allows to correlate the SPT blow count with the friction angle (Table 2.4).

Table 2.4 Correlation between SPT-N values, friction angle and relative density (Meyerhof 1956)

SPT - N3 [Blows/0.3 m -1 ft]	Soil packing	Relative Density [%]	Friction Angle [°]
< 4	Very loose	< 20	< 30
4 - 10	Loose	20 - 40	30 - 35
10 - 30	Compact	40 - 60	35 - 40
30 - 50	Dense	60 - 80	40 - 45
> 50	Very dense	> 80	> 45

When sampling in granular soils, an overburden correction factors should be applied, and other correction factors can be considered if employing different hammers.

Finally, it is possible to note a list of aspects of the Standard Penetration System applied to Mars exploration with rovers: it does not require any drilling fluid to penetrate the soil, the percussive technology is highly efficient in granular soils but it must be considered that a reduced energy will be available on Mars, sampling and testing are performed at the same time. The test procedure will be specifically considered in the design of the sampler and its sampling procedure.

## 2.3 Soil sampling techniques on Mars

### 2.3.1 Mars sample return mission

The process of sample catching is part of the Mars Sample Return (MSR) mission, a proposed spaceflight mission to collect rock and dust samples on Mars and return them to Earth. Plans for this mission are still at a very early stage and three main concepts are under development: one proposed by NASA-ESA (National Aeronautics and Space Administration - European Space Agency) with the support of gathering samples by the Perseverance rover, a Chinese proposal, and a Russian proposal. The “sample catching” process performed by Perseverance is the first ever done and aims to lay the basis for future MSR missions.

### 2.3.2 Perseverance sample handling

The ESA-NASA is working on an international Mars Sample Return campaign, that will be held between 2020 and 2030. Three launches will accomplish the operations of landing, collecting, storing samples and transferring them to Earth. NASA's Mars 2020 mission is dedicated to exploring the surface, document and store samples in strategic areas, to be further retrieved for flights to Earth. This final step will be achieved with two subsequent missions.

NASA started the *Mars 2020* rover mission on the 30<sup>th</sup> of July 2020, with the launch from the Earth on an Atlas V launch vehicle. The mission is defined as a Mars exploration mission and includes the rover Perseverance and a small helicopter called Ingenuity. In particular, the mission aim is to explore Jezero crater, the place of touch down on Mars land that took place on the 18<sup>th</sup> of February 2021.

The three main steps performed are: i) collecting samples, ii) sample sealing and storing on board, and iii) depositing samples on the surface. For this study, the most relevant step is the first one: collecting samples of Mars rock and soil, after an accurate selecting procedure. Then the samples will be sealed in tubes and positioned in specific places on Mars surface where future missions may recover them.

The sample handling equipment consists of three different robotic parts: the rover's two-meter-long Robotic Arm, a second shorter arm (about 0.5 m) called "T-rex arm" and the Bit Carousel (Figure 2.14). The full system architecture is composed by the Adaptive Catching Assembly (ACA) with the Bit Carousel and the Robotic Arm connected to the Turret, as can be observed in Figure 2.15. The Turret is composed by the Coring drill, the Planetary Instrument for X-ray Lithochemistry (PIXL) and finally the Scanning Habitable Environments with Raman & Luminescence for Organics & Chemicals (SHERLOC), assisted by a colour camera (WATSON).

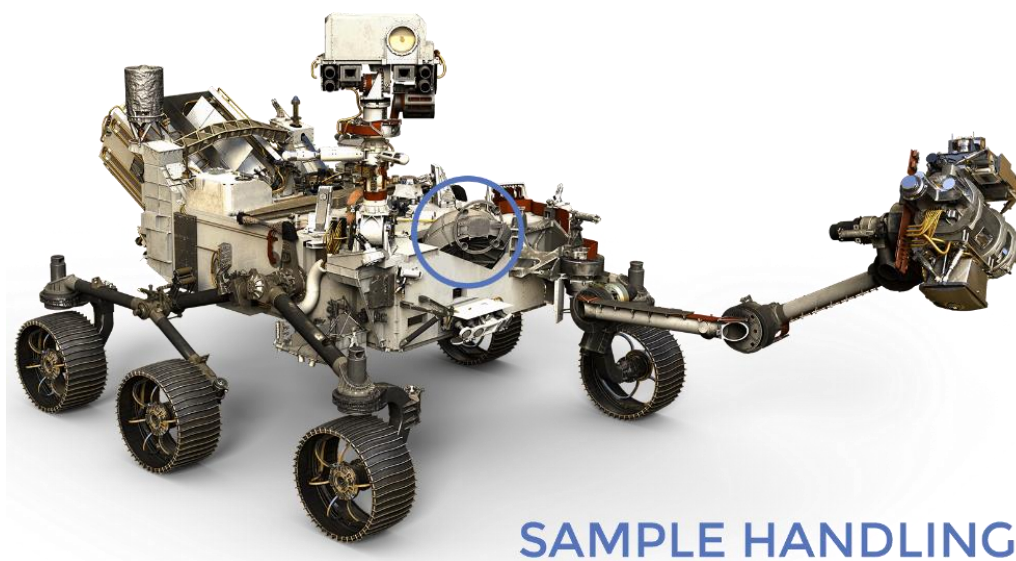


Figure 2.14 NASA's Perseverance rover and sample handling system detail (from "NASA Science Mars 2020 Mission Perseverance Rover - Sample handling" website)

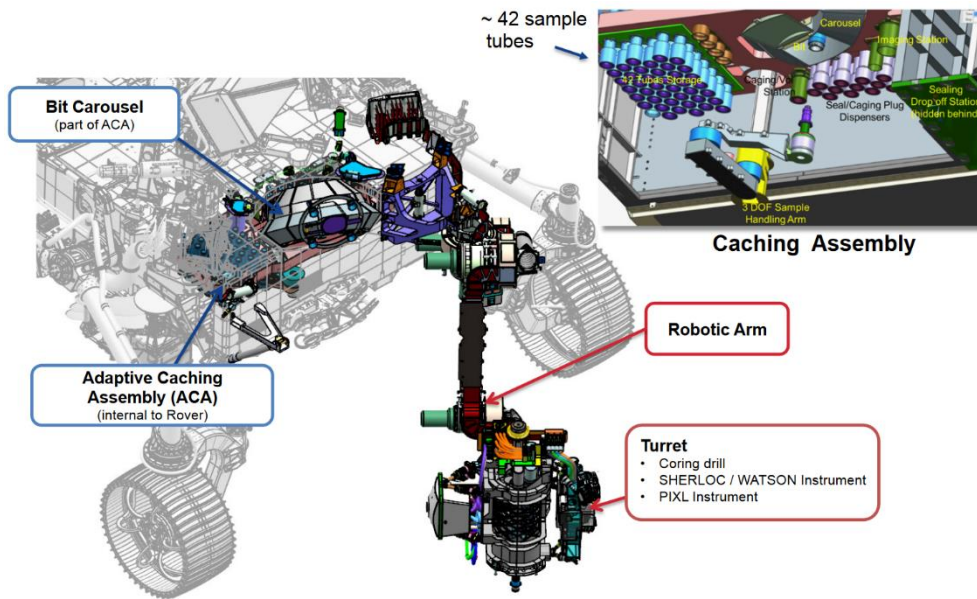


Figure 2.15 NASA's Perseverance rover sampling and caching full system architecture ("Mars 2020 rover Sampling & Caching Subsystem" from Wikipedia commons)

The Bit Carousel can be considered the heart of the sampling and caching subsystem: it holds nine different drill bits and forty-two sample tubes, in this way the system is adaptable to various sampling conditions. Un-weathered surfaces can be studied with more accuracy, for this reason, two drill bits are dedicated to abrading and scraping the top layer of rocks; then one bit is for sampling regolith and the remaining six bits are for coring.

Once operations are defined, the carousel moves to position the desired bit, so that the robotic arm can extract it. Coring operations are performed with the rotary-percussive Coring drill: first, a sample tube is put inside the appropriate coring bit, then the carousel starts to move. At the end of coring, the filled tube and the bit are returned to the carousel by the robotic arm. Every sample taken is hermetically sealed in hyper-sterile vessels, to avoid that any Earth-originating organic material could compromise future studies. A detail of the Drill bit after sampling operations can be observed in Figure 2.16. The coring bit is the bronze-coloured outer ring, the open end of the sample tube is the lighter-coloured inner-ring and inside can be observed the rock core sample.

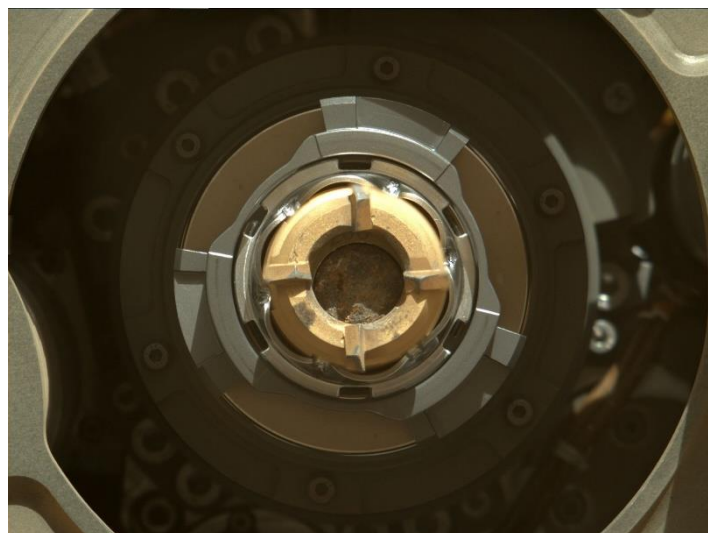


Figure 2.16 NASA's Perseverance Drill with Rock Core collected ("Sample Tube in Perseverance's Coring Drill" from NASA Science Mars Exploration Program website)

Following Perseverance rover mission provides a huge variety of suggestions to the design of a new rover. At the same time, a component of innovation must be implemented during a new design and several limitations

are imposed by competitions design requirements and financial resources. The requirement of modularity of the various systems allows attending different kinds of World Rover Challenges. For this reason, the system of the Bit Carousel completely integrated into the rover body could not be considered. Different considerations should be carried out for the Coring drill with different bits, the one that was considered more challenging is the dimension of the sample taken, characterized by 13 mm diameter and 60 mm length. Those very limited dimensions could provide reduced information about the geological formations, for this reason, one aim during the design will be increasing the depth of sampling below the surface, still collecting a continuous sample.

## 3 Chapter 3: DIANA's soil sampling system

This chapter is related to the design of the prototype of soil sampler. First it is provided an overview of the requirements and limitations to the design related to the ERC competition and rover asset. Then the design of the prototype is described, discussing the four main sub-system and their mechanical and electrical aspects.

### 3.1 Project requirements and main challenges

The main assumptions considered are described in the Introduction Chapter. Some further considerations, deriving from the analysis of the systems studied in the previous chapter are:

- limited space available as the equipment is positioned on ARDITO rover;
- impossibility of human intervention during sampling operations as the rover operates in conditions of autonomous exploration;
- completely dry and cohesionless material at least from the surface to the depth that can be reached in this preliminary operation;
- sandy-gravelly material with presence of superficial dust;
- impossibility of employing drilling fluids, compressed air or freezing techniques;
- different gravity conditions from Earth ( $3,721 \text{ m/s}^2$  on Mars compared to  $9,807 \text{ m/s}^2$  on Earth).

### 3.2 Prototype design

As stated in Chapter 1, the geometrical prototype design started from the definition of the available space on ARDITO rover's, limited by arm movements, position of the connection to the chassis of the rover, avoiding the risk of scraping the soil during rover's movements. This leads to overall height in compact conditions lower than 100 cm.

Then the design was performed working on four different sub-systems: lifting system, sampler, percussion system, control system. A detailed description of the systems is provided in the following paragraphs.

#### 3.2.1 Lifting system

The sampling system is attached to ARDITO rover's chassis through the lifting system, thanks to two plates made of curved stainless steel (5 mm thickness) to resist the different stresses involved during sampler activity. Sampling operations are performed in different phases:

1. electric lock activation and release of sampler;
2. free fall descent of the sampler along stage 1;
3. contact with soil surface by stabilizing system and advanced cutting shoe of the sampler;
4. activation of sampling operations;
5. percussion action and soil penetration with descent of the sampler along stage 2;
6. end of sampling operations;
7. activation of lifting servomotors and recovery of sampler along stage 2 and finally along stage 1;
8. passage through the electric lock and blockage of sampling system in closed position.

When ARDITO rover is moving on the soil, performing exploration tasks, the sampling system must be kept in compact form in order to not disturb the rover's movements (Figure 3.1). Sampling operations are performed keeping the rover completely stationary. The *lifting system* allows the *sampler* and *percussion system* to slide down during terrain approach and soil sampling. At the end of sampling operations the sampling payload is completely elongated, as shown in Figure 3.2.

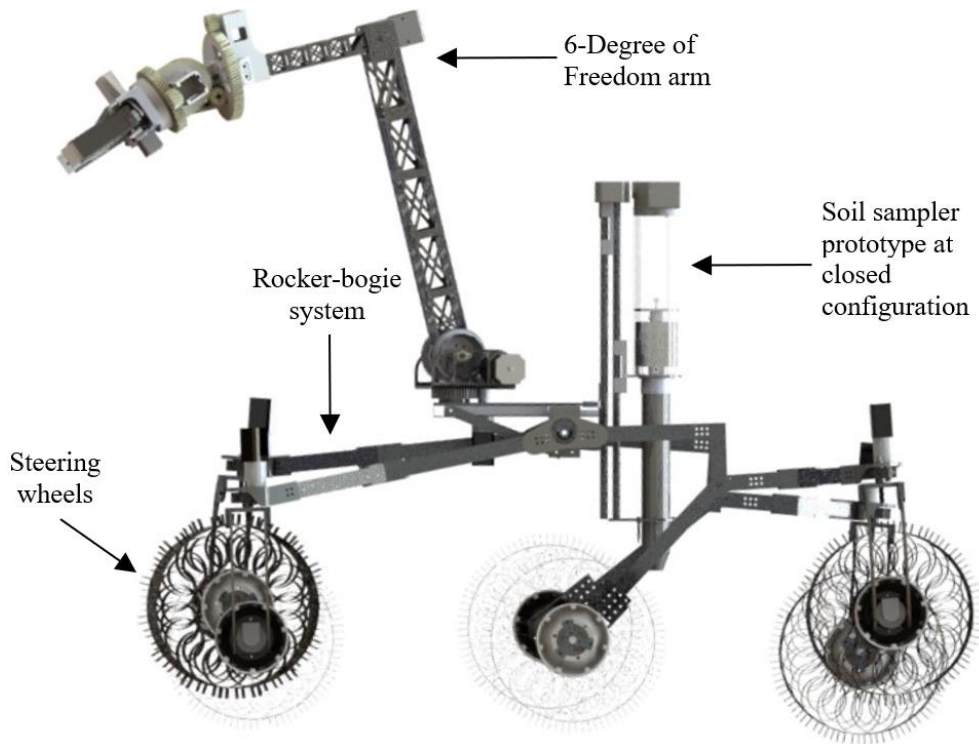


Figure 3.1 ARDITO rover mechanical structure with soil sampler prototype in closed configuration

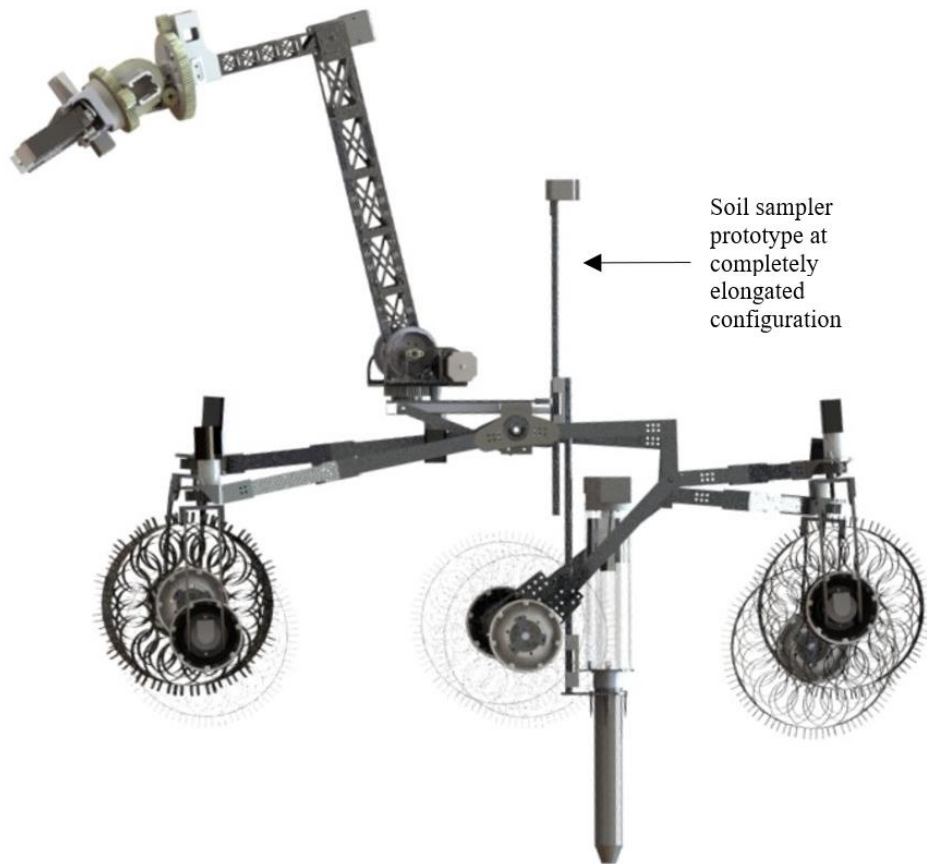


Figure 3.2 ARDITO rover mechanical structure with soil sampler prototype in completely elongated configuration

As can be observed from the lateral view of Figure 3.3, Stage 1 and Stage 2 are both composed of a linear guide and a sliding roller, that can provide a smooth sliding with no disturbance of sampling operations. This

sliding system is made of aluminium that is lighter than steel and at the same time is very thin with only 25 mm for each Stage, as shown in Figure 3.4. This choice was performed following the requirements for a reduced total mock of the sampling payload.

In order to improve vertical stability, the end of stage 2 is equipped with a stabilizing system composed of a stainless-steel plate and three or more nails fixed on it with self-locking nuts.

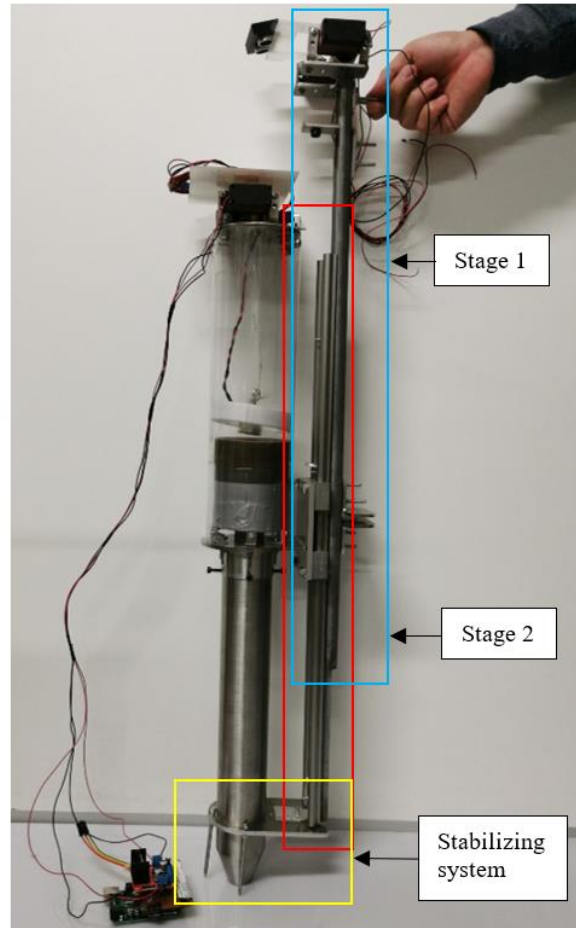


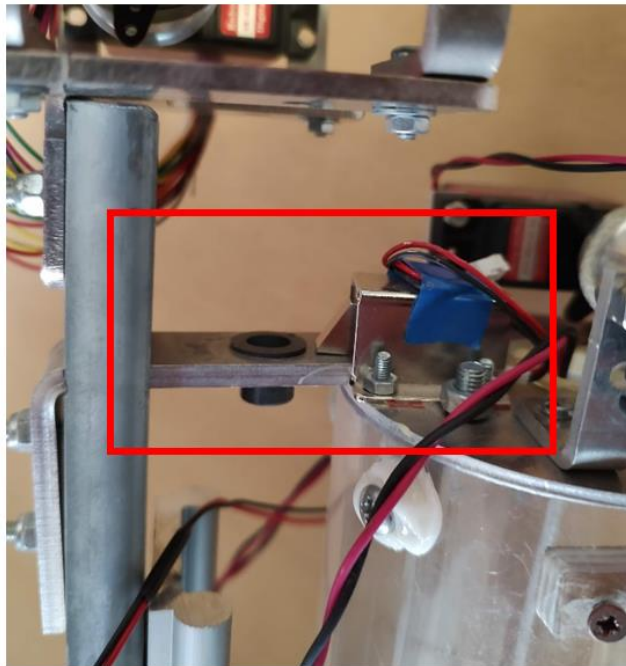
Figure 3.3 Lateral view of DIANA's sampling system with detail of lifting system



Figure 3.4 Detail of linear guide equipped with sliding roller thickness

As stated before, the sampling system must be completely closed if the rover is moving, and this is possible due to a mechanical-electrical lock composed of a stainless-steel blocking plate placed on Stage 1 and an electric lock placed on the top of the percussion system connected to the sampler (Figure 3.4). When the

electric lock is activated (electrical supply) the system is unlocked and the free fall starts. It must be highlighted that for safety aspects when electrical current is not available (possible system failure), the system is kept closed.



*Figure 3.5 DIANA's sampling system: detail of electric lock and blocking plate*

The approach with the terrain is performed through a free fall, allowing the penetration of the nails in the soil. Soil sampling is conducted with the penetration system described in its dedicated paragraph 3.2.3.

Ascent and complete closure of the sampling system, at the end of operations, is performed through two servomotors positioned on top of stage 1. These motors are coupled via a turned aluminium spool which is connected to an eyebolt fixed to the percussion system through a rope. So it is possible to individuate two couples of servomotors: sampling motors and lifting motors, as specified in Figure 3.5.

The strength needed to extract the sampler from the soil at the end of the sampling operation was estimated by performing a test campaign. A tube of diameter 76 mm was infixed in Mars regolith simulant and, a dynamometer allowed to measure the maximum weight during extraction, approximated to the extraction force, (Figure 3.6). Measuring an extraction weight of 12 kg, the motors were all bought with 25 kg capacity for each.

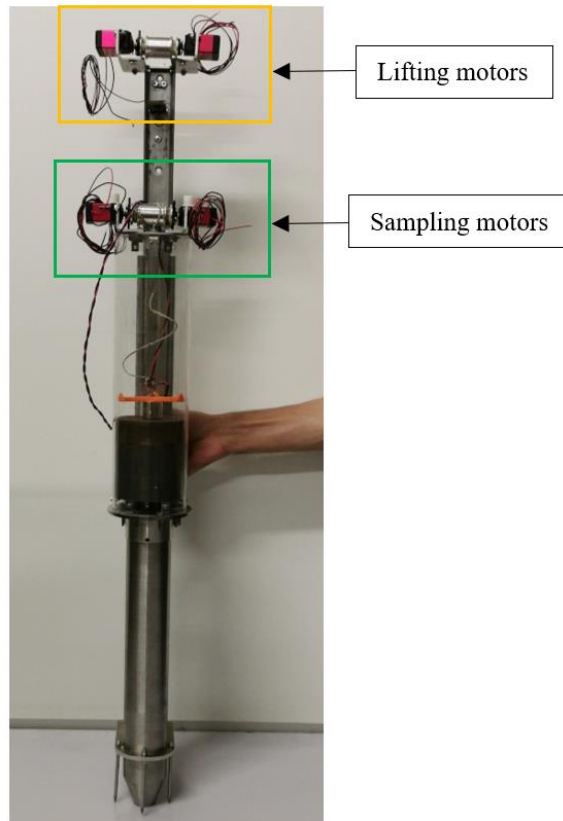


Figure 3.6 Front view of DIANA's sampling system with detail of servomotors



Figure 3.7 Test: measure of extraction weight from Mars regolith

### 3.2.2 Sampler

The design of the sampler for undisturbed sampling is linked to different parameters that affect sample disturbance. In particular, during sampling operations, the predominant causes of sample disturbance are the remoulding and the unloading of soil. Sample remoulding may be caused by friction or smearing of the sampled material along lateral walls and by squeezing of the material into the sampler. At the same time, unloading of soil may cause changes in soil structure. According to these considerations, the following parameters are analysed.

## Degree of disturbance

It can be expressed by a term called Area Ratio, defined as follow:

$$A_r[\%] = \frac{D_0^2 - D_i^2}{D_i^2} 100 \quad (3.1)$$

where  $D_0$  is the outside diameter of the cutting edge and  $D_i$  is the inside diameter of the cutting edge. If the Area Ratio increases, also the penetration resistance of the sampler increases, as well as the possibility of entrance of excess soil and risk of sample disturbance. The allowable Area Ratio intended for obtaining undisturbed soil samples depends on the diameter, design, and penetration method. According to experience, a well-designed tool should have an area ratio lower than 15% (Likos, 2010). The area ratio of the original Denison inner barrel design by Johnson (1940) was about 32%, while for a standard sampler (employed for Standard Penetration Test described in Chapter 2.1.3) is calculated as 112%. A high value of Area Ratio can be accepted if the sampler is provided by a stationary piston or a cutting edge with a very small angle. Good practice guidelines suggest for the cutting edge a minimum inside diameter equal to 75 mm and an angle of 20°. The tube for the holder should be clean, smooth, and uniform with no internal irregularities and should have a length at least equal to the desired sampling length increased by 100 mm, to account for residual soils. Considerations about soft soils, depending on their sensibility, suggest adopting different values for the ratio between the length of the sampler  $L$  and inside diameter of the cutting edge  $D_i$ , described in the following table (Table 3.1). The inside diameter of the cutting edge  $D_i$  will be studied in paragraph 4.4.

Table 3.1 Sampler design parameters (modified from MachenLink web course)

Material sensitivity	L/ $D_i$
>30	20
5 to 30	12
<5	12

## Clearance Ratio

The soil that enters in the sampler is subjected to great stress and tends to lateral expansion, for this reason, the inside clearance should be large enough to partially allow the lateral expansion, but at the same time, some friction is needed to hold the sample. This concept can be expressed by the Clearance Ratio:

$$C_i[\%] = \frac{D_1^2 - D_i^2}{D_i^2} 100 \quad (3.2)$$

where  $D_1$  is the internal diameter of the tube (sample holder) and  $D_i$  is the inside diameter of the cutting edge. The resulting value can be defined as an *inside clearance ratio* and should be kept lower than 3%, in order to avoid excessive deformations that cause disturbance of the sample. For good sampling is usually required that:

$$C_i = \begin{cases} 0.5\%, & \text{for sands, silts and clays} \\ 1.5\%, & \text{for stiff and hard clays} \\ 3\%, & \text{for stiff expansive type of clays} \end{cases}$$

The inside clearance of the original Denison inner barrel design by Johnson (1940) was about 0.6%.

It is also possible to define an *outside clearance ratio*, using the following expression:

$$C_o[\%] = \frac{D_0 - D_2}{D_2} 100 \quad (3.3)$$

The obtained value should be within 0% and 2%.

The following figure (Figure 3.7) shows the sample characteristics parameters described previously.



Figure 3.8 Sample characteristics

### Recovery Ratio

This parameter represents the disturbance of the soil sample and can be computed as follow:

$$R [\%] = \frac{L}{H} 100 \quad (3.4)$$

where L is the length of the sample within the holder tube and H is the depth of penetration of the sampling tube, as described in Figure 3.8.

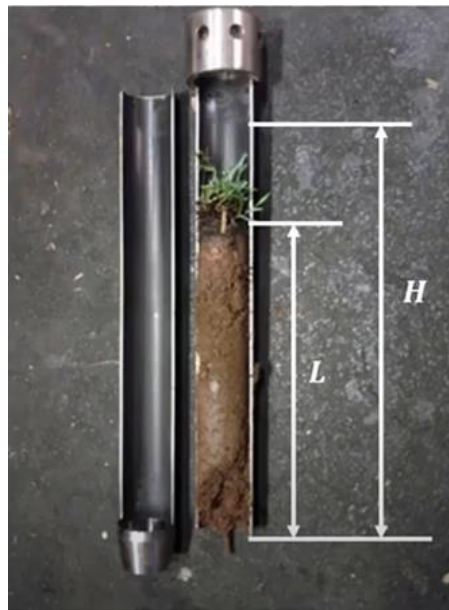


Figure 3.9 Sample Recovery Ratio

A good sample can be described by a value of recovery ratio at least equal to 96%, it should be evidenced that also values higher than 100% can be obtained due to material expansion. The Recovery Ratio is highly influenced by wall friction, which can be reduced with a suitable inside clearance, a smooth finish, and oiling the internal side walls. It is also important to provide holes in the tube for water and air escape.

### Catcher

Several types of research have demonstrate that “even though there is an abundance of ice, Mars has been experiencing a super-drought that may well have lasted hundreds of millions of years” (W. T. Pike, 2012). The same feedbacks are being brought from Nasa’s rover Perseverance site exploration. For this reason, it is possible to assume that sampling operations on Mars will be carried out in total absence of water, at least at

surface. Sampling a granular material (dusty sand) in completely dry conditions means that there will be no cohesion helping sample retaining. A possible device that can be employed is the catcher of the Denison sampler, which main function is to hold the material sampled by means of thin and elastic fingers that close under the weight of the sample during extraction. Figure 3.9 a) shows the triple core barrel Denison sampler specifying the position of the catcher. In Figure 3.9 b) is possible to observe a prototype of spring catcher with harmonic steel fingers developed by Geomarc S.r.l.

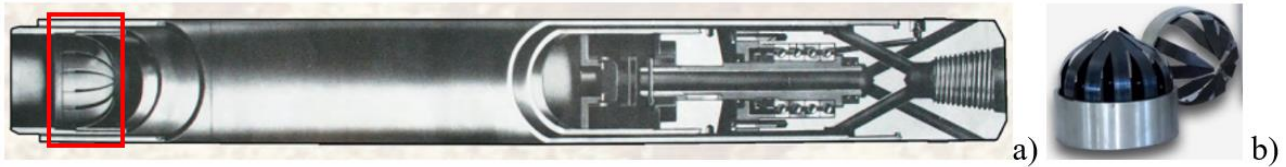


Figure 3.10 (left) Schematization of the triple core barrel Denison sampler with detail of the catcher - (right) catcher prototype developed by Geomarc S.r.l.

Catchers available on market are mainly made by a stainless-steel ring and harmonic steel fingers, with fixed dimensions linked to samplers used for earth purposes and internal diameters around 100 mm. Preliminary evaluations on carried weight available from ARDITO rover suggest keeping the internal diameter of the sampler lower than 60 mm. At the same time, the design requires to be personalized in order to try to hold even the dusty part of the sampled material, in completely dry conditions. For this reason, it is necessary to carry a more detailed analysis of materials that can be employed to produce a catcher.

Starting from the study of requested performances for the element is possible to define the goals like maximizing the deflection and evaluating the fatigue behaviour under a high number of load cycles, reducing the probability of material rupture due to fatigue. Then it is necessary to find restrictions like the resistance to operational loads (limit tension), resistance to cyclic loads, and limitations imposed due to production operations.

It is possible to simplify the catcher analysis by studying only one single finger and schematizing it as a cantilever beam (a rigid structural element fixed at one end and free at the other). Some simplifying assumptions are made. First, the most adequate section to better create a closure of domed section is trapezoidal, having lower stiffness where the section is thicker, a regular rectangular section is assumed. The fixed end is the joint between the fingers and the ring. Finally, due to the curved shape of fingers, the tips of the fingers are the first to keep in contact with the sampled material (cylindrical shape) that transmits the tension necessary to open them. As a consequence, the load distribution is assumed as triangular.

Working with CES Edupack Software (Ansys Inc., 2016), the process for the material choice adopted is the “funnel-shaped method”. Starting from 4026 materials available on the software database and inserting the defined restraints on material properties and characteristics of the production process, a reduced list of appropriate materials is obtained. The huge availability of materials is limited with the application of borderline properties and the definition of Material Performance Index (MPI) that allow sorting materials starting from their capacity of maximising performances. MPI is usually obtained combining properties. The evaluations develop starting from design requirements, in particular the “function” defines what the component does, the “objective” what performance is necessary to maximize or minimize and “bonds” which conditions must be satisfied. The performance ( $p$ ) of the component will be function of functional requirements ( $F$ ), geometrical parameters ( $G$ ) and material properties ( $M$ ):  $p = f(F, G, M)$  (Maizza, 2019-2020). An optimal design defines geometry and material that maximize the performance, so it is better to separate the performances and find a new equation that allows individuating the MPI that optimizes the performance:

$$p = f_1(F) \cdot f_2(G) \cdot f_3(M) \quad (3.5)$$

The first objective studied is the **maximizing of deflection ( $\delta_{max}$ )**. The single finger must bend elastically due to the load imposed by the cylinder of soil entering in the sample. So it is possible to schematize the system as a cantilever beam (total length  $L$ ) with a distributed triangular load and resultant applied at a distance equal to  $\frac{2}{3}L$  from the fixed end. The equivalent system is a cantilever beam with a concentrated load  $F$  applied at distance  $\frac{2}{3}L$  from the fixed end. The shear force diagram is constant from the fixed end until the point of application of the force  $F$  and the bending moment diagram is linear with maximum value at the fixed end and null in the point of application of the force  $F$ . The maximum deflection  $\delta_{max}$  is computed at the free end of the beam:

$$\delta_{max} = \frac{7}{27} \frac{FL^3}{EI} \quad (3.6)$$

where:

- $F$  is the force applied;
- $L$  is the length of the beam;
- $E$  is the elastic modulus of the material;
- $I$  is the area moment of inertia of the beam cross section.

The *bond* equation is obtained from the material resistance and correlated to the failure tension. In case of a ductile material (elastoplastic behaviour) it depends on the beginning of plastic deformations:

$$\sigma = \frac{F}{A} \leq \sigma_f \quad (3.7)$$

where:

- $F$  is the force applied;
- $A$  is the area of the section;
- $\sigma_f$  is the failure tension.

In practice, a safety factor  $SF$  is applied in order to keep the tension lower than  $\sigma_f/E$  instead of  $\sigma_f$ . Removing the force  $F$  from equation 3.6 and 3.7 it is possible to obtain:

$$\delta = \frac{7}{27} \cdot \left( \frac{L^3 A}{I} \right) \cdot \left( \frac{\sigma_f}{E} \right) \quad (3.8)$$

The process of identification of the MPI starting from material properties allows to exclude the geometrical properties, so it is possible to identify the material index that if maximized allows to maximize the deflection:

$$IM = \frac{\sigma_f}{E} \quad (3.9)$$

This index is known from technical literature (Ashby, 2003) for efficient and light springs. It is useful to rewrite equation 3.9 in logarithmic form:

$$\log IM = \log \sigma_f - \log E \quad (3.10)$$

From which is obtained:

$$\log \sigma_f = \log E + \log IM \quad (3.11)$$

This last form allows visualizing the results on CES Edupack software through the *bubble chart* (material property chart) developed by Ashby. The plot obtained having set the filters defined above can be observed in Figure 3.10. The drawn line with slope equal to 1 describes the equation 3.10 and the materials with the same MPI. Moving the line intercept from the origin to higher values of yield strength is possible to exclude materials with lower performances. In addition, a lower limit for Young Modulus has been imposed, considering the one for medium to high-quality springs, equal to 207 GPa (ACE wire and springs company). The preliminary

resultant materials mainly belong to the groups of “Fibers and particulates” and “Metals and alloys”, it is possible to evidence the tool steel and the Silicon carbide.

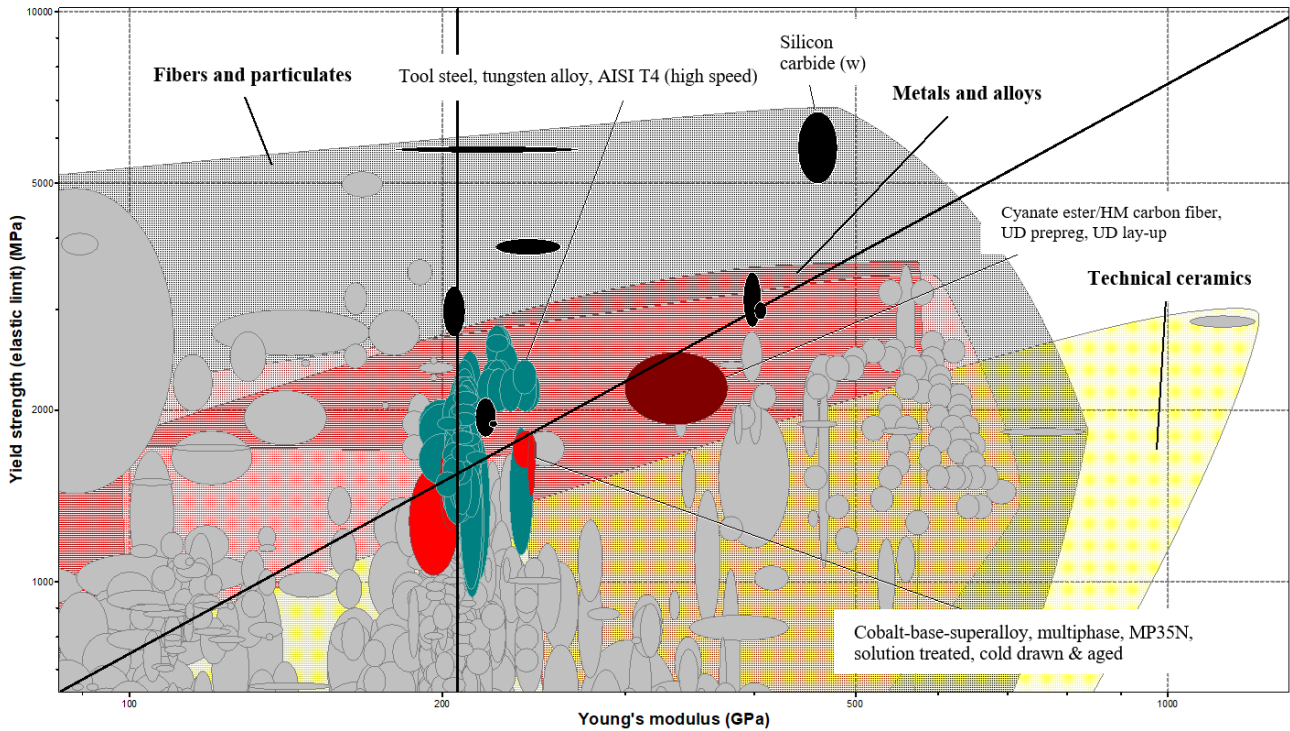


Figure 3.11 Ashby logarithmic plot for strong and elastic beam (obtained with CES Edupack software)

The second objective analysed is **fatigue behaviour**. The fatigue resistance of a material is generally studied by means of two different approaches: considering the points of weakness (fracture mechanics) or correlating the durability of a component (number of cycles before breakage) with the acting stress. Considering the very small thickness of the component under investigation, the fracture resistance approach is excluded because the probability of having significant faults is very low.

Wöhler tension-cycles ( $\sigma-N$ ) plots can be used to determine the domain of non-failure of the component. These semilogarithmic graphs are obtained from interpolation of the experimental data obtained from fatigue tests performed on standard samples. Different type of curves are obtained for different materials: for example, steel describes a particular sharp bend while light alloy show a horizontally asymptotic behaviour. In the following figures the experimental Wöhler plots are shown in relation with the amplitude of cyclic stress (Figure 3.11 left) and the range of cyclic stress (Figure 3.11 right).

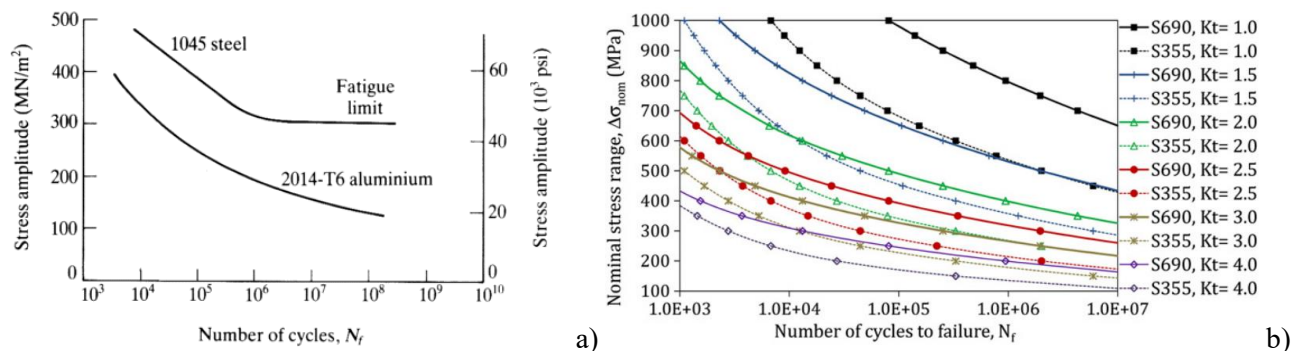


Figure 3.12 Experimental Wöhler plots (a) from generic literature and (b) from (de Jesus, et al., 2012)

The component will have to resist to a low number of cycles (a maximum of  $10^4$ ): for this reason, a resistance to fatigue equal to 400 MPa is chosen and will be applied in the Ashby plot for the evaluation of the index to fatigue resistance.

Parameters involved in the study of the resistance to fatigue are: cyclic stress range, defined as the difference between maximum peak ( $\sigma_{max}$ ) and minimum peak of the cycle ( $\sigma_{min}$ ); amplitude of the cyclic stress ( $\sigma_a$ ) equal to half of the cyclic stress range; limit of resistance or fatigue ( $\sigma_e$ ) that correspond to the amplitude of stress that a smooth and intact sample can resist without fracture for  $10^7$  cycles and finally the load ratio R, commonly used as measure of the medium stress of the cycle, and defined as  $R = \sigma_{min}/\sigma_{max}$ .

The equation *bond* for fatigue resistance is:  $\frac{F}{A} \leq \sigma_e$ .

With reference to studies performed by Fleck et al. (Fleck, et al., 1994), existent MPIs are considered, already determined for components different in shape and load. Proposed solutions have been determined with the focus of minimizing the mass, but in this case study it is not a particular need (component with very small dimensions). For this reason the line on the plot will have a very small intercept, corresponding to very low resistance to fatigue. Taking reference to beams, the MPI for cyclic loads or cyclic bending moments with defined length and free section is:

$$IM = \frac{\sigma_e^{2/3}}{\rho} \quad (3.12)$$

where  $\rho$  is the density of the material.

Writing equation 3.12 in logarithmic form the result is:

$$\log IM = \frac{2}{3} \log \sigma_e - \log \rho \quad (3.13)$$

$$\log \sigma_e = \frac{3}{2} \log \rho + \frac{3}{2} \log IM \quad (3.14)$$

In this way is possible to obtain the bubble plot represented in Figure 3.12 with a line with a slope of 1.5 that maximises the behaviour and minimum fatigue resistance equal to 400 MPa. The preliminary resultant materials mainly belong to the groups of “Fibers and particulates”, “Technical ceramics” and “Metals and alloys”. From a preliminary evaluation it is possible to evidence the carbon fibers and the maraging steel.

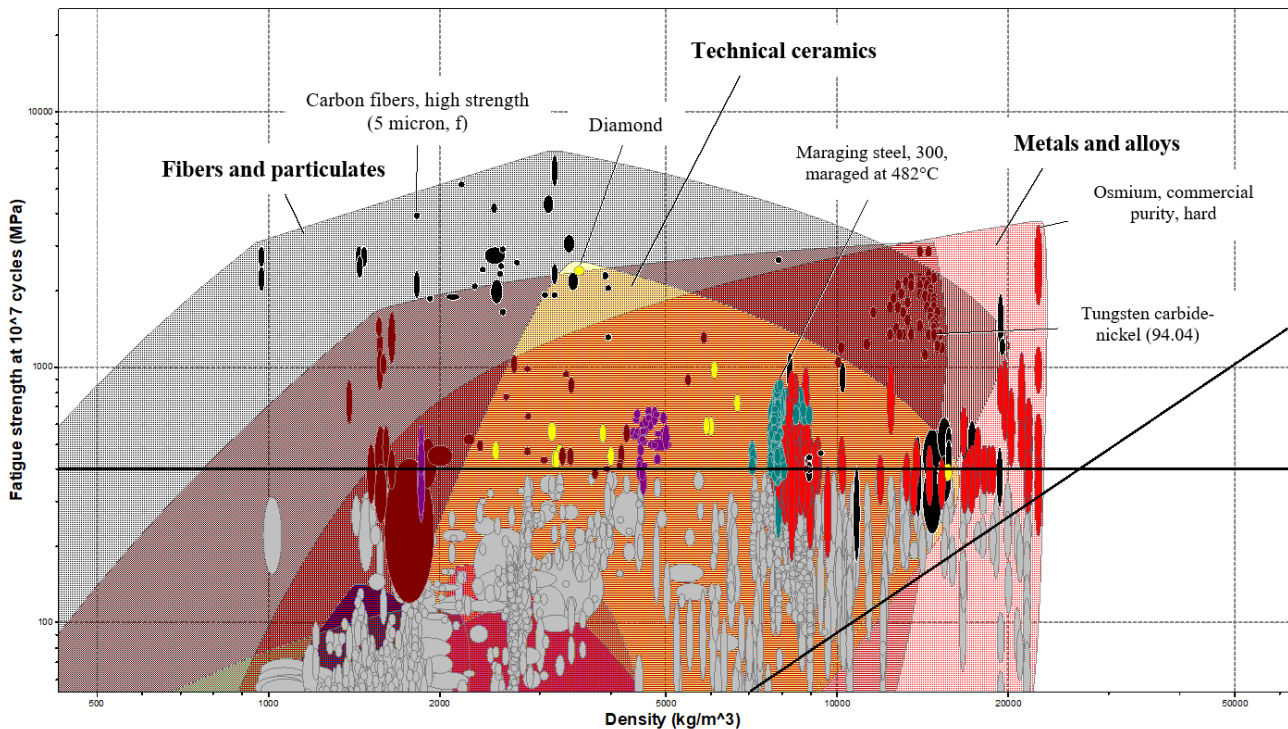


Figure 3.13 Ashby logarithmic plot for fatigue resistance of a beam element (obtained with CES Edupack software)

Considering a possible production of the catcher in metal, the component would be produced with cold lamination, for this reason on CES Edupack software more filters related to the production have been imposed: excellent capacity of cold lamination, which also includes hot forming and excellent printing capacity. In addition, an excellent galling resistance is required, because the function of the catcher is to allow the passage of the soil sample cylinder inside the sampler, so there is a high risk of material being lost due to friction with the soil. Considering a production with steel a minimum percentage of carbon about 0.5% is set to obtain stronger steel.

The resultant materials, obtained overlaying all the filters imposed on CES Edupack, are low alloy steels. American designation AISI (American Iron and Steel Institute) requires for low steel alloy the use of 4 digits, where the first two numbers describes the series and last two the carbon content multiplied by 100. Series 51 is related to Chromium steels (composition Cr 0.80, 0.87, 0.92, 0.95, 1.00 e 1.05), the result is acceptable because Cr is responsible of an increment of hardness, elastic limit, wear resistance, stability at temper and fragility at cold temperatures. Carbon content for obtained steel of series 51 is 0.5 or 0.6 that describes the so known *harmonic steel* (composition C 0.55-0.65, Mn 0.75-1.00, Cr 0.70-0.90) a type of steel applied in springs production. Series 91 describe Silicon and Manganese steels (composition Si 1.40 e 2.00, Mn 0.65, 0.82 e 0.85, Cr 0 e 0.65). In fact there is a presence of Silicon and Manganese in all steel products because increase hardness, resistance, durability, resistance to temper and resistance to wear. At the same time contribute to increase the elasticity, for this reason are highly applied in the production of springs. Silicon steels have tendency to fragility, fibrousness and grain size increasing. Manganese element reduces hot fragility caused by sulphurs and increases temper, mechanical resistance and in high content also wear resistance but increases steel embrittlement.

It should also be highlighted that the three elements individuated, are tempering steels, characterized by thermal treatments like quench and temper, that lead to high yielding resistance.

The limited number of catchers needed implies that the production of a harmonic steel catcher cannot be requested to a factory, but a prototype can be handmade produced starting from a very thin plate (0.4 mm) of C67 harmonic steel, cutting and bending it giving the requested shape and curvature. The result can be observed in Figure 3.14 where the catcher prototype is fixed directly to the holder with self-locking nuts, useful to better resist loosening through vibration and normal use.



Figure 3.14 DIANA's harmonic steel catcher prototype

Considering the high stiffness of the obtained fingers also other prototypes made with different materials are produced and tested. In particular 3D printing technology allows to obtain and self-design different possible solutions. The material used for this study is Polylactic acid (PLA), the most 3D printing material available. This material is characterized by a high detail reproduction between the common filaments, it is also low cost, stiff, and with good strength. Problems related to this material are the low heat resistance, the risk of brittle behaviour in time and as it is biodegradable the contact with humidity reduces the durability. The very reduced costs anyway can permit to produce a very large number of prototypes to be substituted after a few cycles. The following figures show the 3D printing model (Figure 3.15 a) and the resultant assembly (Figure 3.15 b). Fingers width is fixed at 8 mm and two different thicknesses will be produced and tested, 1 mm and 0.5 mm, in order to obtain different stiffness and yielding resistance.

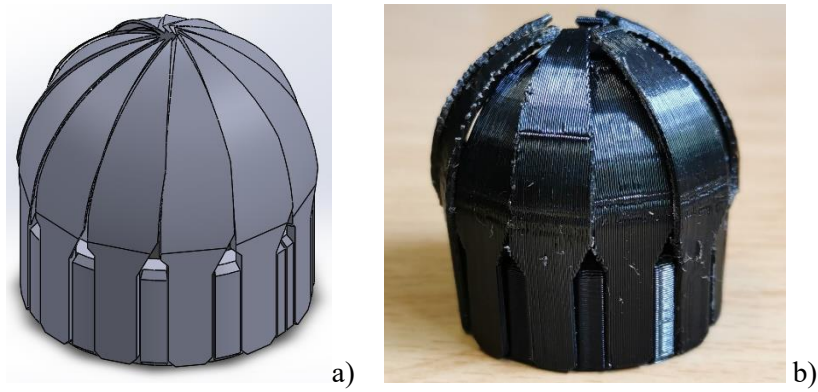


Figure 3.15 DIANA's PLA catcher prototype (1 mm finger thickness): a) CAD model, b) 3D printed prototype

### Sampler prototype design

Following the indications provided in the previous paragraphs, the sampler assembly design is composed of an external stainless-steel tube, an internal transparent holder, and an advanced cutting shoe equipped with the catcher. The first prototype produced is shown in Figure 3.16 and in Figure 3.17 with detail of advanced shoe and catcher. The external tube and the advanced shoe are produced in AISI 304 steel, in order to be able to resist to wear and stresses provided by the sample soil penetration. The holder tube is produced in transparent Polycarbonate (PC). In this way the sampled material can be observed simply extracting the holder from the sample. Inside the holder will be positioned a humidity and temperature sensor (Figure 3.17), in this way soil parameters can be monitored in real time.

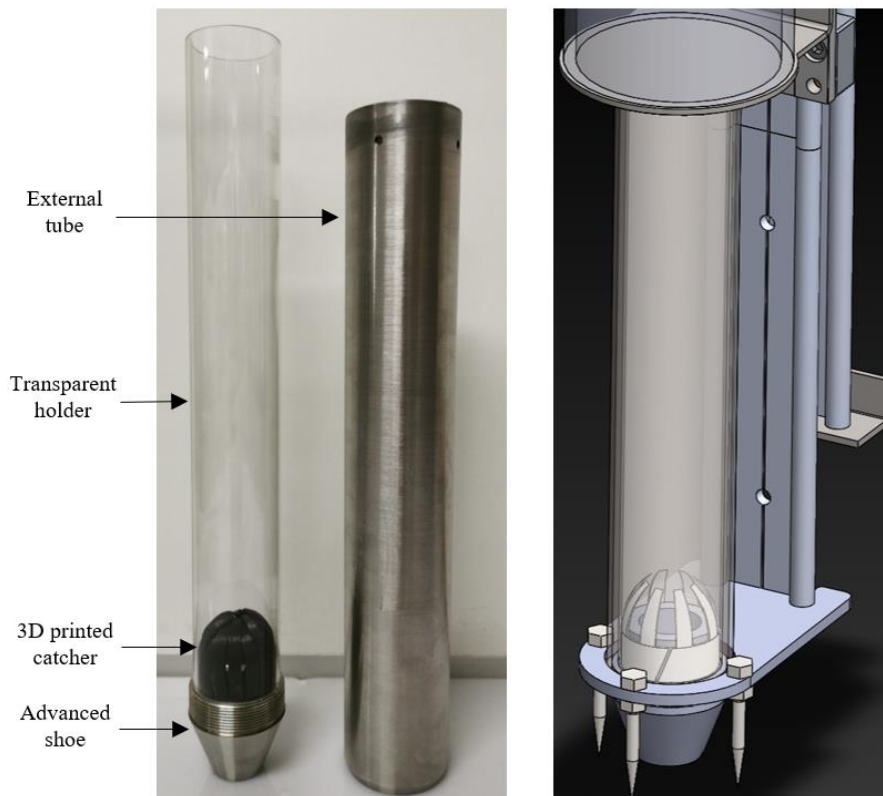


Figure 3.16 DIANA's sampler assembly



Figure 3.17 Humidity and temperature soil sensor to be positioned inside the holder

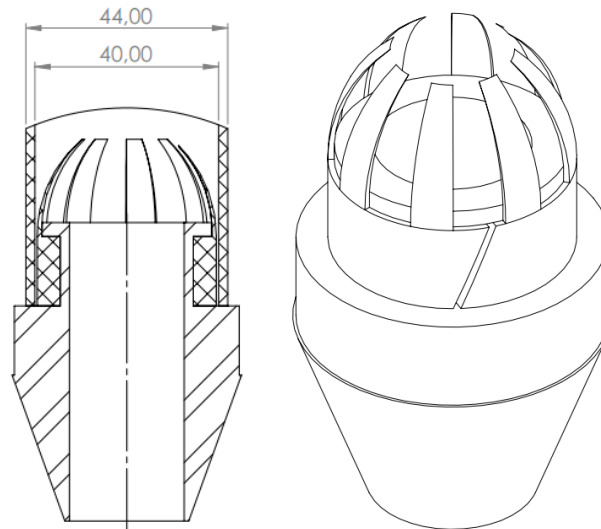


Figure 3.18 DIANA's advanced shoe and catcher

From the quoted section of the advanced shoe (Figure 3.19) is possible to compute the parameters defined at the design stage. In particular:

- Degree of disturbance:  $A_r[\%] = \frac{D_0^2 - D_i^2}{D_i^2} 100 = \frac{50^2 - 25^2}{25^2} 100 = 300\%$

This parameter largely exceeds the reference one (15%) but this design solution was obtained with the purpose of permitting a fast and easy replacement of the catcher, as well as the fixed cutting angle on  $20^\circ$  derived from good practice suggestions. For this reason, this solution will still be produced and tested in order to understand the effectiveness of the cutting advanced shoe in soil penetration.

- Inside Clearance Ratio:  $C_i[\%] = \frac{D_1^2 - D_i^2}{D_i^2} 100 = \frac{37^2 - 25^2}{25^2} 100 = 119\%$  also this value largely exceeds the limit suggested (3%), but the difference of space between the inside diameter (25 mm) and the internal diameter of the holder (37 mm) is imposed to block the catcher base.
- Outside Clearance Ratio:  $C_o[\%] = \frac{D_0 - D_2}{D_2} 100 = \frac{50 - 50}{50} 100 = 0\%$  this value is within the fixed range (0-2%).
- The Recovery Ratio will be determined during test phase.

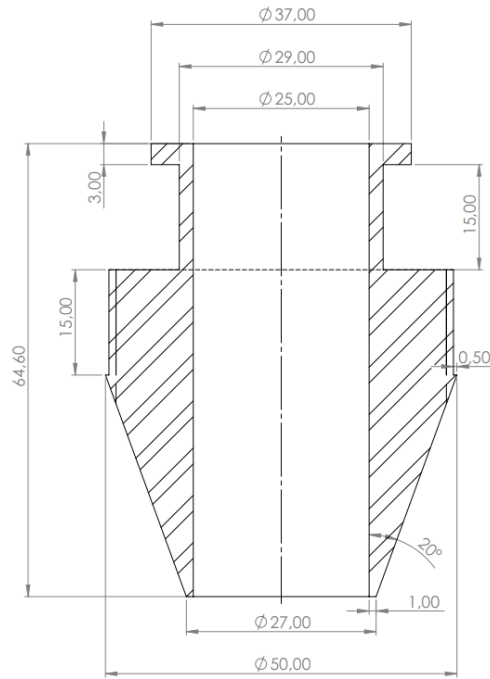


Figure 3.19 Quoted section of DIANA's advanced shoe

### 3.2.3 Percussion system

Two different penetration systems were evaluated to design the sampler: percussion boring and rotary drilling.

Tests were performed manually, using a tube of diameter 100 mm and to penetrate a completely dry sample of mars regolith simulant. In order to simulate *rotary drilling*, the drilling is obtained from the continuous scraping of the lower part of the tube under constant pressure. Penetration was difficult to be achieved and a great contrast force was required, impossible to be granted only through the rover's weight. Considering percussion drilling, usually it is performed with a heavy bit repeatedly lifted and dropped, progressively boring through the soil. In this case, a hammer was used and penetration was immediately effective. The percussive penetration system is the one adopted in Standard Penetration Test explained in 2.1.3. As previously stated this test is characterised by several positive aspects, in particular it can be applied to all types of soils (Cestari, 2009). For this reason a site test was performed from Thales Alenia Space Italy S.p.A. in order to verify the effectiveness of the procedure.

Thales Group is a French-Italian aerospace manufacturer specialised in the space industry. Thales Alenia Space Italy S.p.A. is based in Turin and its ROvers eXploration facility (ROXY) is a technological area located in TAS-I Turin site. This facility is dedicated to robotic systems design, development, validation, and verification in a real-world weather conditions. Outdoor yard has dimensions 23x19 m (437 m<sup>2</sup> and height 0-2 m), and reproduces Mars planetary morphology in terms of colour, landscape, statistic distribution of boulders, smaller rocks and slopes. It can be observed in Figure 3.20.



Figure 3.20 Thales Alenia Space ROXY facility: internal view of test area (courtesy of Thales Group S.p.A.)

Tests were performed looking for a position where soil looked mostly composed of sand, as in many areas there was a great quantity of gravels and pebbles. The same procedure of evaluating the best test position will be performed by a formed operator during competitions simulating Mars exploration (ERC). The chosen position can be observed in Figure 3.21.

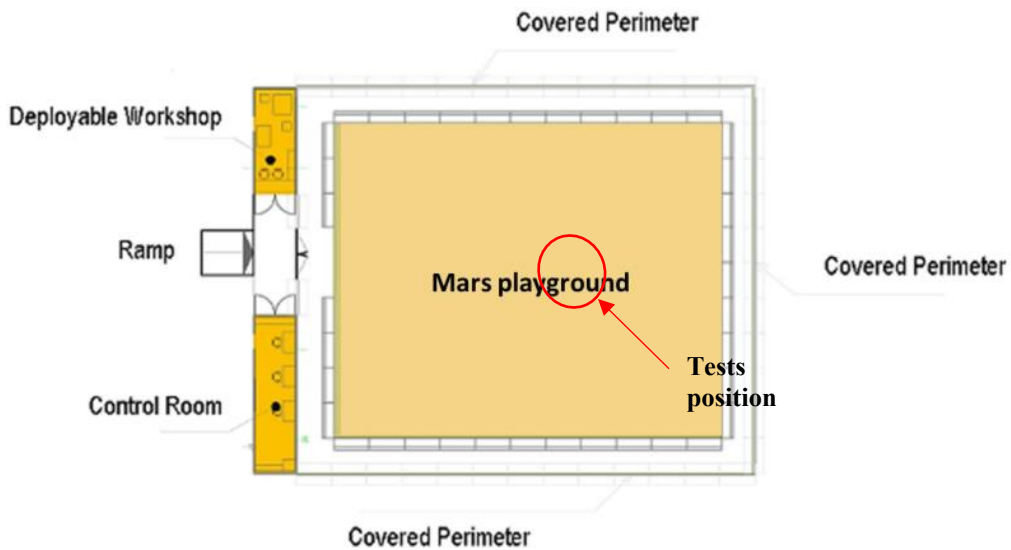


Figure 3.21 Thales Alenia Space ROXY facility: plan and tests position

A test was planned in order to estimate the minimum mass and drop height necessary to penetrate the soil with two different tubes. The first was a stainless-steel tube with external diameter equal to 76.1 mm and 2 mm wall thickness, while the second tube was made of Polyvinyl chloride (PVC) with external diameter equal to 50 mm and 1.5 mm wall thickness..

The test equipment involved is shown in Figure 3.22. It was composed by:

- stainless-steel or PVC sampler tube;
- graduated wooden stick working as linear guide for the hammering weights and reference for the depth of penetration of the sampler tube;
- tube holder assembled with 3D printed parts in Polyethylene terephthalate glycol (PETG) and employed to extract the tube from the soil at the end of penetration;
- stroke stabilizer made with 3D printed PETG;
- different weights utilised as mallets;
- wooden board for mallets support;
- measuring instruments like a dynamometer for measuring the extraction force and a meterstick.



Figure 3.22 DIANA's test equipment for evaluation of weight and dropping height

Three series of tests were performed by fixing the dropping height at 30 cm. First, the penetration of the stainless-steel tube was tested using a heavy bit of about 2.5 kg, then the same tube was tested using 4.5 kg. Finally, the PVC tube was tested with the heavy bit of about 2.5 kg, at the end of the test the tube resulted damaged so a test with 4.5 kg was not carried out. Results obtained can be observed in the plot of Figure 3.23.

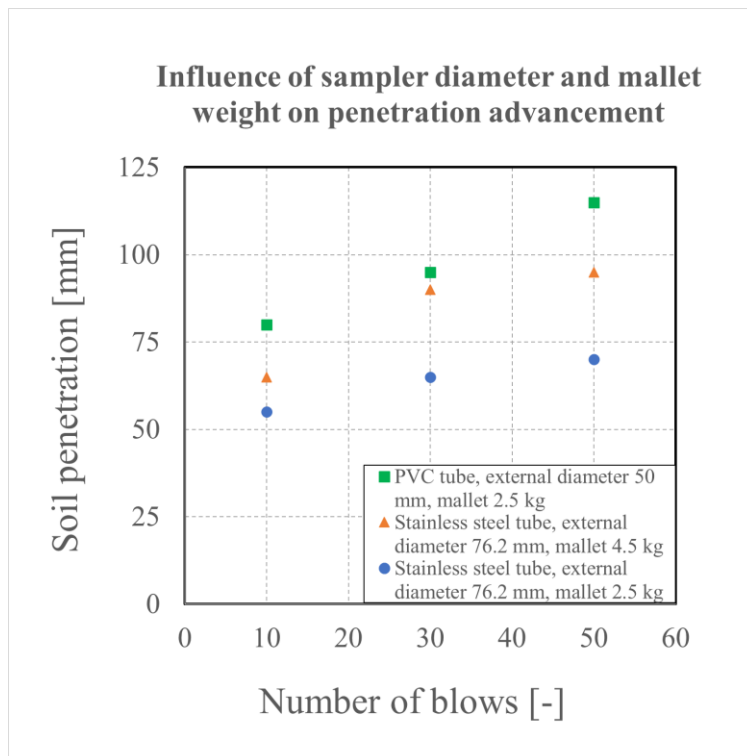


Figure 3.23 Results of test campaign at ROXY facility of Thales Alenia Space

Some observations can be carried out after this site test:

- the extraction force measured weren't reliable because of the water content of the soil that develop an initial apparent cohesion (ROXY facility is placed outdoor), so the borehole could self-sustain and extraction forces measured were related only to the tube weight;
- the PVC tube, despite being less rigid, allowed an easier penetration into the soil, having kept the drop height constant (300 mm) but adopting a lighter mallet (2.5 kg). That result depends on the reduced external diameter (50.0 mm for the PVC tube instead of 76.1 mm for the stainless-steel tube) and also the wall thickness was slightly smaller (1.5 mm instead of 2.0 mm);
- gravels slightly disturbed the operations, breaking the PVC tube and affecting the test;
- an advanced shoe is necessary to increase the depth of penetration keeping the same number of blows and same drop height and mallet.

Site test confirmed the idea of developing a percussion system, having understood that a smaller diameter for the sampler requires much less energy for penetrating the soil. Balancing the overall weight of the sampling payload and trying to keep it under 10 kg, the available weight for the hammer to be lifted and dropped is 4 kg, while the diameter of the sampler will be kept the same as the PVC tube, so 50 mm. It is important to remember that the available total weight of the mallet would be less working with Mars gravity, but the whole system is scalable according to rover's available power and dimensions. As indication gravity on Mars is equal to  $3.721 \text{ m/s}^2$  compared to  $9.807 \text{ m/s}^2$  on Earth, to the total available weight would be 1.5 kg.

It was necessary to reduce the mallet dimensions as much as possible, with a diameter about 80 mm, so for this reason the central part made by lead. The small hammering head is composed of a silicon-iron alloy cylinder, connected to a screw (diameter 15 mm) passing through the lead cylinder and finally to another silicon-iron alloy cylinder, as shown in Figure 3.24. The choice of a silicon-iron alloy is due to its ferromagnetic properties, as the upper cylinder connects with an electromagnet, the innovative lifting and dropping system. The produced mallet can be observed in Figure 3.25.

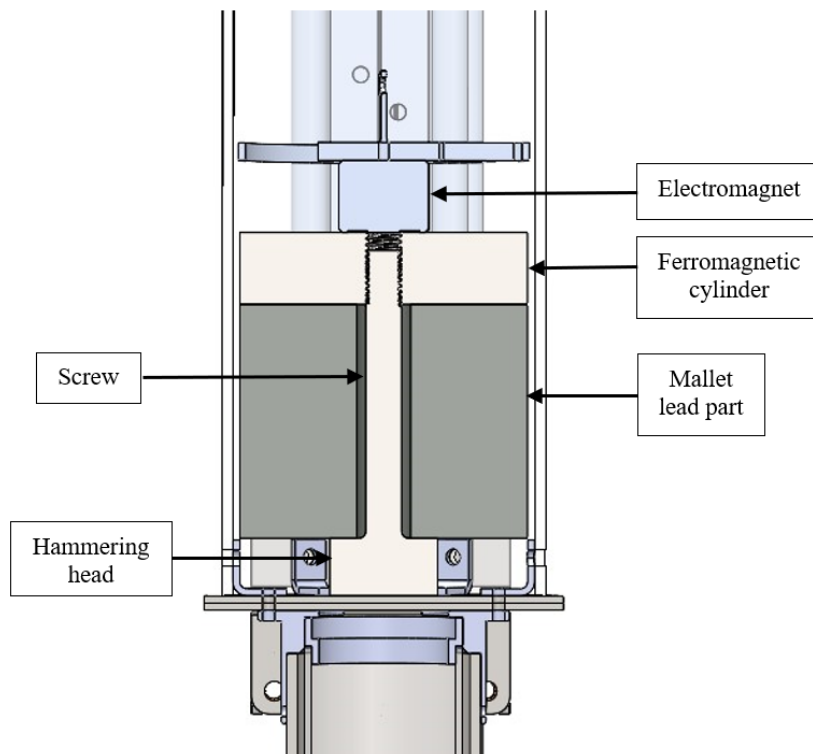


Figure 3.24 DIANA's sampling system: mallet section



Figure 3.25 DIANA's sampling system: mallet

The complete percussion system is positioned inside a mallet guide made of transparent Polycarbonate, so the operations can be visually checked. Following the need for an instantaneous drop of the mallet with free fall, a mechanised system for lifting and dropping the weight would have resulted in too complex in terms of electronic control, spatial disposition, and the need for more servomotors. For this reason, a small electromagnet, (capacity of 150 N, diameter of 25 mm) is equipped and electrically controlled simply providing energy during lifting and interrupting energy supply when the dropping height is reached and the free fall of the mallet starts (Figure 3.26 a). The dropping height is set as 200 mm due to space limitations. During lifting operations, the mallet is anchored to the electromagnet by means to a ferromagnetic silicon-iron alloy cylinder. The feedback of having reached the dropping height is given by an endstop (Figure 3.26 b), mechanically protected and anchored with small slabs of plywood.

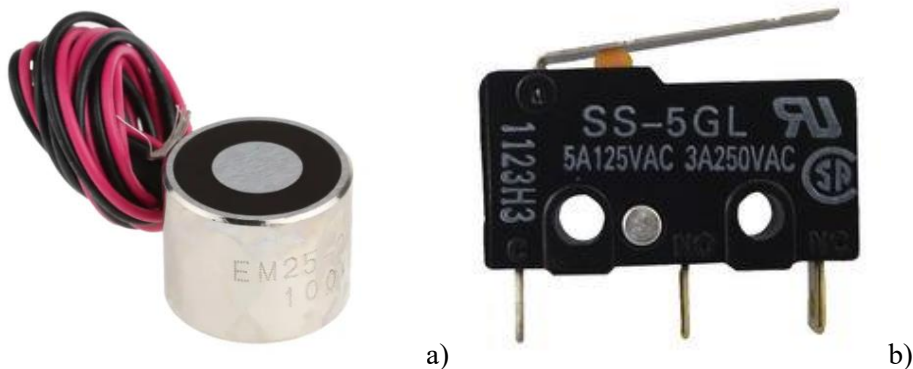


Figure 3.26 DIANA's sampling system: particular of (a) electromagnet, (b) endstop

After the electromagnet has dropped the mallet, it is dropped down too, inverting the rotation of the servomotors. The magnetic anchorage is more effective if the contact between the electromagnet and the metallic cylinder is perfectly in the middle of the cylinder's upper surface. This also allows the system to work in conditions of non-perfect verticality. For this reason, it was necessary to design a centering device, positioned inside the percussion system guide.

The complete percussion system is shown in Figure 3.27.



*Figure 3.27 DIANA's sampler: detail of the percussion system*

The various connections and supports are made with aluminium curved and laser-cut plates. One of the most interesting is the connection between the percussion system and sampler, represented in Figure 3.28. This element allows to easily remove only the sampler from the sampling system, to extract the holder with the sampled material at the end of operations and replace it with an empty one. At the same time, this component transmits the impulsive forces provided by the percussion system directly to the sampler without damaging the internal holder made of fragile Polycarbonate.



*Figure 3.28 DIANA sampler: detail of the aluminium connection between sampler and percussion system*

### 3.2.4 Control system

The sampling system is electronically controlled. The test activity was performed by integrating the hardware electric components with a code, specifically developed for the purpose, on Arduino Integrated Development Environment (IDE). Arduino is an open-source electronic prototyping platform. The developed sampling code can be analysed in Annex 1 and allows to automatically perform sampling operations setting the number of blows. Further integrations will allow to automatically interrupt the sampling procedure if the maximum penetration distance is reached or if the sampling time limit has expired (ERC limitations).

The electronic control can be observed in Figure 3.29, it is composed by:

- ELEGOO UNO R3: microcontroller compatible with Arduino IDE, connects to the computer with a standard USB cable and the various electronic parts through jumpers and cables;
- L298: two equal boards containing two H-Bridges each. One boards dedicate the two H-Bridges drivers to interface the two servomotors, dedicated to the percussion system, with the microcontroller. This is necessary because the tension provided by the microcontroller is 5V and is not sufficient for the alimentation of each servomotor. Each H-bridge is composed of 4 transistors used to move a motor with a certain velocity and change the direction of rotation (clockwise or counter-clockwise). Regarding the other board, only one H-Bridge of the two available is used to turn on and off the electromagnet providing the necessary alimentation equal to 19V.
- DC-DC step-down, that allows lowering the input tension from 19V to 5V needed for the H-bridges power supply;
- Matrix board: base where the input/output, alimentation, and ground lines are soldered via jumpers.

The connection to the rover's system will be made with an ethernet shield, an expansion board with a dedicated IP address to control the microcontroller of the sampling system.

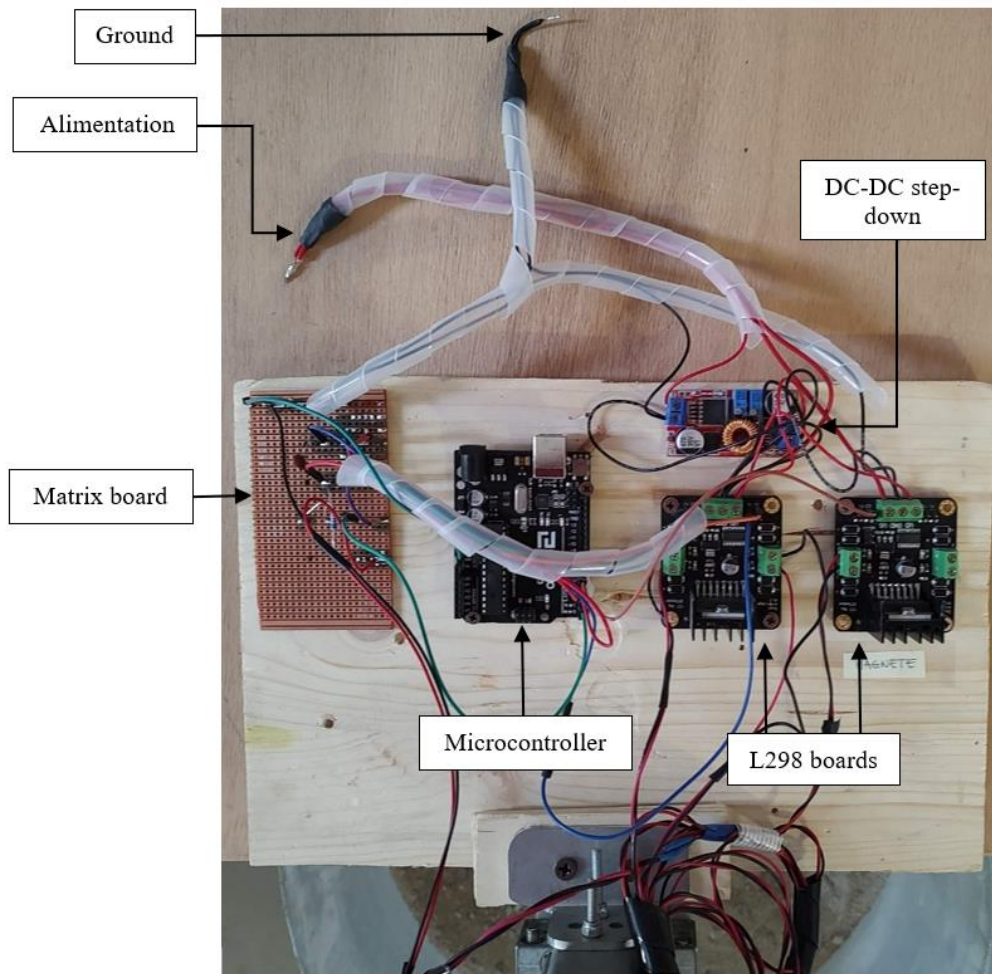


Figure 3.29 DIANA's sampler: electronic control (test configuration board)

## 4 Chapter 4: laboratory tests

The tests on the soil sampler prototype were performed at MastrLAB of Department of Structural, Building and Geotechnical Engineering (DISEG) of Polytechnic of Turin. The main purposes of the sampling test campaign were the following:

- verify the robustness of the system;
- collect penetration information such as number of blows and distance reached;
- check the quality of soil recovered.

In addition, some specific preliminary tests were performed on two parts of the sampler subsystem of the soil sampler prototype: the holder and the catcher. Two main parameters were considered: the quantity of soil entered in the holder (L) and the quantity recovered when extracting the holder having equipped a catcher (R). In this chapter it was referred to this parameters only through the effective measure of length performed, the length of soil entered in the holder without and with the catcher equipped, and the length of the soil recovered inside the holder having equipped the catcher. The preliminary test campaign is described in two specific paragraph as divided in two main test activity: “holders test” and “catchers tests”, both performed on loose soils. In general this two test campaigns were performed inserting the holder by percussion in different types of soil. From the results of this tests, the behaviour of samplers was analysed in terms of soil entered in the holder changing its diameter, soil and with or without the presence of a catcher equipped inside the holder. Finally it was studied the variation of the length of soil recovered having equipped different types of catchers with different stiffnesses of the fingers.

After this preliminary test campaign, the soil sampler prototype was tested on loose and compacted soils, evaluating the number of blows necessary for the total descent of the sampler (whole length available) and the quantity of soil recovered.

All the tests mentioned were performed in a test bench specifically design and built, in order to not compromise the sampling operations.

Soils involved in tests, and in particular the simulant of Mars regolith anticipated in Chapter 2, are described in a dedicated paragraph 4.2, as well as the procedure adopted to prepare the soils at loose and compacted condition.

Finally, the last paragraph is dedicated to the definition of the new parameters for the improved version of the prototype.

### 4.1 Test bench

It was necessary to test the soil sampler prototype using an appropriate test bench. A special attention was paid to the container dimensions and considering a schematization of the sampler as a cylinder with diameter 50 mm and maximum penetration length 300 mm, the container that will be filled with the soil to be sampled must have diameter and overall height big enough to avoid creating interferences during sampling operations. The possible disturbances that could be encountered are boundary effects and consist of a resistance to soil penetration generated by the soil-tool interaction (Xi et al., 2019). These considerations lead to identify as optimal test container a cylindrical bin with both diameter and height at least equal to 400 mm. The container used is realised in transparent Poly Methyl Methacrylate (PMMA) with a height of 600 mm and a wooden base with diameter 400 mm, as can be observed in Figure 4.1. The choice of transparent material was made to permit external check and measurements of the filling soil.

Even if the soil sampler prototype was developed to sample also from a tilted position, this first test campaign will be performed with the full system positioned vertically from the soil surface. This with the purpose of simulate the condition of sampling on a plain Mars surface. Considering that the rover can explore also inclined surfaces, future tests in different conditions, not treated in this thesis, will be performed. These tests will allow to understand the maximum inclination that the soil sampler prototype can tolerate in terms of efficiency and workability.

The attachment to ARDITO's chassis is simulated anchoring the sampler to one side of a stable wooden table with height higher than 600 mm.



Figure 4.1 Container for tests: a) lateral view, b) upper view with dimensions reference

## 4.2 Soils employed

A picture of the soils supplied for test activity can be observed in Figure 4.2. Gravel, sand and silt provided came from the crushing of cave soil commercially called “tout venant”, in unwashed conditions. It was necessary to perform some preliminary operation to adapt the soil for tests application. Repeating the procedure with 10 kg of soil per time, the wet soil was dried for 24 hours in an electric oven, at a constant temperature of 104 °C. Then a mechanical screening was performed in order to reach the desired granulometric range, following the UNI EN ISO classification (UNI EN ISO 14688-2:2018) recalled in Figure 4.3.



Figure 4.2 Starting soils for sampling test

Soil fractions	Sub-fractions	Symbols	Particle sizes mm
Very coarse soil	Large boulder	LBo	>630
	Boulder	Bo	>200 to 630
	Cobble	Co	>63 to 200
Coarse soil	Gravel	Gr	>2.0 to 63
	Coarse gravel	CGr	>20 to 63
	Medium gravel	MGr	>6.3 to 20
	Fine gravel	FGr	>2.0 to 6.3
	Sand	Sa	>0.063 to 2.0
	Coarse sand	CSa	>0.63 to 2.0
	Medium sand	Msa	>0.2 to 0.63
	Fine sand	Fsa	>0.063 to 0.2
Fine soil	Silt	Si	>0.02 to 0.063
	Coarse silt	CSi	>0.02 to 0.063
	Medium silt	MSi	>0.063 to 0.02
	Fine silt	Fsi	>0.002 to 0.0063
	Clay	Cl	$\leq 0.002$

Figure 4.3 Soil classification modified from UNI EN ISO 14688-2

The resultant soil, with unit weight provided by the supplier, is:

- gravel: particles granulometric range  $2 \div 20$  mm, dry unit weight  $\gamma_d$  equal to  $1500 \text{ kg/m}^3$ ;
- sand: particles granulometric range  $0.06 \div 2$  mm, dry unit weight  $\gamma_d$  equal to  $1600 \text{ kg/m}^3$ ;
- silt: particles granulometric range  $0.002 \div 0.06$  mm, dry unit weight  $\gamma_d$  equal to  $1700 \text{ kg/m}^3$ .

This soils were employed to build the reference soils for test activity. The available volume for the test container with diameter 400 mm and filled for a height of 400 mm is  $V_{container} = \pi \cdot r^2 \cdot h = \pi \cdot 0.2^2 \cdot 0.4 = 0.05 \text{ m}^3$ . Considering the dry unit volume of soil available ( $\gamma_d$ ), is possible to calculate the total amount of soil ( $W_s$ ) to be employed to fill the test container for the desired height of 400 mm:  $W_s = \gamma_{d,soil} \cdot V_{container}$ . Four different conditions are obtained:

- **uniform sand:** granulometric range  $0.06 \div 2$  mm, resultant  $W_s = 80.0 \text{ kg}$ . The uniform sand poured in the test container can be observed in Figure 4.4;
- **uniform gravel:** granulometric range  $2 \div 20$  mm, resultant  $W_s = 75.0 \text{ kg}$ . The soil can be observed in Figure 4.5;
- **Mars regolith simulant:** it was created by means of the curve of grain size distribution described in Figure 4.6. The percentual fractions considered are 16% for gravel, 74% for sand and 10% for the clay/silt component (Pizzamiglio et al., 2018). For each granulometric fraction is possible to evaluate the quantities to be employed to fill the test container for the desired height of 400 mm:  $W_{s,gravel} = 12.0 \text{ kg}$ ;  $W_{s,sand} = 59.2 \text{ kg}$ ;  $W_{s,silt} = 8.5 \text{ kg}$ , for a total amount  $W_s = 79.7 \text{ kg}$ . The simulant was obtained manually mixing the defined quantities in parts of 1/3 per time, the mixing procedure can be observed in Figure 4.7 left while the resultant soil in Figure 4.7 right;
- **50% sand - 50% gravel:** homogeneous mixture obtained mixing in equal parts uniform sand and uniform gravel. The following quantities are necessary to fill the test container for the desired height:  $W_{s,gravel} = 37.5 \text{ kg}$  and  $W_{s,sand} = 40.0 \text{ kg}$ . For a total amount  $W_s = 77.5 \text{ kg}$ . Again a manual mix procedure was adopted and the resultant soil is shown in Figure 4.8.



*Figure 4.4 Test soil: uniform sand*



*Figure 4.5 Test soil: uniform gravel*

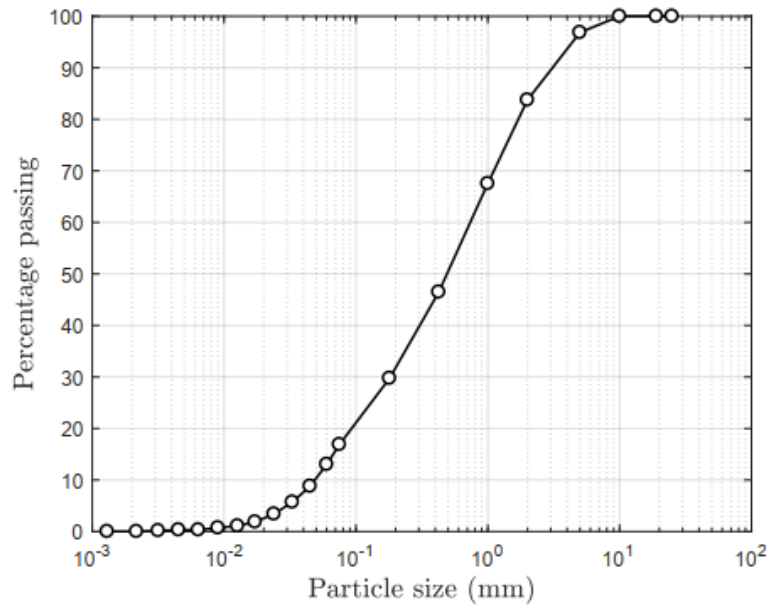


Figure 4.6 Mars soil simulant: reference grain size distribution from ALTEC S.p.A.

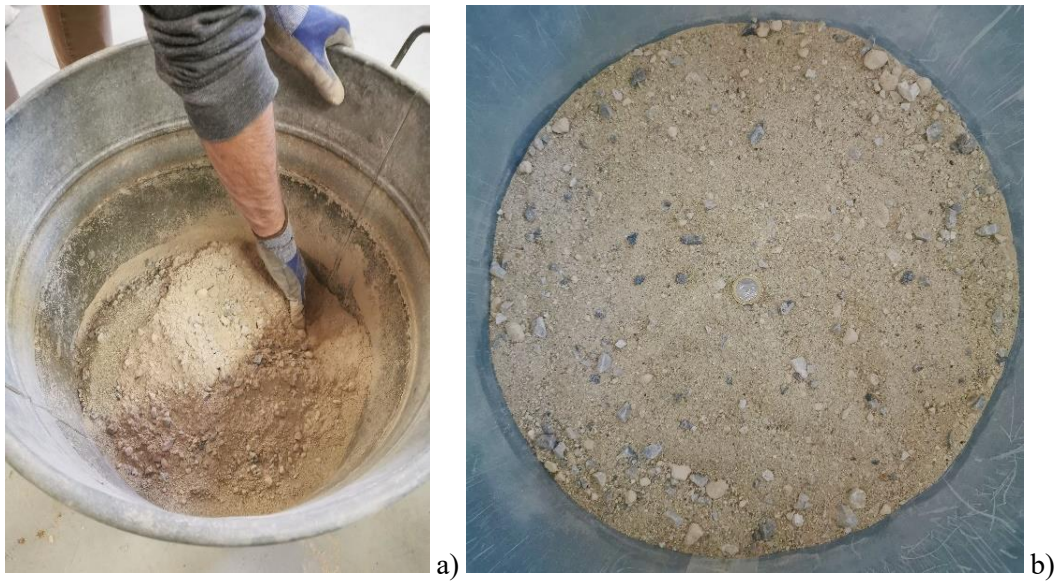


Figure 4.7 DIANA's simulant of Mars regolith: a) mixing procedure, b) resultant soil



Figure 4.8 Test soil: 50% sand - 50% gravel

### 4.3 Preparation technique

All the tests were performed by using the soils and the mixtures described in the previous paragraph under loose and dense conditions. A standard procedure is defined in this paragraph to obtain the loose and the compacted condition and will be followed for all the tests performed.

#### 4.3.1 Loose soil

This condition is obtained slowly pouring the soils in the test container, with the aim of reaching the maximum void ratio possible.

The procedure followed for the determination of the void ratio obtained is:

- 1) definition of the mass of soil  $W_s$ , necessary to fill the test container (fixed dimensions of diameter 400 mm and height 400 mm). These quantities have already been calculated in paragraph 4.2 for the four soils involved in tests;
- 2) definition of the specific gravity (or specific weight) of the soil  $G_s$ : the ratio between the unit weight of the solid part ( $\rho_s$ ) and the unit weight of water ( $\rho_w$ ):

$$G_s = g \cdot \frac{\rho_s}{g} \cdot \rho_w = \frac{\rho_s}{\rho_w} \quad (4.1)$$

For practical purposes  $\rho_w$  can be considered as  $1000 \text{ kg/m}^3$  while  $\rho_s$  depends on the type of soil. The specific weight of the grains depends on the mineralogic composition of the soil, in a range between 2.4 and 3.2. Some average values of specific weight for some types of soil are provided in the following table (Table 4.1).

Table 4.1 Specific gravity  $G_s$  for different types of soil particles

Type of soil	Specific gravity $G_s$ [-]
Kaolinite	2.4
Quartz	2.65
Limestone	2.72
Dolomite	2.8-2.95
Mica	2.7-3.2

The specific gravity for silts, sands and gravels employed in this test campaign is the same, because all soils came from the same cave. Giuggia Costruzioni S.r.l. provided this value equal to 2.6;

- 3) evaluation of the volume of grains  $V_s = \frac{W_s}{G_s \cdot \gamma_w}$ ;
- 4) evaluation of the total volume  $V_{tot} = r^2 \cdot \pi \cdot h$ , considering the dimensions r (radius), h (height) of the cylinder;
- 5) evaluation of void volume  $V_v = V_{tot} - V_s$ ;
- 6) evaluation of void ratio  $e = \frac{V_v}{V_s}$ .

The resulting theoretical void ratios, calculated considering the quantities obtained at the beginning of the paragraph, are listed in the following table (Table 4.2).

Table 4.2 Theoretical void ratio for each test soil

Test soil	Total height, h [mm]	Total weight, W <sub>s</sub> [kg]	Void ratio, e [-]
Uniform sand	400	80.0	0.63
Uniform gravel	400	75.0	0.74
Mars regolith simulant	400	79.7	0.64
50% sand - 50% gravel	400	77.5	0.69

Slowly pouring the soils inside the container, the amount necessary to fill it for a height of 400 mm was different depending on the soil type. The resulting void ratios are listed in Table 4.3.

Table 4.3 Experimental void ratio for each test soil at loose condition

Test soil at loose condition	Total height, h [mm]	Total weight, W <sub>s</sub> [kg]	Void ratio, e [-]
Uniform sand	400	78.0	0.68
Uniform gravel	400	74.0	0.77
Mars regolith simulant	400	77.0	0.70
50% sand - 50% gravel	400	75.0	0.74

The different values of void ratio described in Table 4.2 and Table 4.3 are probably due to an overestimation of the specific gravity G<sub>s</sub> provided by the soil supplier.

### 4.3.2 Compacted soil

The soil sampler prototype was tested also on compacted soil. The purpose of this paragraph is to individuate a compaction procedure suitable for the test container built. Having defined the procedure, the maximum level of compactness that could be reached with this procedure was individuated for each soil to be tested. Finally, the resulting void ratio and the compaction energy involved were calculated. The procedure for obtaining the final void ratio is defined in paragraph 4.3.2, while the total compaction energy per unit volume can be obtained from the following equation (Al-Khafaji, 2016):

$$E = \frac{W_{hammer} \cdot h \cdot n_b \cdot n_l}{V_{sample}} \quad (4.2)$$

where:

- $W_{hammer}$  is the total weight of the hammer;
- $h$  is the dropping height of the hammer;
- $n_b$  is the number of blows for each layer;
- $n_l$  is the total number of layers compacted;
- $V_{sample}$  is the overall volume of the sample compacted.

For the determination of the compaction parameters and procedure, it should be evidenced that this process must allow to obtain a uniformly compacted soil, at least in the central part of the test container where sampling

tests are performed. Some suggestions are provided by the Proctor Compaction Test (UNI EN 13286-2). In particular, the fundamentals of compaction were introduced by R. R. Proctor in 1933 in order to investigate the dependency of soil density on the moisture content. The water content is a key parameter of the Proctor test, but no water is considered in this test campaign, for this reason only the indications related to the compaction process are evaluated. Compaction in Proctor Compaction Test is performed in pre-weighed layers (three or five layers) and, in the manual soil compaction, the hammer is lifted to the maximum defined height and allowed to fall freely over the soil specimen, for the required number of blows.

For this test campaign a cylindrical hammer made of cast iron was produced (Figure 4.9). It was designed in order to have a diameter similar to the one of the test container and the weight has been estimated in a way that could efficiently compact a layer made with 20.0 kg of soil. The design process led to the following characteristics: 350 mm diameter, 260 mm thickness, total weight of the hammer  $W_{hammer} = 19.6 \text{ kg}$ .



Figure 4.9 Compaction hammer overall weight

The operations of soil compaction were conducted adopting a dropping height of the hammer ( $h$ ) equal to 200 mm. This value was defined according to space limitations: the total height of the test container is 600 mm and when it is filled with the test soil for a height about 400 mm, only 200 mm remains as guide for the mallet descent. The measurement of the compaction attained  $\Delta h$  (difference between initial and final height) was always made after a sequence of five blows. The path followed by the blows was defined in order to obtain a level of compaction as homogeneous as possible. First four circumferential blows were performed and the fifth final blow was done in the center of the container, as illustrated in Figure 4.10. A picture from the performing of compaction procedure is shown in Figure 4.11. This procedure of performing five blows and measuring the compaction was repeated until the value of final height did not showed significant variations for three consecutive sequences. In this way, the total number of blows for each layer  $n_{b/l}$  was directly established and an asymptotic trend can be observed plotting the void ratio ( $e$ ) versus the number of blows performed (Figure 4.12). The compaction parameters for the defined procedure are resumed in Table 4.4. The weight of the mallet, the initial height and the number of layers are parameters fixed a priori. Also the volume of the sample can be obtained measuring the height of soil obtained slowly pouring the four layers made with 20.0 kg each into the container before performing the compaction operation. The number of blows results the only parameter that could be incremented in order to obtain the maximum compaction reachable with the above defined procedure. When the asymptotic trend is reached and no further variations can be obtained with the incrementation of the number of blows, the maximum level of compaction that could be obtained with the defined procedure is reached.



Figure 4.10 Soil compaction sequence



Figure 4.11 Soil compaction procedure on test bench

Table 4.4 Compaction parameters for the defined procedure

Compaction parameter	Value
$W_{\text{hammer}}$ [kg]	19.6
$H$ [mm]	200
$n_{\frac{b}{t}}$ [-]	Different for each soil
$n_i$ [-]	4
$V_{\text{sample}}$ [mm <sup>3</sup> ]	Different for each soil

Having defined the compaction procedure for the four different soils created, the resultant void ratios computed for one layer made with 20.0 kg of each soil are resumed in Table 4.5. During the test campaign on the soil sampler prototype performed with compacted soil, the compaction procedure was executed compacting four layers made with 20.0 kg of material, not only one. The overall compaction energy employed for the compaction of four layers made with 20.0 kg of soil is resumed in Table 4.6.

Table 4.5 Experimental void ratio for one layer with 20 kg of soil at compacted condition

Test soil	Initial height, $h_0$ [mm]	Initial void ratio, $v_0$ [-]	Final height, $h_f$ [mm]	Final void ratio, $e_f$ [-]
Uniform sand	110	0.80	85	0.39
Uniform gravel	115	0.88	100	0.63
Mars regolith simulant	95	0.55	80	0.31
50% sand - 50% gravel	105	0.72	88	0.44

Table 4.6 Compaction energy for four layers made with 20.0 kg of soil

Test soil	Hammer weight, $W_{hammer}$ [kN]	Dropping height, $h$ [m]	Number of blows per layer, $n_b$ [-]	Number of layers, $n$ [-]	Volume of sample $V_{sample}$ [m <sup>3</sup> ]	Compaction energy [ $\frac{kJ}{m^3}$ ]
Uniform sand	0.0196	0.20	30	4	0.055	8.5
Uniform gravel	0.0196	0.20	15	4	0.058	4.1
Mars regolith simulant	0.0196	0.20	15	4	0.048	4.9
50% sand - 50% gravel	0.0196	0.20	20	4	0.053	5.9

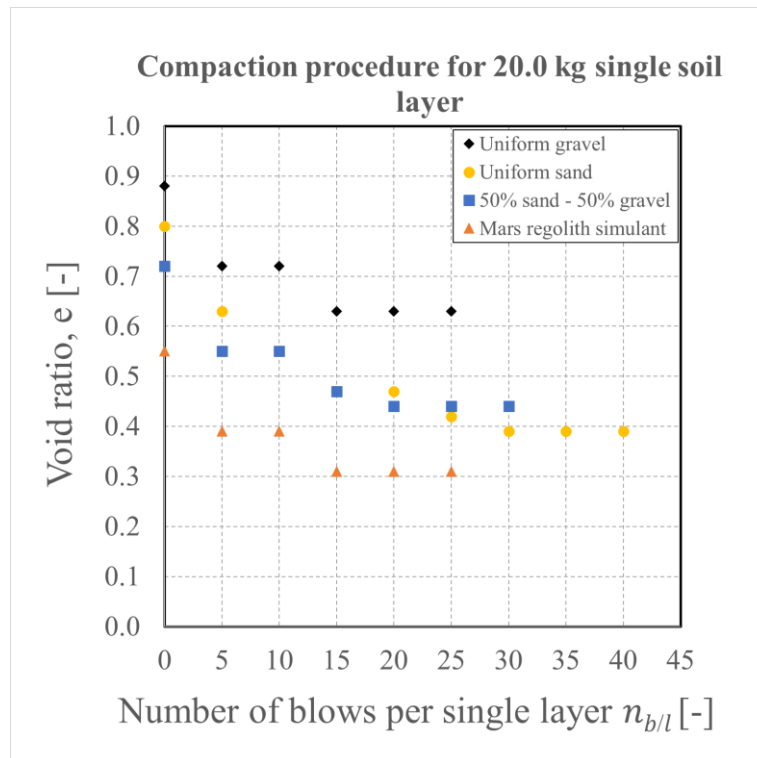


Figure 4.12 Trend of compaction for one layer of 20 kg of soil

#### 4.4 Holder tests on loose soils

An important aspect to be considered when a tube is inserted into the soil through a percussive system, is that the length of soil entering inside the tube ( $L$ ) during the descent may not be exactly the same as the length of penetration in the soil ( $H$ ), as illustrated in Figure 4.13. This concept was anticipated in Chapter 3, by introducing the Recovery Ratio parameter (equation 3.4) aimed to describe this type of sampling disturbance. Indeed, what is experimentally observed is that reducing the internal diameter of the tube ( $D_{int}$ ), the overall quantity of soil entered during soil penetration reduces significantly.

For this reason, a test campaign was carried out to investigate the different lengths of soil entered into the holder, by varying the type of tested soil and the holder diameter. At this preliminary stage all the soils were

tested at loose condition. A manual percussion using a hand hammer was performed and the height of penetration of the holder (H) was measured during the soil penetration until a value equal to was 200 mm reached.. The experiments were realised using six holders having different diameters, (Figure 4.14), and their main characteristics are summarised in Table 4.6. It is highlighted that different materials, and so different stiffness do not influence the outcome of this preliminary test because these parameters only affects the required percussion energy. Results could be affected by the different levels of internal wall friction of the holders, but in this research the effect is minimized by choosing holders having a good internal smoothness. For this reason the influence of the wall friction was neglected at this preliminary stage.

Table 4.7 Main characteristics of the holders tested

Internal diameter, $D_{int}$ [mm]	Material [-]	Length, $L_{tot}$ [mm]	Thickness, $t$ [mm]
26	Polyvinyl chloride (PVC)	293	3
40	Polycarbonate (PC)	310	2
48	Polyvinyl chloride (PVC)	500	2
60	Polylactic acid (PLA)	220	2
72	AISI 304 steel	480	2
85	Polycarbonate (PC)	315	2

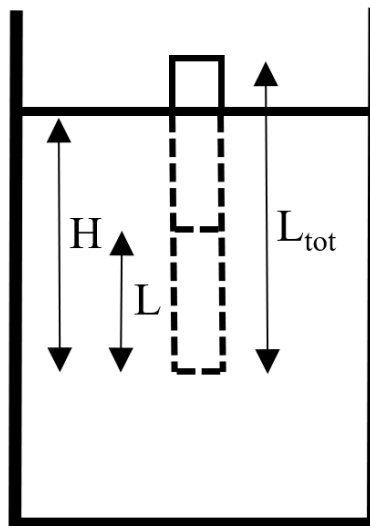


Figure 4.13 Length of soil entered in the holder  $L$  and height of penetration  $H$

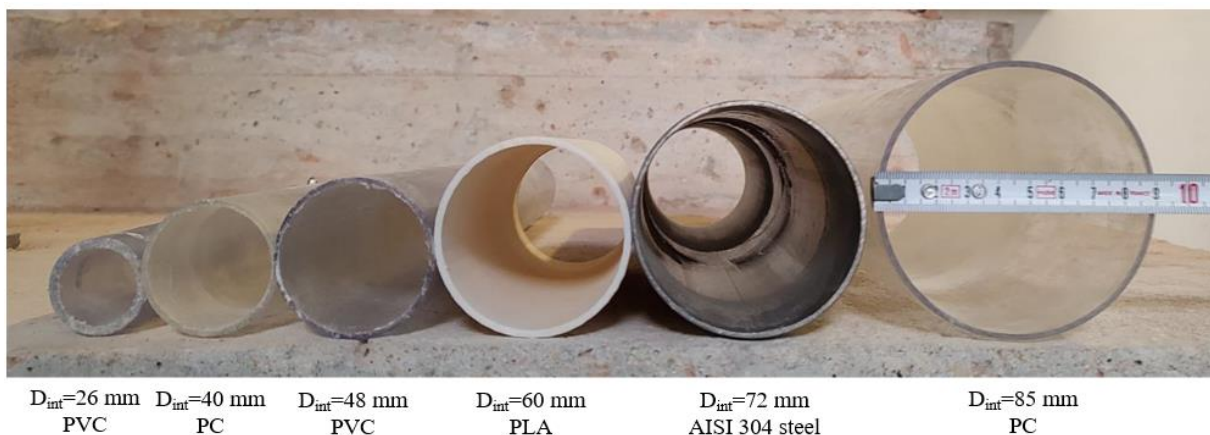


Figure 4.14 Holders involved in the test campaign

The experimental results are summarised in Figure 4.15. While the Recovery Ratios associated at each test is given in Table 4.7. Results showed a great variation, both changing the holder diameter having fixed the soil tested, both changing the soil having fixed the holder diameter. The length of entrance  $L$  is never equal to the length of penetration  $H$ , and it is greatly reduced with smaller diameters of the holders, regardless the type of the tested soil. At the same time, an increase of the grain size of the soil led to a reduction of the length of entrance  $L$ . The best results were obtained with uniform sand, for which an internal diameter of 85 mm allowed the entrance of almost the whole length of penetration (Recovery Ratio equal to 98.5%). On the opposite side, an increasing of the fraction gravel in the soil mixture, lead to a reduction of the entrance length. The uniform gravel when using a holder diameter equal to 85 allowed to obtain the maximum Recovery Ratio similar to that would probably be obtained with the uniform sand and a holder diameter equal to 35 mm. With the smaller internal diameter tested, equal to 26 mm, the Recovery Ratio ( $R$ ) varies from a value of 83% with the uniform sand to a value of 32.5% with the uniform gravel. Remembering that, according to literature, a good sample should be characterised by a value of Recovery Ratio at least equal to 96%, tests performed with uniform gravel showed critical results but the occurrence of sampling uniform gravels could be considered remote and so it represents an extreme condition. The highest value reached was 87.5 % with an internal diameter equal to 85 mm.. At the same time, the optimization of the Recovery Ratio is not possible because of space and weight restrictions imposed by ARDITO's dimensions and ERC requirements. For this reasons it is not possible to equip and adapt the design of the soil sampler prototype to a holder with diameter equal to 85 mm. Weight simulations performed considering the different materials involved in the full sampling system, get 50 mm as the maximum external diameter that could be equipped for the sampler, with consequently less than 46 mm for the holder to placed inside. Considering the expected soil conditions, the curve related to the Mars regolith simulant (Figure 4.6) is the reference and this type of mixture is mainly made by sand (74%). The holder with internal diameter equal to 40 mm allow to obtain a Recovery Ratio equal to 81.5% with the Mars Regolith simulant, 90.5 % with uniform sand and to 57.0% in the limit condition of uniform gravel. For this reason the holder already employed in the design phase, with diameter equal to 40 mm, is adopted in this test campaign. Future design updates may consider a diameter equal to 46 mm, changing the design of the sampler system of the soil sampler prototype.

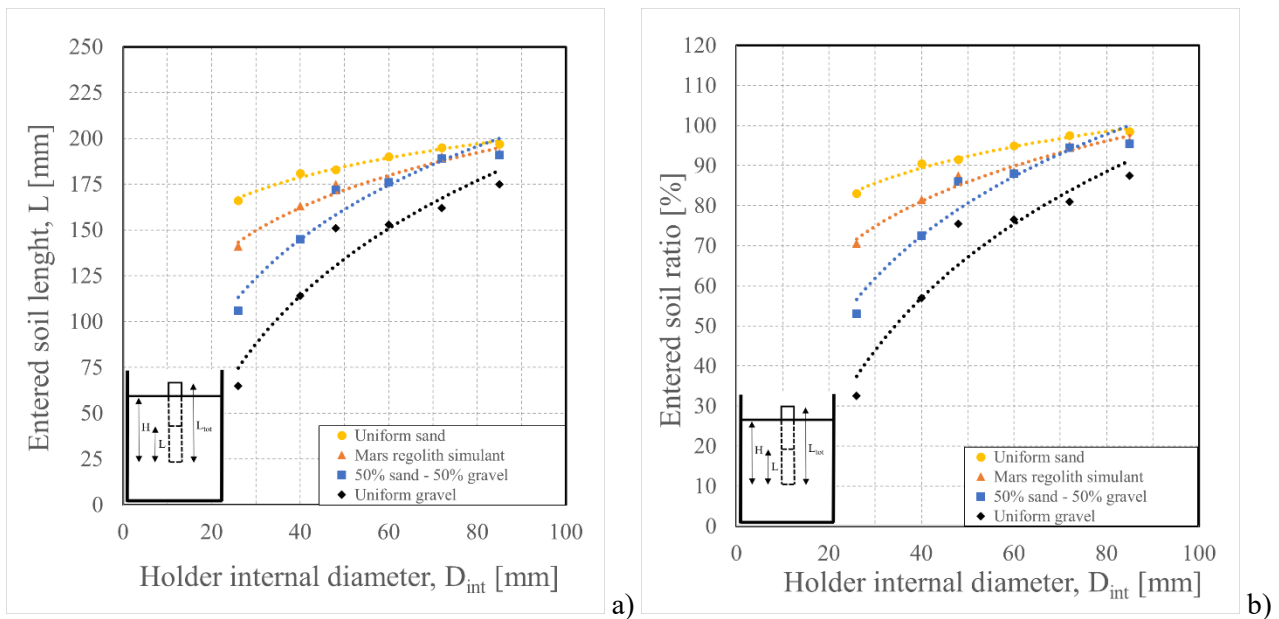


Figure 4.15 Variation of soil entrance length (a) and ratio (b) in the holder, changing the type of soil and diameter of the holder

Table 4.8 Recovery Ratio computed for the test campaign on different soils with holders characterised by different internal diameters

$D_{int}$ [mm]	Uniform sand [%]	Mars regolith [%]	50% sand - 50% gravel [%]	Uniform gravel [%]
26	83.0	70.5	53.0	32.5
40	90.5	81.5	72.5	57.0
48	91.5	87.5	86.0	75.5

60	95.0	88.5	88.0	76.5
72	97.5	95.0	94.5	81.0
85	98.5	96.0	95.5	87.5

Analysing the experimental results, it is possible to make some preliminary considerations about the possible reasons that led to a similar reduction of soil entrance with the decrease of the diameter and the increase of the grain size. Two main possible effects can be considered. The first one, a sort of “**pile effect**”, describes a situation in which the material does not even enter in the holder during the descent. The penetration of the holder within the soil is possible due to lateral compaction of the soil, as for percussion driven piles applied for deep foundations. Indeed, if the grain size is comparable with the internal diameter, grains can rearrange their position due to percussion solicitation and possibly block the entrance. A qualitative representation with small and big grains if compared to the holder internal diameter is given in Figure 4.16. The case of “big grains” can be described by the condition of the internal holder diameter equal to 26 mm and uniform gravel with biggest grain size equal to 20 mm. This effect can explain the resultant Recovery Ratio equal to 32.5%: a very limited amount of material entered due to interlocking of big grains that, with the percussive solicitation, changed their position blocking the entrance into the holder. A second effect is a type of “**arch effect**”. In tunnelling this effect allows a redistribution of the stresses and increases the soil self-sustain in terms of free-span ( $L_{max}$ ) and time during tunnel excavation advancement. In this case the “arch effect” is encountered when the soil already entered into the holder and the rearrangement of particles during entrance movements builds an antagonist arch. The stress redistribution between the soil particles along the antagonist arch could contrasts the entrance of soil and also the advancement along the holder of the soil already entered (Figure 4.17). Both this effects reduce with the holder diameter increase. Regarding the “pile effect” this occurs because a higher holder diameter leads to the condition of small grains also for the coarser soils (i.e. gravels), while for the “arch effect” higher holder diameters do not allow the development of the antagonist arch. Finally, it should be highlighted that also the ratio between external diameter and internal diameter of the holder can influence the length of material entered in the holder. In this case, similar thicknesses of the different holders tested were adopted, so this influence was the same in this campaign test. A proper campaign test, not object of this thesis, will be performed having fixed the internal diameter of the holder but changing the thickness and so the external diameter.

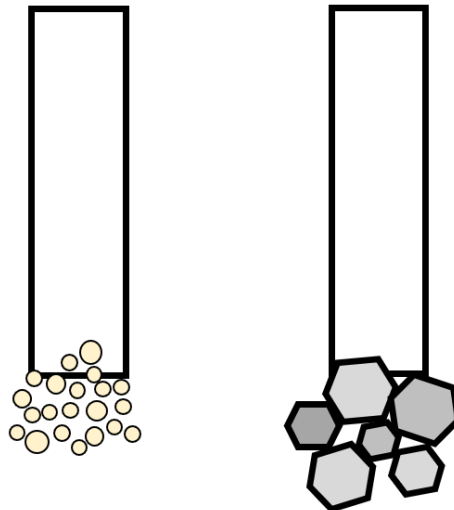


Figure 4.16 “Pile effect” during sampling operations

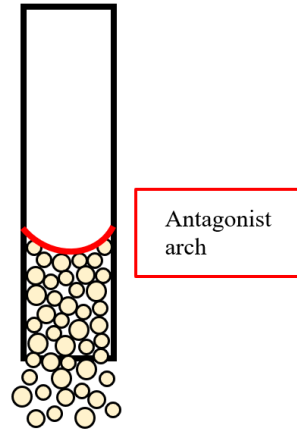


Figure 4.17 “Arch effect” during sampling operations

## 4.5 Catcher tests on loose soils

Catcher tests on loose soils were performed by choosing a holder diameter equal to 40 mm on the basis on the results obtained from the previous experimental campaign (Cap. 4.4). The holder was so tested by equipping different types of catchers in order to measure the soil sampled (L) and recovered length (R), so evaluating the Recovery Ratio associated to different fingers’ stiffness. Fingers stiffness influence the capability of the fingers to open during soil advancement in the holder. If the stiffness is too high the fingers stay closed and create contrast to soil advancement into the holder. The stiffness of the fingers can also be determinant at the end of sampling operations, in the retaining phase of the soil sampled. The aim of this test campaign is defining if fingers with low stiffness can allow higher entrance of soil but offer lower resistance to soil loss during sampler extraction.

Tests are performed with length of penetration of the holder (H) fixed equal to 200 mm and performing a manual percussion with a hand hammer. Four different catchers were built and tested:

- “**PLA 1 mm**” catcher made of 3D printed Polylactic Acid with thickness of the fingers equal to 1.0 mm (Figure 4.18);
- “**PLA 0.5 mm**” catcher made of 3D printed Polylactic Acid with thickness of the fingers equal to 0.5 mm (Figure 4.19);
- “**Harmonic steel**” catcher made of folded harmonic steel class C67 with thickness of the fingers equal to 0.4 mm (Figure 4.20);
- “**PMMA**” catcher made of thermally curved Poly(methyl methacrylate) with thickness of the fingers equal to 0.5 mm (Figure 4.21).

In particular the stiffness of each finger was evaluated through the simplifications made in paragraph 3.2.2, where the single finger is schematized as a cantilever beam with constant rectangular section. The stiffness is computed as the ratio between the force applied and the deflection exhibited by the element. If the deflection is small and the material does not yield, a linear relationship is available for a cantilever beam correlating the force (F) to the deflection (d):

$$F = \left[ \frac{3 \cdot E \cdot I}{L^3} \right] \cdot d \quad (4.3)$$

where:

- E is the elastic modulus of the material;
- I is the area moment of inertia of the beam cross section;
- L is the length of the beam.

For a beam with rectangular section, the area moment of inertia can be computed as:

$$I = \frac{1}{12} \cdot w \cdot t^3 \quad (4.4)$$

where:

- $w$  is the width of the beam;
- $t$  is the thickness of the beam.

Including equation 4.4 in 4.3, the resultant force generated by a given deflection results:

$$F = \left[ \frac{E \cdot w \cdot t^3}{4 \cdot L^3} \right] \cdot d \quad (4.5)$$

The stiffness of the beam is given by the terms in brackets. Figure 4.22 shows a detail of the four single fingers produced, while Table 4.8 resumes the parameters and the computation of the stiffness of each finger. Different thickness were tested (0.5 mm and 1.0 mm), especially for the PLA catchers. These two catchers were produced with two different thicknesses and width because the first attempts of equipping fingers made in PLA with 1.0 mm thickness and width equal to 8.0 mm led to a condition of too high stiffness and fragility, so a reduced width equal to 5.0 mm was considered in this test campaign. The connection between each single finger and holder is made with stainless steel screws and interlocking nuts. The configuration of the fingers is a parameter that can highly influence tests. At this preliminary stage a configuration where all the fingers have same length is chosen. The main characteristics of each catcher developed are listed in Table 4.9.

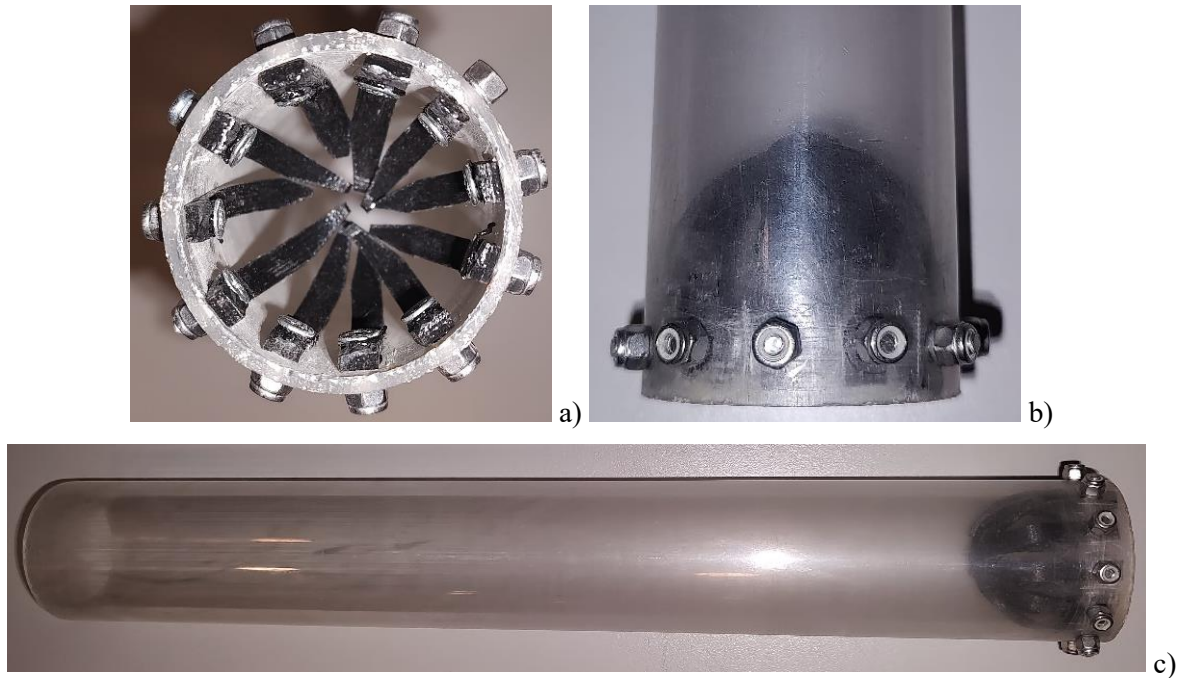


Figure 4.18 “PLA 1 mm” catcher equipped on the holder: a) bottom view, b) lateral view, c) top view

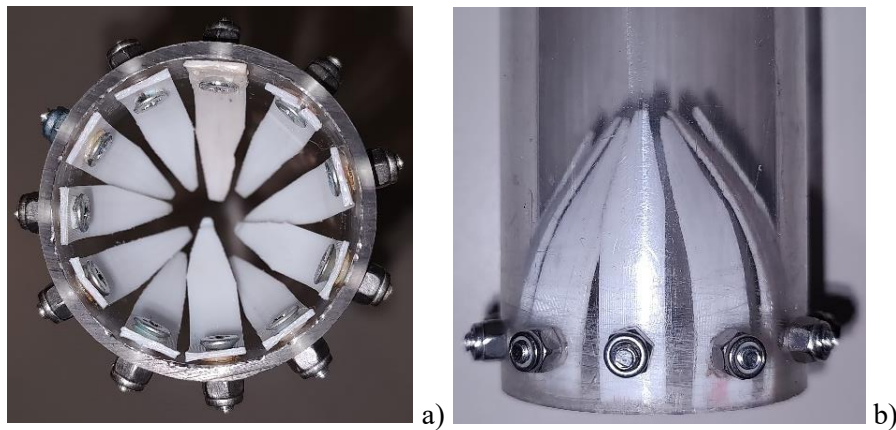




Figure 4.19 "PLA 0.5 mm" catcher equipped on the holder: a) bottom view, b) lateral view, c) top view

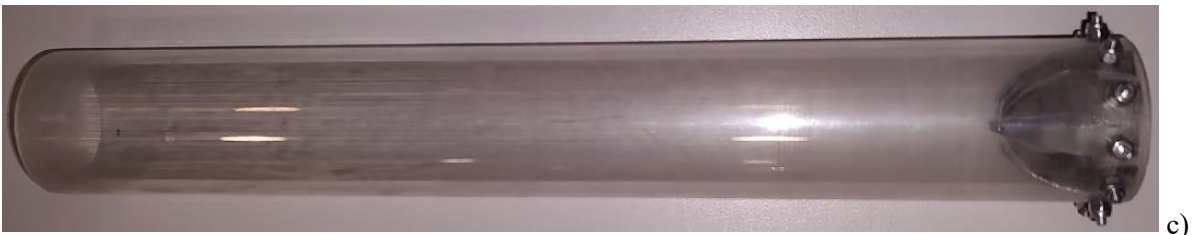


Figure 4.20 "Harmonic steel" catcher equipped on the holder: a) bottom view, b) lateral view, c) top view



Figure 4.21 "PMMA" catcher equipped on the holder: a) bottom view, b) lateral view, c) top view

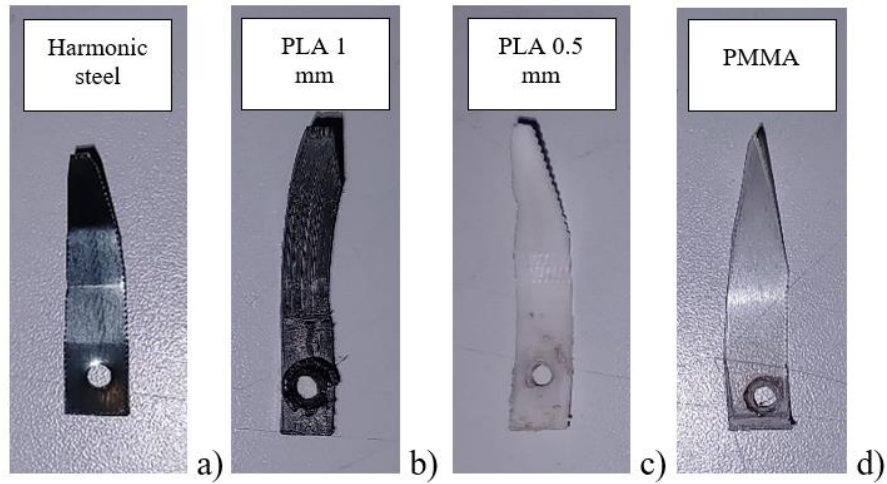


Figure 4.22 Fingers made in different materials: a) harmonic steel, b) PLA 1 mm, c) PLA 0.5 mm, d) PMMA

Table 4.9 Stiffness evaluation for different fingers

Material	Elastic modulus, E [N/mm <sup>2</sup> ]	Width, w [mm]	Thickness, t [mm]	Length, L [mm]	Stiffness [N/mm]
Harmonic steel C67	205000	8.0	0.4	50.0	0.2099
Polylactic Acid	3500	5.0	1.0	50.0	0.0350
Polylactic Acid	3500	8.0	0.5	55.0	0.0053
Poly(methyl methacrylate)	2800	8.0	0.4	50.0	0.0029

Table 4.10 Catchers main characteristics

Name	Material	Number of fingers, N [-]	Stiffness of the fingers [N/mm]
Harmonic steel	Harmonic steel C67	11	0.2099
PLA 1 mm	Polylactic Acid	11	0.0350
PLA 0.5 mm	Polylactic Acid	11	0.0053
PMMA	Poly(methyl methacrylate)	11	0.0029

The results obtained from the different tests performed are shown in the following figures, in terms of lengths of material entered in the holder (L) and recovered after having extracted the holder from the test bench (R). Figure 4.23 shows a comparison plot with results of tests on loose soil entrance without any catcher equipped and with the different types of catchers equipped. Figure 4.24 is related to a comparison between the soil recovery obtained with the different types of catchers equipped. All the Recovery Ratios are computed and listed in Table 4.11 for the entered soil and Table 4.12 for the recovered soil.

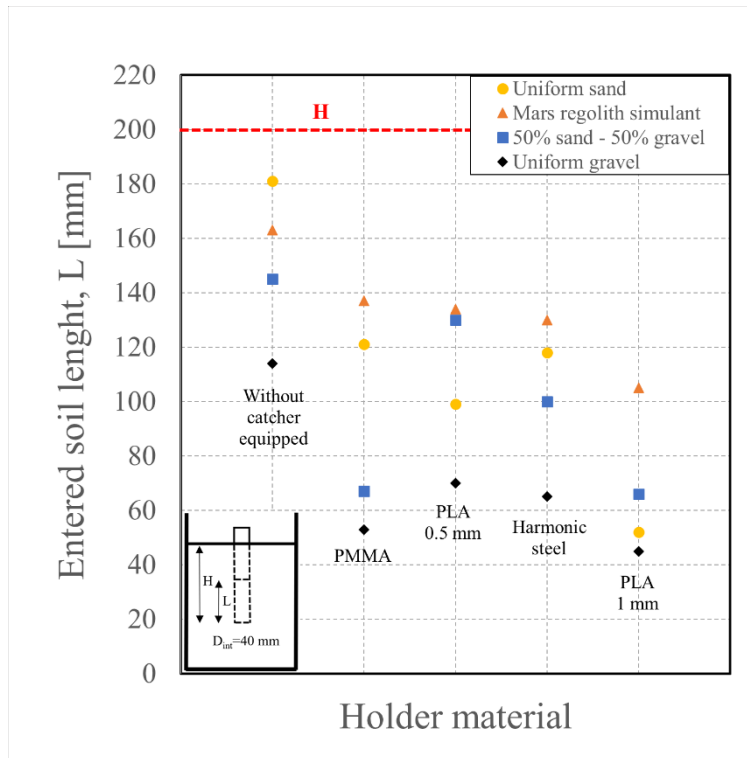


Figure 4.23 Soil entrance for different catchers and soil tested (the first column “without catcher” is obtained from figure 4.15 for a diameter of the holder equal to 40 mm)

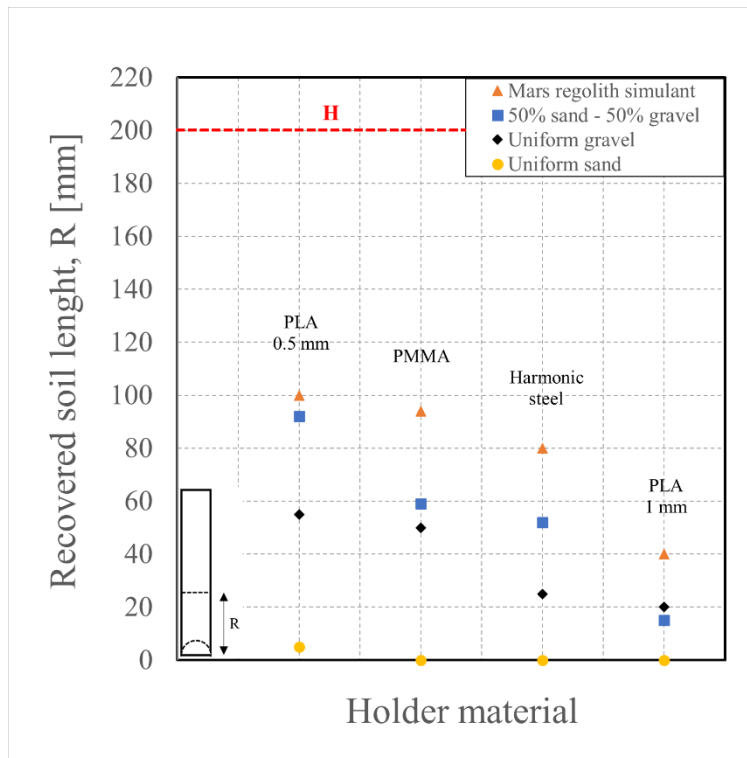


Figure 4.24 Soil recovery for different catchers and soil tested

Table 4.11 Evaluation of the recovery Ratios of entered soil (L)

Catcher name	Uniform sand [mm]	Mars regolith [mm]	50% sand - 50% gravel [mm]	Uniform gravel [mm]
No catcher	90.5	81.5	72.5	57.0
Harmonic steel	59.0	65.0	50.0	32.5

PLA 1 mm	26.0	52.5	33.0	22.5
PLA 0.5 mm	49.5	67.0	65.0	35.0
PMMA	60.5	68.5	33.5	26.5

*Table 4.12 Evaluation of the recovery Ratios of recovered soil (R)*

Catcher name	Uniform sand [mm]	Mars regolith [mm]	50% sand - 50% gravel [mm]	Uniform gravel [mm]
Harmonic steel	0.0	40.0	26.0	12.5
PLA 1 mm	0.0	20.0	7.5	10.0
PLA 0.5 mm	2.5	50.0	46.0	27.5
PMMA	0.0	47.0	29.5	25.0

It is possible to observe that the worst values of the soil entrance are obtained with gravel and the same was obtained for the recovered soil. It is also possible to individuate a tendency to obtaining better results by testing the Mars regolith simulant, both in terms of soil entrance and of soil recovery. The PMMA catcher is characterised by a very low stiffness and gives the highest Recovery Ratios of entered soils testing the uniform sand and for the Mars regolith simulant, but generally the lowest testing the others two mixtures. The PLA 1 mm catcher, even if not being the more rigid, gives the lowest values both for soil entrance and soil recovery. These low Recovery Ratios can be justified by the smaller width of the fingers, that led to bigger gaps allowing the escape of soil. A different configuration of the catcher, increasing the number of fingers, should be tested in future. Different lengths of the fingers, probably two, could be considered in order to reduce the gaps between the fingers but still avoiding positioning them in contact, that would increase the overall stiffness of the catchers. The worst case related to soil recovery is encountered testing the uniform sand, with all the catchers tested. This soil, at dry conditions, is completely loose and the small dimensions of grains allow to pass through the gaps between the fingers. Mixtures of grains with different sizes allow a better interlocking between grains and more material is recovered. More considerations can be made by observing the following four figures, showing plots related to the results obtained with the different catchers singularly, in order to highlight the trends experimented.

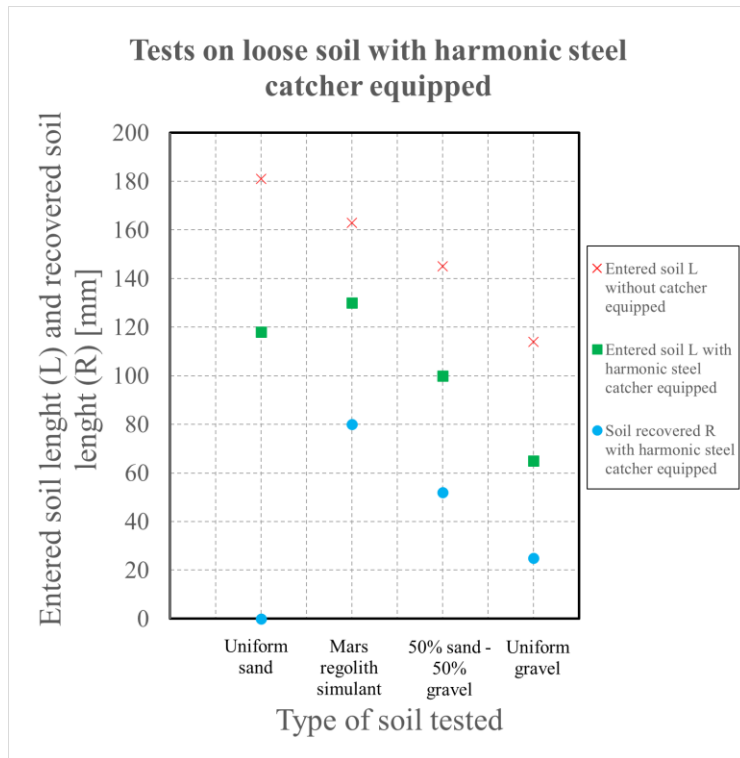


Figure 4.25 Entered soil length and recovered soil length with harmonic steel catcher equipped (holder internal diameter equal to 40 mm)

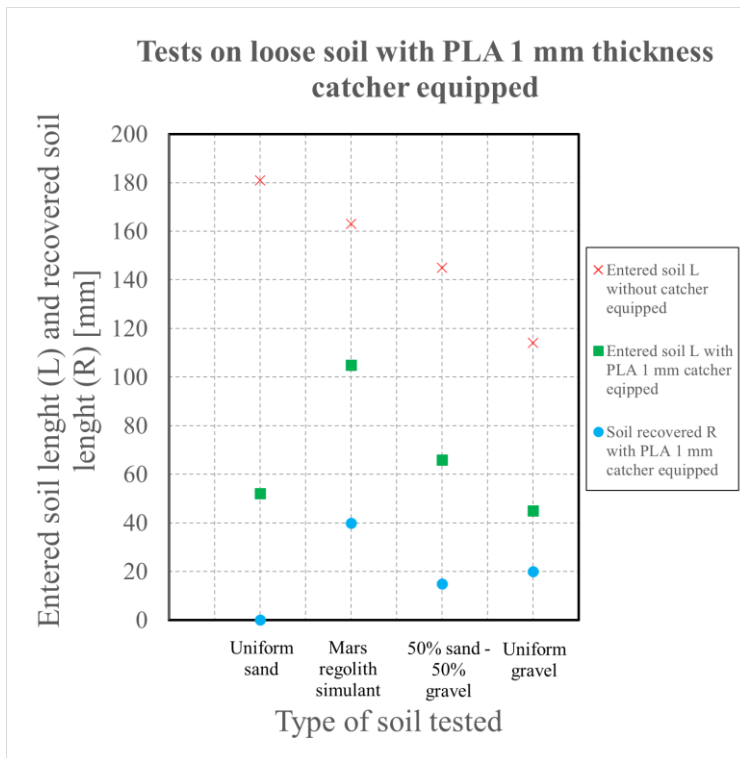


Figure 4.26 Entered soil length and recovered soil length with PLA 1 mm catcher equipped (holder internal diameter equal to 40 mm)

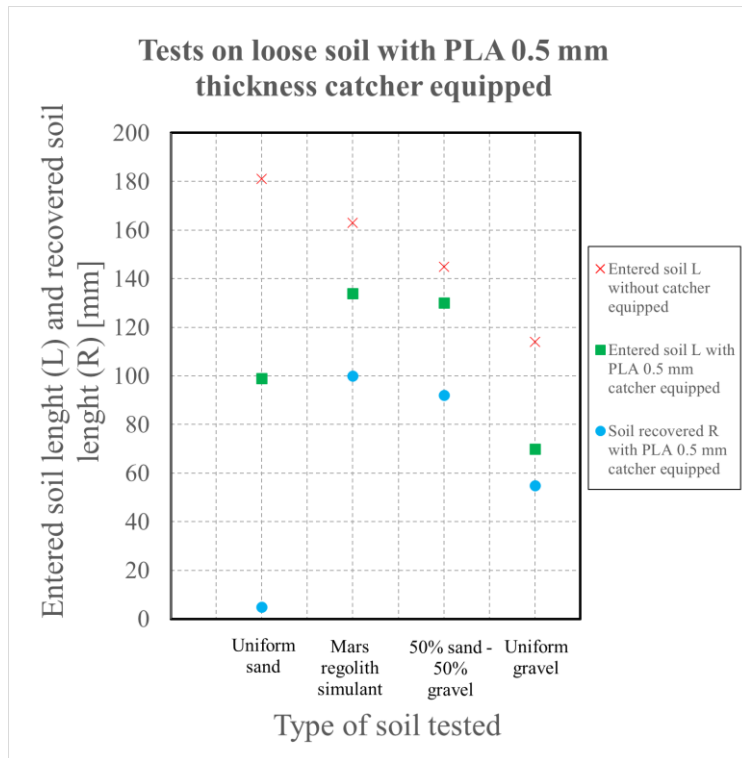


Figure 4.27 Entered soil length and recovered soil length with PLA 0.5 mm catcher equipped (holder internal diameter equal to 40 mm)

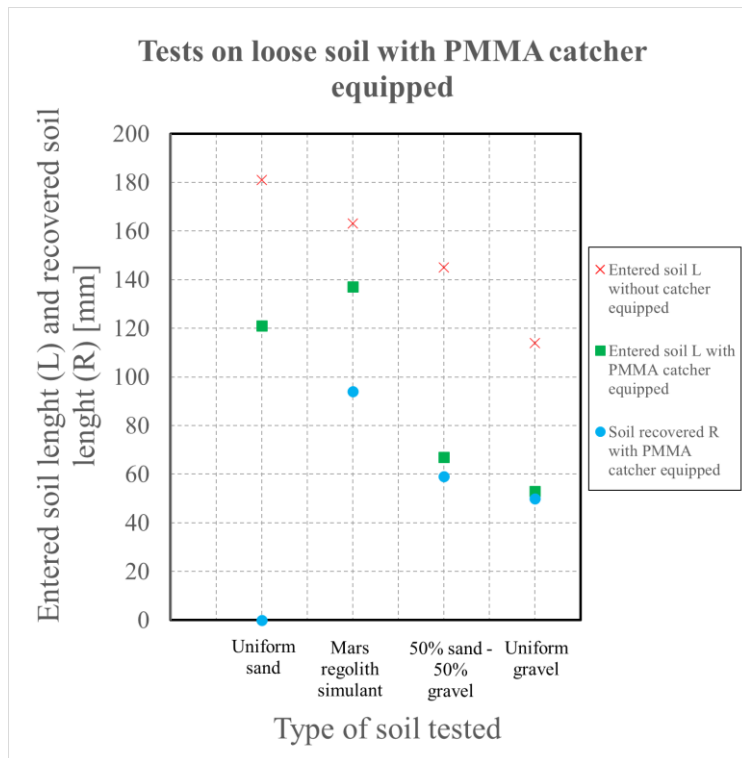


Figure 4.28 Entered soil length and recovered soil length with PMMA catcher equipped (holder internal diameter equal to 40 mm)

It can be observed that while the curve of entered soil with no equipped catcher describes a linear decrease, by increasing the gravel content, the curves related to the test conditions with catchers equipped are characterised by a different trend. In all cases, a peak of L and R is obtained testing the Mars regolith simulant, then the values decrease by increasing the gravel content. The curve related to soil recovered (R) seems to follow the one of material entered with a catcher equipped (L).

Analysing the curves of entered soil with a catcher equipped, it can be evidenced that all the values of R and R are lower than the ones reached with no catcher equipped. The highest values of entrance are obtained with the Mars regolith simulant and the holder equipped with PMMA catcher or PLA 0.5 mm, showing similar results. Testing the uniform gravel again provided the worst results in all cases and in general the worst results are obtained with the PLA 1 mm catcher, for the reasons previously described (small width of each finger and bad configuration of the catcher). The different stiffnesses of the catchers seemed not influence the outcomes in terms of L and R. Indeed the harmonic steel catcher, characterised by the highest stiffness, showed regular curves with a regular decrease of values from the condition with no catcher equipped but on the other side, the PMMA catcher, characterised by the lower stiffness, showed a better capability to retain the soil.

A parameter that was initially evaluated, is the resistance to cyclic loads (paragraph 3.2.2). During this experimental campaign the resistance assumed an important role, because only the fingers made with harmonic steel catcher did not need to be replaced during tests, the others needed some replacements. The point of failure was the connection between the fingers and the holder, in particular no one of the fingers broke up at the tip, but the damages and failures occurred always where a hole was created in order to allow the passage of the screw connecting the finger to the holder. Is possible that also blockage operations with interlocking nuts created the first fractures that propagated during tests. Holes in the plastic materials were created with a fine point of the electric welder and this probably made the material more fragile in that position. Holes in the harmonic steel catcher were directly made by the manufacturer of the plate. In Figure 4.29 is possible to observe the fragility of the finger made of PLA 1 mm thick, that broke up during assembly after having performed only three tests with uniform sand, Mars regolith simulant and the mixture of 50% sand - 50% gravel. Figure 4.30 is related to the failure of PLA 0.5 catcher after tests with uniform gravel, for a total of 10 cycles with various materials. Finally Figure 4.31 shows the deformed conditions of the catcher made of PMMA at the connection with the holder and the two fingers broken after a cycle of five tests. It is possible to highlight that, regarding the plastic materials, the PLA 0.5 catcher showed the better resistance, and could still be employed imposing to change the fingers every five cycles or even more frequently.



*Figure 4.29 PLA 1 mm catcher failure during assembly*



*Figure 4.30 PLA 0.5 mm catcher failure after tests with uniform gravel*

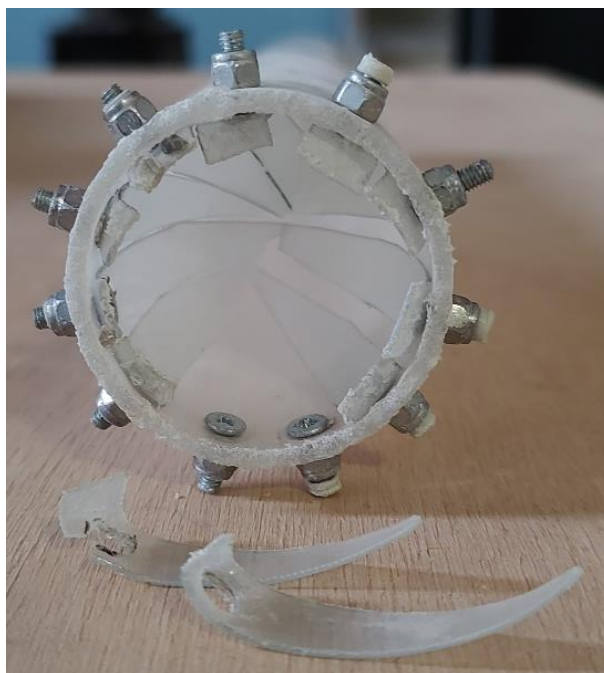


*Figure 4.31 PMMA damaged after tests with uniform gravel*

As anticipated, future upgrades of the catcher may consider different configurations of the fingers in order to allow also holding the finest part of soil mixtures and soils made of uniform sand. The following Figure 4.32 shows three pictures taken of the holder with recovered soil after tests made in Mars regolith simulant, 50% sand - 50% gravel and finally with the uniform gravel. In this cases when the holder was extracted from the soil a small amount was lost passing through the gaps between the fingers. The limit condition is shown in Figure 4.33 with the holder completely empty after the test in uniform sand. The 3D printed solution with PLA

material and thickness equal to 0.5 mm will still be tested with improved versions, as 3D printing technology allows to create a very wide variety of shapes of the fingers.

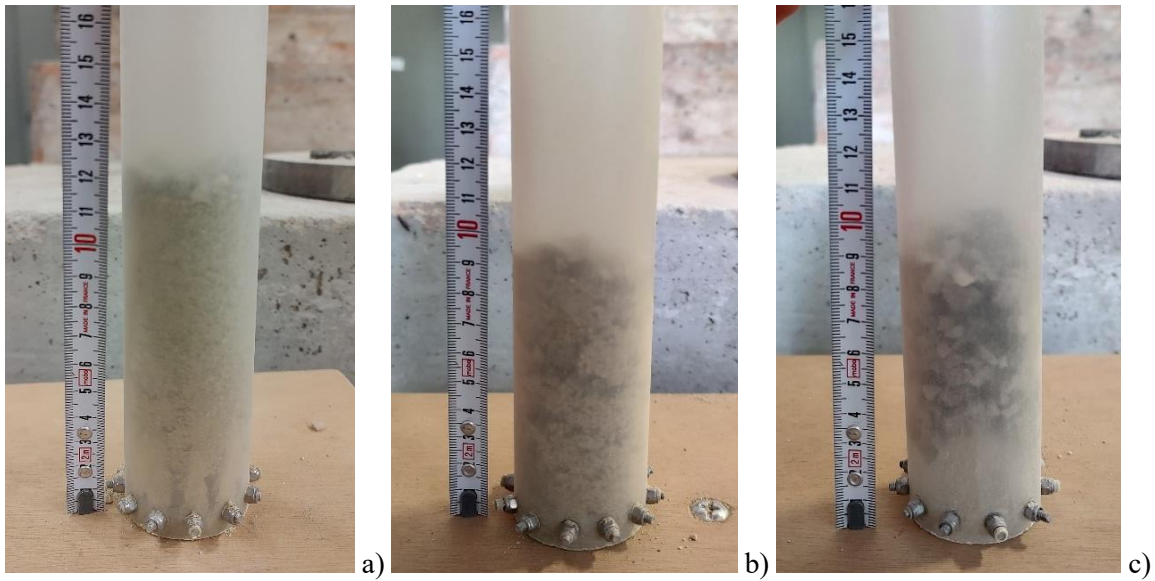


Figure 4.32 Recovered soil after tests with a) Mars regolith simulant, b) 50% sand - 50% gravel, c) uniform gravel.



Figure 4.33 Recovered soil after test with uniform sand

## 4.6 Sampler prototype test

Having tested different holders and catchers, the soil sample prototype was tested in its entire configuration having equipped the holder with diameter 40 mm and the catcher made of Poly-lactic Acid (PLA) with 0.5 mm thickness. The choice of the holder with diameter 40 mm was a compromise between performances and space restrictions, while the PLA 0.5 mm catcher provided the best results in terms of material entered in the holder and recovered. In this case the catcher was equipped as from design explained in paragraph 3.2.2 and shown in Figure 3.34, without creating holes to allow the passage of screws and holding with self-locking nuts, but through interlocking between advanced shoe and holder having glued the fingers on a 3D printed ring. The aim of the test is simulating a real soil sampling procedure, checking the overall system designed and produced, measuring the number of blows necessary to penetrate the soil for almost 300 mm (ERC requirement and physical limit of the sampler imposed by design) and the progressive advancement. At the end of sampling operations the quantity of soil sampled (soil recovery R) is evaluated, as well as the conditions of the prototype. Tests are performed first with uniform sand and Mars regolith simulant in loose condition and then with the

same soils in compacted conditions with the procedure described in paragraph 4.3.2. The idea was to slowly increase the stresses applied to the sample with a slow trend: first increasing only the gravel quantity keeping a non-compacted and soft soil, then also increasing the hardness of the soil to be sampled.

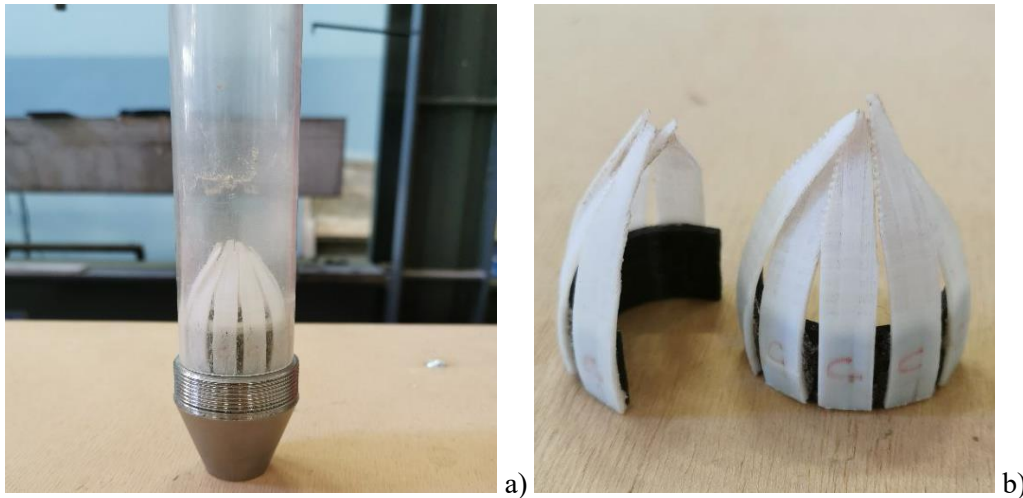


Figure 4.34 a) PLA 0.5 mm catcher equipped on the system composed by advanced shoe and holder, b) detail of the PLA 0.5 mm catcher

#### 4.6.1 Uniform sand at loose condition

The test bench was assembled as shown in Figure 4.35. The end of sampling operations can be observed in Figure 4.36 where the sampler prototype is completely penetrated into the soil. A total amount of 22 blows were necessary to penetrate the uniform sand for 261 mm: the sequence of blows versus the penetration can be observed in the comparative plot of paragraph 4.6.5 Figure 4.47 (yellow curve). The theoretical soil penetration was 300 mm while the experimental value reached was lower, this was due to a slight inclination of the prototype from the vertical position and to a movement of the lower plate equipped with nails from the original position. Future prototype updates will provide stronger connections between the various plates in order to avoid this reduction of soil penetration. The first three blows can be considered the less representative as the soil penetration is higher than the average one of the following blows, consequently the maximum advancement obtained with a single blow is 15.1 mm, with an average of 9.2 mm. The overall conditions of the sampler prototype were step-by-step checked and no damages were observed. The lifting system allowed a smooth descent in the soil as well as the lifting up, the electromagnet efficiently caught and lifted up the mallet during percussion operations and servomotors did not show fatigue during lifting operations. At the end of sampling procedures the holder was extracted from the sampler and the quantity of sampled material was almost null (Fig. 4.36). This result could be compared with those obtained with campaign performed only with the penetration of the catcher and the same catcher made of PLA with 0.5 mm thickness (Figure 4.27). The reason could be found in the absence of cohesion and the homogeneity of the soil with characterized by uniform small grains if compared to the gaps between the fingers of the catcher. Further improvements of the catcher's configuration will probably led to better retain of the soil, but in this research test will all be performed without any additional variations.



*Figure 4.35 Beginning of sampling test with sampler prototype on loose uniform sand*



*Figure 4.36 End of sampling test with sampler prototype on loose uniform sand*



*Figure 4.37 Holder with sampled material of loose uniform sand*

## **4.6.2 Mars regolith simulant at loose condition**

Figure 4.38 shows the beginning of sampling test on the Mars regolith simulant in loose condition, while the end of sampling operations can be observed in Figure 4.39. A total amount of 20 blows were required to penetrate the regolith simulant for 251 mm and the sequence of blows versus the penetration can be observed in Figure 4.47 (orange curve). Again, the first three blows were excluded, so the maximum advancement with a single blow was 16 mm with an average of 10 mm. Again, the overall system performed the sampling operations without damages. At the end of sampling procedures the holder was extracted from the sampler and the quantity of recovered soil was almost null (Fig. 4.38). Only some gravels were blocked within the space between the holder and the fingers, while the finest fraction was completely lost or did not even enter in the holder. From this observation some preliminary considerations can be made. First, the condition of completely loose soils could have led to a preliminary compaction of the soil inside the advanced shoe, before effectively opening the fingers of the sampler, so reducing the quantity of soil entered into the sampler. At the same time, the penetration of the cone sampler shape (external tube and advanced shoe) on a loose soil can possibly compacted laterally the soil during the descent, instead of allowing it entering in the holder. Finally, a significant loss of material occurs with the volume that enters from the advanced shoe but it does not overcome the fingers, for a height that can be approximated as 100 mm.



*Figure 4.38 Beginning of sampling test with sampler prototype on Mars regolith simulant*



*Figure 4.39 End of sampling test with sampler prototype on Mars regolith simulant*



Figure 4.40 Holder with sampled material of Mars regolith simulant

### 4.6.3 Uniform sand at compacted condition

After having performed the compaction operations described in paragraph 4.3.2, the test bench was assembled (Figure 4.35) and sampling operations were performed on the compacted uniform sand. A total amount of 198 blows occurred to penetrate the soil for 259 mm and the sequence of blows versus the penetration can be observed in the comparative plot of paragraph 4.6.5 Figure 4.47 (green curve). It can be observed that the number of blows increased significantly and also the time necessary to ultimate for the procedure. The system takes about 3 seconds to perform one blow, having automatized the measurement operations, less than 10 minutes were necessary to penetrate the soil for the whole length of the sampler in a uniform sand with void ratio equal to 0.39. Excluding the first three blows, the maximum advancement obtained in this case with a single blow is 11.0 mm with an average of 6.0 mm, and also this values were lower than those obtained for loose soil. During this test some critical aspects were detected with the servomotors. First, it was noticed an increase in the temperature of the servomotors. It was not so high to cause disturbance to operations or damaging the motors, but a proper cooling system is recommended. Then, the holding L-plates of the servomotors (Figure 4.41) slightly separated from the design position, this due to an insufficient number of fixing points through self-locking nuts. This increase of distance led to a damage of the servomotors flanges and one was completely levigated during the rotation and it needed to be replaced. A future design of this plates should include a stronger attachment for these plates. At the end of sampling procedures the holder was extracted from the sampler and the quantity of sampled material was again almost null (Figure 4.42).

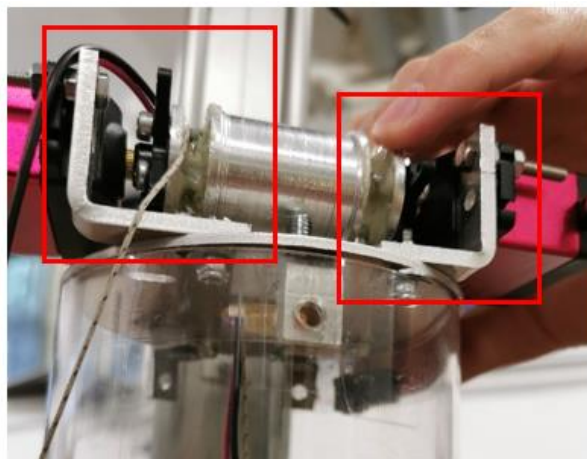


Figure 4.41 Detail of servomotors holding L-plates



Figure 4.42 Holder with sampled material of compacted uniform sand

#### 4.6.4 Mars regolith simulant at compacted condition

After having performed the compaction operations described in paragraph 4.3.2 on the Mars regolith simulant, the test bench was assembled (Figure 4.38). A number of 180 blows was necessary to penetrate the mars regolith simulant for 253 mm. The sequence of blows versus the penetration is given in Figure 4.47 (blue curve). Excluding the first three blows, the maximum advancement obtained in this case with a single blow is 12.0 mm with an average of 6.0 mm. The overall system worked efficiently. At the end of sampling procedures the holder was extracted from the sampler and, as shown in Figure 4.43, the quantity of sampled material was very low, almost 45 mm measured externally, removing the 3.5 mm of the height of the curved fingers, results 10 mm sampled. The Recovery Ratio evaluated by considering the total length of 253 mm was approximately equal to 4.0%, much lower than the one obtained with tests only with the holder equipped with the catcher, equal to 67.0% (Table 4.11). It should also be noticed that the most part of loss material is composed by the fine part of the mixture (sand and silt), mainly the gravelly part was sampled. In this case it can be assumed that the compacted condition reduced the lateral compaction of soil during the descent and effectively the soil entered in the holder, but only the gravel was recovered and the fine part was again almost completely loss.



Figure 4.43 Holder with sampled material of compacted Mars regolith simulant

#### 4.6.5 Uniform sand at compacted condition, without equipping the catcher

Due to the critical results obtained with soil recovery, a different type of test is performed with the prototype. The uniform, compacted sand was tested without equipping the catcher inside the holder of the soil sampler prototype. The aim was to understand if the soil effectively enters into the holder or if the system is composed by an advanced shoe and the catcher creates a sort of impedance to the material entering. The followed procedure was the same as previously explained, with the test bench assembled as shown in Figure 4.35 and compaction procedure performed as previously explained (paragraph 4.6.1). As the external tube is made of stainless steel (non-transparent material), the only way to approximately read the height of material entered into the sampler was accurately wash the holder and letting it a little wet, so that the dirty level will show the material passage. At the end of the soil penetration, the holder was extracted from the sampler and approximately 120 mm were measured from the highest level of sand trace observed in the holder and the beginning of the advanced shoe, as described in Figure 4.44.

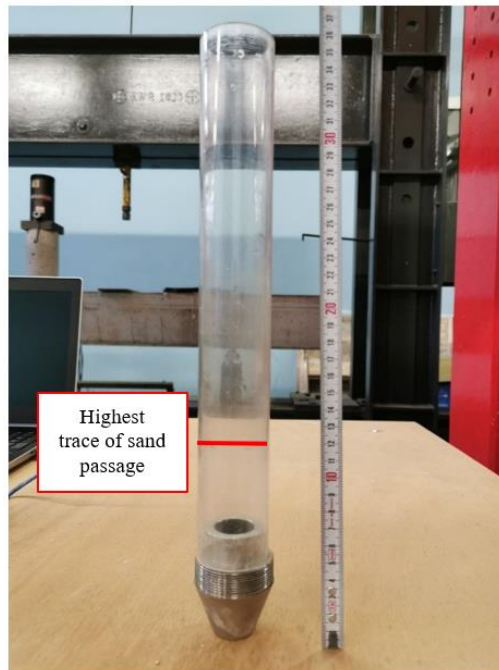


Figure 4.44 Trace of sand passage inside the holder

A comparison between volumes can be performed. First, it is possible to define an ideal cylinder of material sampled ( $V_{s,ideal}$ ), with diameter equal to the width of the toe of the advanced shoe, equal to 25 mm, and height equal to the depth of penetration of the sampler ( $h$ ), in this case equal to 251 mm. Obtaining:

$$V_{s,ideal} = \pi r^2 h = \pi \left(\frac{25}{2}\right)^2 251 = 123'209 \text{ mm}^3$$

Then, the volume sampled inside the holder ( $V_s$ ) is computed, having diameter equal to 40 mm and height approximately equal to the trace of sand passage ( $h_{sand}$ ), equal to 120 mm, having removed the height of the advanced shoe ( $h_{shoe}$ ), approximately equal to 65 mm. The result is:

$$V_s = \pi r^2 (h_{sand} - h_{shoe}) = \pi \left(\frac{40}{2}\right)^2 (120 - 65) = 69'115 \text{ mm}^3$$

As showed in Figure 4.45, the total loss of soil is given by two components. The most impacting loss owes to the material that remains between the advanced shoe toe and the fingers in closed configuration. The height of the advanced shoe is equal to 65 mm, while the height of the dome created by the fingers in closed position is equal to 35 mm. The total height of loss material ( $h_{lost}$ ) is at least equal to  $65 + 35 = 100 \text{ mm}$ , an additional quantity is lost during the closure of the fingers but cannot be estimated a priori. The resultant volume lost ( $V_{lost}$ ) can be preliminarily evaluated considering the certain height of loss material  $h_{lost}$  and the internal diameter of the advanced shoe, equal to 25 mm.

$$V_{lost} = \pi r^2 h_{lost} = \pi \left(\frac{25}{2}\right)^2 (65 + 35) = 49'087 \text{ mm}^3$$

The sum of the sampled volume  $V_s$  and the lost volume  $V_{lost}$  provides a value equal to 118'202  $\text{mm}^3$ . Comparing this volume with the ideal  $V_{s,ideal}$ , equal to 123'209  $\text{mm}^3$ , is possible to state that effectively the soil enters inside the sampler, but the loss of soil is too high. At the same time, the higher diameter of the holder referring to the one of the advanced shoe provides a relaxation of the cohesion-less soil inside the holder, with a reduction of the overall height over the fingers.

The new design of the sampler sub-system should strongly reduce the quantity of material loss. In particular, the advanced shoe height ( $h_{shoe}$ ) and the fingers dome height contain a material that cannot be retained by the catcher's fingers and will always be loss. For this reason, these heights should be reduced with a new design of the advanced shoed and an increased curvature of the catcher's fingers. It should be highlighted that an initial loss of material will still occur during the closure of the fingers.

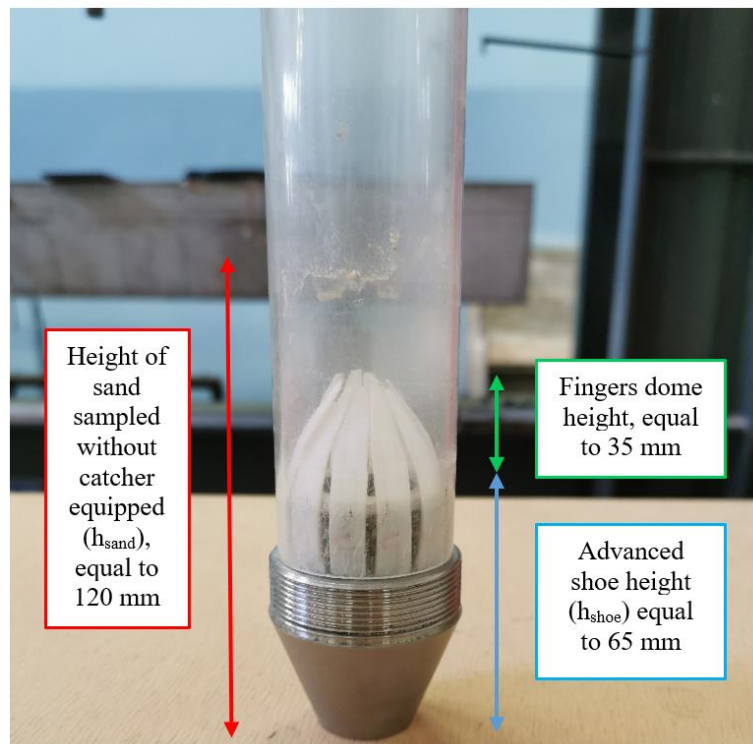


Figure 4.45 Trace of sampled soil and reference heights for loss soil

#### 4.6.6 Comparison of results about soil penetration with the sampler prototype

During the sampler prototype penetration into the soil, each blow performed by the percussion system was correlated to the progressive distance measured from the upper plate of the percussion system to the position of the ranging sensor, as shown in Figure 4.46. From the comparison plot of Figure 4.47 is possible to observe that moving from the loose condition to the compacted one, the number of blows needed for complete the sampling operations significantly increased and the penetration obtained with a single blow is reduced. In any case, uniform sand and Mars regolith simulant showed a similar behaviour, both in loose and in compacted conditions. This was due to the very similar composition, as the Mars regolith simulant is mainly composed by sand. The void ratio for the uniform sand and the Mars regolith simulant at loose condition were comparable (0.68 for the uniform sand and 0.70 for the Mars regolith simulant) and the same for the compacted condition (0.39 for the uniform sand and 0.31 for the Mars regolith simulant), this justifies that the trend of curves was almost equal in both the conditions. Additional tests campaign, not object of this thesis, will consider different soils (starting from the mixture 50% sand - 50% gravel and the uniform gravel) and compaction levels to investigate if the number of blows can be representative of the sampled material, like for Standard Penetration Tests. During this preliminary test campaign, the number of blows allowed to distinguish the different

compaction conditions. Performing more tests it would be possible to create a sort of reference database linking different soils and degrees of compaction with the penetration.

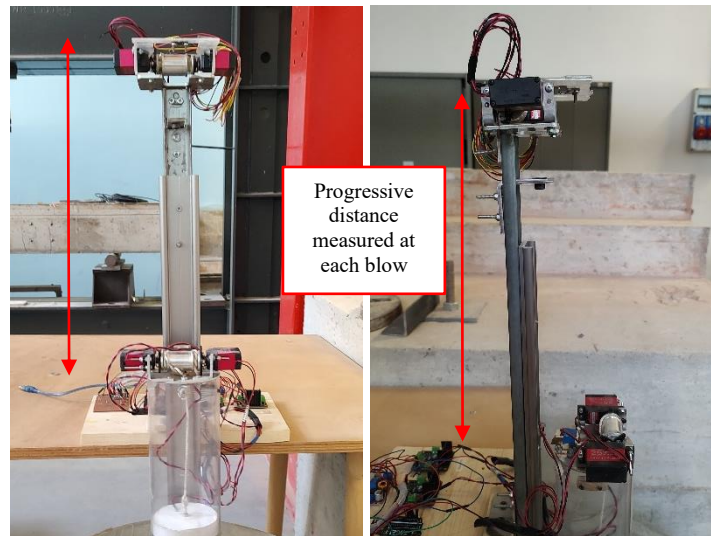


Figure 4.46 Progressive distance measured at each blow performed by the soil sampler prototype

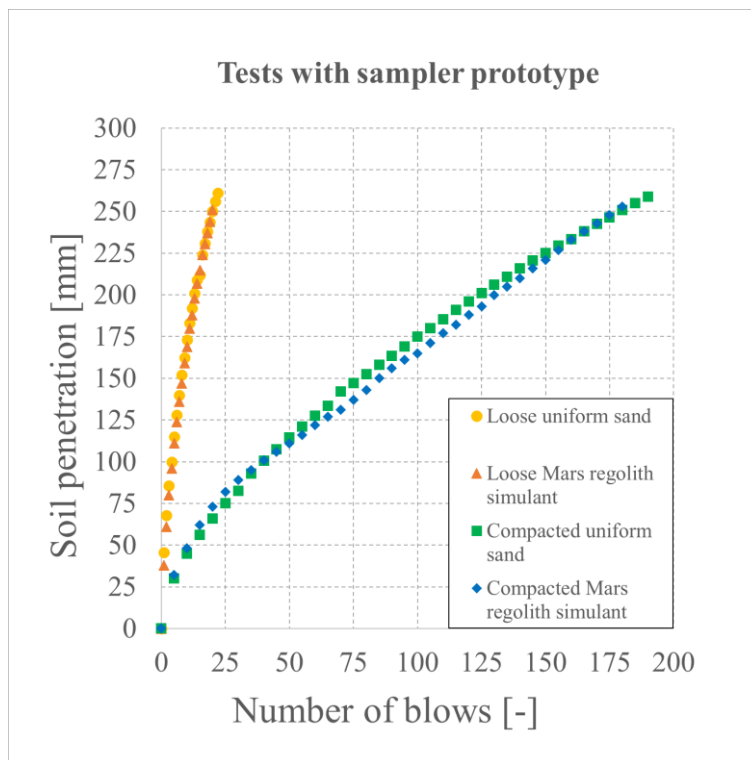


Figure 4.47 Comparison of results of sampling test

## 4.7 Safety aspects

### 4.7.1 Prototype manual of operation and maintenance

Test activity of the sampler prototype was performed in MASTRLAB laboratory of Politecnico di Torino. Working with a prototype machinery requires to individuate and protect workers and other employers of the laboratory from any possible risks, following the current normative regulation.

A prototype can be defined as the first device and original model of a series of subsequent realizations.

Devices specifically designed and built with research purposes and employed for limited time in laboratories are excluded from the application of Machinery Directive (Directive 2006/42/EC of the European Parliament and of the Council of 17 May 2006), a European Union directive concerning machinery and certain parts of machinery. This Directive was received and implemented in Italy through the Legislative Decree n.17 of 27<sup>th</sup> January 2010.

Article 9 of Ministerial Decree n. 363 of 5<sup>th</sup> August 1998 “Regolamento recante norme per l’individuazione delle particolari esigenze delle università e degli istituti di istruzione universitaria ai fini delle norme contenute nel decreto legislativo 19 settembre 1994, n.626, e successive modifiche e integrazioni”, is dedicated to the design and use of prototypes and new devices. In particular, is indicated the responsibility for the responsible of research activity to:

- a) guarantee the correct protection of employees, evaluating at the design stage the possible risks connected to the realization of the project and adopting the necessary precaution based on the available knowledges;
- b) provide adequate formation and information to the operators about the specific risks and particular measures of prevention and protection.

Following the previous indications, a *prototype manual of operation and maintenance* was developed and kept with the prototype during the whole duration of the test campaign. It can be reviewed in Annex 2.

Directions provided by Legislative Decree n.81 of 9<sup>th</sup> April 2008 “Testo unico sulla salute e sicurezza sul lavoro” are still valid and observed, as MASTRLAB laboratory of Politecnico di Torino is classified as working place.

## 4.8 Synthesis of the results

It is possible to briefly resume the results attained during all the campaign test performed.

- A compaction procedure was defined using a mallet with diameter equal to 350 mm and weight 19.6 kg; a container with diameter equal to 400 mm and filled with four layers made of 20.0 kg of soil and a dropping height of 200 mm. With this procedure a number of 30 blows per layer is necessary to obtain the maximum compaction with the uniform sand (granulometric range  $0.06 \div 2$  mm and final void ratio  $v_f = 0.39$ ); 15 blows with the uniform gravel (granulometric range  $2 \div 20$  mm and final void ratio  $v_f = 0.63$ ); 15 blows with the Mars regolith simulant (percentual fractions from Pizzamiglio et al. 2018 and final void ratio  $v_f = 0.31$ ); 20 blows with the 50% sand - 50% gravel mixture (final void ratio  $v_f = 0.44$ ).
- Penetration tests on different soil mixtures with holders (tubes) with internal diameter from 26 mm to 85 mm were performed. The main result revealed is that the quantity of soil effectively entering in the holders significantly increases with the internal diameter but reduces as the gravel quantity of the soil mixtures is increased.
- Penetration tests on different soil mixtures with a holder with internal diameter equal to 40 mm and equipped with catchers with different stiffnesses of the fingers were performed. The evidence is that equipping a catcher reduces the quantity of soil entered in the holder. Catchers with lower stiffness of the fingers like Poly (methyl methacrylate) and 3D printed Polylactic Acid with thickness of the finger equal to 0.5 mm, provided better results in terms of soil entrance, than ones with higher stiffness.
- Recovery tests on different soil mixtures with a holder with internal diameter equal to 40 mm and equipped with catchers with different stiffnesses of the fingers were performed. The 3D printed Polylactic Acid with thickness of the finger equal to 0.5 mm provided the best results in terms of soil retained.
- Recover loose uniform sand with null water content is very critical. In order to reach this objective, the design of the catcher must focus on avoiding the gaps between the fingers. Similar considerations are valid for the dusty part of Mars regolith simulants.
- Sampling tests performed with the soil sampler prototype were performed on the uniform sand and the Mars regolith simulant at loose and compacted conditions. The sampled soil was almost null due to the small internal diameter of the advanced shoe. The penetration of the soil was successful and the

number of blows correlated to the penetration of the soil allowed to distinguish between the loose and compacted conditions with both soils.

## 4.9 Considerations on future prototype updates

A series of problems were encountered during test campaigns. In this paragraph the main updates necessary for the soil sampler prototype are listed. Future test campaign will check if the proposed updates effectively improve the prototype performances. The main focus must be kept on the problems encountered with sampling. The Recovery Ratio in this preliminary test campaign was almost null or severely reduced from the results obtained testing only the holder with diameter 40 mm equipped with the catcher made of PLA with thickness of the fingers equal to 0.5 mm. Future test campaigns will also allow to individuate more limits of the sampler and define possible mechanical and electrical updates.

### 4.9.1 Prototype updates

The more relevant design updates to be performed to the soil sampler prototype are related to the mechanical system, some evidenced during the test campaign are listed below:

- develop a new design of the system composed by advanced shoe, holder and catcher: designing a new advanced shoe with lower height and internal diameter almost equal to the one of the holder, avoiding the relaxation of the soil. It should be remembered during this design stage that a higher holder diameter provided better results in terms of length of material entered and recovered (paragraph 4.4);
- provide a new positioning for the catcher, considering that interlocking between fingers and holder reduces the risk of failure of the fingers that occurred having created holes and fixed the fingers with screw and nuts (paragraph 4.5);
- develop new designs of catcher prototypes;
- provide a cooling system to the servomotors of the percussion system;
- design new L-plates devoted to stably fix the servomotors to the percussion system upper plate.

Finally, a module devoted to soil sampling still needs to be developed on the SawaGUI webapp of team DIANA. This will allow to control and perform the operations remotely, by real-time checking the conditions of the system and receiving the needed information from a series of dedicated sensors.

### 4.9.2 Future test campaigns

More test campaigns, not object of this thesis, will be performed with the sampler prototype, and the most relevant planned are the following:

- test campaign focused on the conditions on non-perfect verticality of the sampler prototype during sampling operations. The aim is to understand the limits of the soil sampler prototype in terms of maximum inclination from the vertical condition. The condition of non-verticality is probable during surface exploration and the opportunity of sampling also on inclined conditions would allow to test soils of dunes and craters borders. The main limitations faced by the prototype when sampling in conditions of non-verticality will be provided by the efficiency of the electromagnet, as preliminary tests have already shown that a non-vertical condition led to lower weights that can be lifted up. At the same time also the sliding of the mallet inside the transparent Polycarbonate (PC) guide during percussion operations can be lowered, this due to the friction developed between mallet and PC guide that, in fact, could be easily faced applying oils or positioning sheets made of materials that reduce friction along the walls of the PC tube. Also the linear guides of the lifting system could encounter friction problems, but these elements are certified by the seller and sliding problems could be solved moving to better alternatives;
- test campaign on different configurations of the catcher: the 3D printing technology allows to design and print in reduced time different catcher prototypes. In this way it is possible to produce new versions of the catcher (PLA 0.5 mm), that provided the highest results in terms of length of material entered in the holder and length of material retained. In particular, it was observed during test campaign that a solution with more curved fingers would lead to a smaller height of the dome created by the fingers in closed condition, reducing the material loss. Also the voids between the fingers should be reduced, trying to retain also the soil composed by uniform sand and the silty part of the Mars regolith simulant;

- test campaign on the sampler prototype on different soils: testing at least also the mixture 50% sand - 50% gravel and the uniform gravel will allow understanding if the number of blows performed with this soil sampler prototype can describe the type of material crossed. Same considerations can be made with the level of compaction evaluated through the void ratio.

## 5 Chapter 5: conclusions

This thesis deals with the design, build and test of a prototype of soil sampler to be equipped on team DIANA's rover ARDITO to attend the Rover Challenge series dedicated to the surface exploration of Mars planet. The design of the prototype was carried out by team's DIANA Core Drill Group under the coordination of Sara Sacco, author of this thesis. Test campaigns were performed at MastrLAB of Department of Structural, Building and Geotechnical Engineering (DISEG) of Politecnico di Torino.

A study of the technologies already existing was first carried out, to quantify and evaluate the relevant design parameters of a soil sampler and to evaluate the criticalities of obtaining a portion of soil from the original mass. On the basis of the available literature results, the Mars soil, known as "Mars regolith", was classified as a gravelly sand with a small silt fraction in dry conditions and cohesionless. This type of soil was rarely sampled on Earth, therefore the existing technologies were not fully designed for this kind of conditions, but in any case, some devices were taken as a reference in the current investigations. In particular, the Denison rotary core-barrel sampler in its triple tube configuration, provided a suggestion in terms of equipping an inner stationary tube that receives and holds the soil sample by means of a "catcher". A similar tool for retaining cohesionless soil is adopted in Cable Percussion Drilling, with a clack valve made of steel or leather: this device was taken as a reference for what concerns the penetration system. Indeed, a rotary percussive system like the one adopted in the Denison sampler was not suitable for sampling sands and requires a lot of energy, while a percussion system made with a mallet like in Cable Percussion Drilling can be easily implemented, even at a small scale. The last equipment evaluated was the one involved in Standard Penetration Tests. Some design specifics evaluated from this apparatus are the drive advanced shoe that cuts the crossed soil, the percussive system with a mallet, and the evaluation of the number of blows correlated to the soil penetration attained. Regarding the soil sampling techniques applied on Mars, the only results obtained at the moment derive from NASA's Perseverance rover, which is performing sampling missions thanks to the "sample handling" system. The main operations successfully performed consist of drilling of rocks, while the sampling of soil is still at a critical phase as the dusty part of the soil was still not retained in the sample tubes, probably due to its completely cohesionless characteristics.

The design of the new prototype was performed starting from a list of project requirements provided by the European Rover Challenge Onsite rules, in terms of sampling depth and characterizations of the retrieved soil. In particular, the Collection and Probing Task intends the rover to demonstrate the ability of the system to collect one deep sample, reaching up to 300 mm below the surface and collecting information on the sample gathered. Some further considerations carried out on ARDITO's rover, imposed space and weight limitations. Then the design of the prototype was performed dividing it into four different sub-systems:

- lifting system: mainly composed of linear guides, rollers and two coupled servomotors. It allows the sampler and the percussion system to approach the soil surface, perform soil sampling operations and recover them at the end of sampling operations.
- sampler: constituted by an external tube connected to an advanced shoe that directly cuts and penetrates the soil, then, the internal part of the sampler is made by a transparent holder equipped with a catcher that is devoted to receiving and holding the soil sample;
- percussion system: allows penetrating the soil by means to several blows carried out lifting up and releasing a 4 kg mallet. The uplift is made by two coupled servomotors and an electromagnet that holds the mallet, while the release of the mallet is performed removing the electric supply from the electromagnet. Each blow performed is linked to the soil penetration attained, automatically measured with a Time-of-Flight distance ranging sensor;
- control system: electronic and developed on Arduino Integrated Development Environment (IDE). It allows to automatise the sampling operations setting the number of blows and providing energy supply to the servomotors, the electromagnet and the installed sensors. It is connected to the rover's system with an ethernet shield.

The soil sampler prototype was built and tested to understand its operational limits, robustness and main criticalities. A suitable test bench with geometry 400 mm diameter and 600 mm height was built and filled with the soil to be samples for a total height of 400 mm. Then, different types of soil mixtures were created:

uniform sand (granulometric range 0.06 ÷ 2 mm); Mars regolith simulant (16% gravel, 74% sand and 10% clays/silts); mixture of 50% sand and 50% gravel, and uniform gravel (granulometric range 2 ÷ 20 mm).

Two preliminary campaign tests were performed on two parts of the sampler sub-system: the holder and the sampler. After defining a proper compaction procedure, the prototype was tested on the uniform sand and the Mars regolith simulant in loose and compacted condition. The tests performed on the holders were aimed to investigate the influence of the tube diameter on the penetration into loose soil mixtures. Six holders with internal diameter ranging between 26 mm to 85 mm were tested. It was observed that the entrance length  $L$  was never equal to the penetration length  $H$  that, in turns, was reduced by decreasing the holder diameter and by increasing the percentage of gravels of the soil mixture. Some hypothesis were assumed to explain these outcomes, with a combination of two different effects. The “pile effect”, related to the difference between internal diameter of the holder and soil grains dimensions. Soil grains with dimensions close to the holder’s diameter can fit together and being blocked during the entrance inside the holder. At the same time, the “arch effect” favours the creation of an “antagonist arch” of soil particles inside the holder, that obstacles the advancement of soil inside the holder and so the entrance of new soil grains. A holder with an internal diameter equal to 40 mm was adopted, allowing to obtain a Recovery Ratio equal to 81.5% penetrating into the Mars Regolith simulant.

Once the internal diameter was fixed, a second test campaign was performed equipping different catchers on the holder to evaluate the influence of the catcher’s fingers stiffness on the quantity of entered ( $L$ ) and recovered soil ( $R$ ). Four catchers having different stiffnesses were tested on the four soil mixtures created. The catcher built with fingers made of 3D printed Polylactic Acid with thickness of the fingers equal to 0.5 mm provided the overall best results considering all the soils tested. The Mars regolith simulant provided the best results both in terms of material entrance ( $L$ ) and soil recovery ( $R$ ). The retention of a uniform sandy soil revealed to be critical with recovery ratios close to zero. In order to retain also soils made of sands and silts, it is necessary to plan further tests on catchers adopting different shapes of the fingers and reducing the gaps between each finger.

The final campaign was related to the soil sampler prototype on uniform sand and Mars regolith simulant in loose and compacted conditions. The soil sampling with the prototype was not performed due to the configuration of the advanced shoe whose small diameter of the toe, comparable with the smaller holder tested in preliminary test campaigns, significantly reduced the soil entrance. At the same time, the soil remaining in the space between the shoe toe and the catcher’s fingers, is always lost and can nullify the length of soil entered. An improved design of the advanced shoe would be necessary by reducing its internal height, and so providing a toe diameter similar to the one of the holder. The other aspect analysed is the soil penetration of the soil sampler prototype: this was efficiently performed and the maximum penetration possible for the prototype was reached in every test. The number of blows requested to penetrate the uniform sand and the Mars regolith simulant was similar, both in the case of loose and compacted conditions. These results were a consequence of the high percentage of sand (74%) into the Mars regolith simulant. The most evident difference is the higher number of blows necessary to penetrate the compacted soils mixtures, from an average of 20 blows at loose conditions to an average of 180 blows at compacted conditions. This latter result could establishes the basis for a possible use of the correlation between the number of blows and penetration reached for a preliminary definition of the crossed soil.

Working on a Mars exploration scenario, it could be possible to preliminary estimate the recent or old age of the sampled soil, assuming that older or unaltered deposits requires a higher number of blows with lower values of penetration attained for each blow. For example, during the same mission, different sampling operations would be performed in different strategic positions on the surface and, in the end, it could be evaluated if the borders of a crater or of an ancient river, would require a lower number of blows than the bed of the crater or of the ancient river. In any case, a high number of tests campaign would be required to collect the necessary information and to obtain the empirical correlations necessary to associate the number of blows to the density of the ground.



## 6 Annex

### 6.1 Annex 1: sampling system control code

```
#define MotSPEED 3 //fwd is to rise //Pins for Outputs
#define MotDIR 4

#define Magnet 6

#define TopStop 2 //Pins for Endstop
#define CheckPin 7 //Endstop signal check

#define Mot_PWM_ON 20

#define Mot_PWM_Hold 10
#define Mot_PWM_OFF 0

#define Mag_ON 255
#define Mag_OFF 0

volatile boolean endstop_flag = 0;

//-----
void setup() {
  pinMode(MotSPEED, OUTPUT); //Motor FWD - Going UP
  pinMode(MotDIR, OUTPUT); //Motor REV

  pinMode(Magnet, OUTPUT); //Magnet

  pinMode(TopStop, INPUT_PULLUP); //Endstop Top

  pinMode (CheckPin, INPUT); //Endstop signal check

  attachInterrupt(0, endstop_ISR, CHANGE); // Endstop ISR

  Serial.begin(115200); //Start the Serial Communication

  campiona ();
}

//-----
void loop() {

}

void endstop_ISR () {
  delay(200);

  if ((digitalRead (CheckPin)) == HIGH) {
    endstop_flag = 1;
  }
  else {
    endstop_flag = 0;
  }
}
```

```

int campiona() {
  int a=1;
  while(a<=1){
    initialize_core ();
    Serial.print("\n\rHit number ");
    Serial.print(a);
    a++;
  }
  return 1;
}

void initialize_core() {
  //called at start, rise all since the endstop flag is triggered

  analogWrite(Magnet, Mag_ON);

  delay(500);
  //then go up until the endstop is reached
  goUp(200); //when return from this the endstop as been reached, wait and then release the magnet
  endstop_flag = 0;

  delay(50);

  analogWrite(Magnet, Mag_OFF);

  // go down for n seconds, slowly, to be sure the magnet is on the mallet
  goDown(950, 200);
}

void goDown(int t , int s) {
  //int t define how many second make the magnet go down
  //int s define the speed
  analogWrite(MotSPEED, s); //Fall
  digitalWrite(MotDIR, LOW);
  delay(t);
  analogWrite(MotSPEED, 0); //Fall
}

void goUp(int s) {
  endstop_ISR ();
  while (endstop_flag == 0) {
    analogWrite(MotSPEED, s); //Rise
    digitalWrite(MotDIR, HIGH);
  }
  analogWrite(MotSPEED, 0); //Fall
}

```

## 6.2 Annex 2: prototype manual of operation and maintenance

### MANUALE D'USO E MANUTENZIONE

#### per l'uso del prototipo di campionatore del team DIANA, da equipaggiare su un Rover per l'esplorazione di Marte

Il presente manuale di istruzioni è stato redatto con grande cura. Ciononostante, il team DIANA (Politecnico di Torino) non si assume alcuna responsabilità:

per eventuali errori presenti nel manuale di istruzioni per l'uso e ne declina la responsabilità per le relative conseguenze;

per danni diretti o indiretti che derivano da un utilizzo non conforme alle disposizioni del dispositivo stesso.

L'utilizzo del dispositivo è soggetto al rispetto delle relative normative di sicurezza e alla normativa antinfortunistica, nonché a tutte le disposizioni presenti nel manuale di istruzioni.

Il Team diana si riserva il diritto di modifiche ed aggiornamenti.

### 1 Informazioni importanti

**Leggere il manuale di istruzioni.** Prima di iniziare qualsiasi tipo di lavoro con il dispositivo o nelle vicinanze dello stesso, si deve leggere accuratamente e rispettare tutto il contenuto del presente manuale di istruzioni e le relative avvertenze di sicurezza e di pericolo. **Il presente manuale di istruzioni deve sempre essere conservato vicino al dispositivo.**

### 2 Indicazioni di sicurezza

Tutte le avvertenze di sicurezza e le istruzioni devono essere lette. Eventuali omissioni per quanto riguarda il rispetto delle avvertenze di sicurezza e delle istruzioni possono provocare gravi lesioni. **Tutte le avvertenze di sicurezza e le istruzioni fanno parte integrante del prototipo di campionatore.**

#### 2.1 Sicurezza sul posto di lavoro

**L'ambiente di lavoro deve essere mantenuto pulito e ben illuminato.** Il disordine e gli spazi di lavoro non illuminati possono comportare infortuni.

**Con l'utensile elettrico si deve lavorare in un ambiente dove non sussista pericolo di esplosioni, e dove non si trovino sostanze infiammabili liquide, gassose o in polvere.** Gli utensili elettrici provocano scintille che potrebbero costituire da innesco per polveri o vapori.

**Durante l'utilizzo dell'utensile è necessario mantenere a distanza le altre persone.** Distraendosi è possibile perdere il controllo dell'attrezzatura.

#### 2.2 Sicurezza elettrica

**Si deve evitare che il proprio corpo entri in contatto con superfici collegate a terra come tubazioni, riscaldamenti, stufe e frigoriferi.** Sussiste il rischio elevato di scarica elettrica se il corpo dell'operatore addetto all'utilizzo del dispositivo è collegato a terra.

**Gli utensili elettrici devono essere tenuti lontano dalla pioggia e dall'umidità.** La penetrazione di acqua in un utensile elettrico aumenta il rischio di scossa elettrica.

**I cavi non devono essere usati per scopi estranei alla loro funzione, come per esempio trascinare il dispositivo o per appenderlo. I cavi devono essere tenuti lontano da fonti di calore, da oli, da spigoli vivi o da parti mobili dell'apparecchiatura.** I cavi danneggiati o attorcigliati aumentano il rischio di scosse elettriche.

**Se si sta lavorando con l'utensile elettrico all'aria aperta è necessario usare cavi di prolunga che siano idonei per l'uso all'aria aperta.** L'impiego di cavi di prolunga idonei per l'uso all'aria aperta riduce il rischio di una scossa elettrica.

**Se è inevitabile l'impiego dell'apparecchiatura elettrica in un ambiente umido, allora è necessario usare un interruttore automatico di sicurezza per correnti di guasto.** L'impiego di un interruttore automatico di sicurezza per correnti di guasto riduce il rischio di scosse elettriche.

## **2.3 Sicurezza delle persone**

**Si raccomanda di essere cauti e di prestare la massima attenzione a quello che si sta facendo e si raccomanda di procedere con raziocinio quando si sta lavorando. Non si deve utilizzare il dispositivo quando ci si sente stanchi oppure quando si è sotto l'effetto di droghe, alcool o medicinali.** Un momento di distrazione durante l'uso del prototipo può avere conseguenza molto serie.

**Devono essere sempre indossati i dispositivi per la protezione personale.** Il rischio di lesioni si riduce indossando i dispositivi di protezione come la maschera antipolvere, i guanti di protezione e le scarpe di sicurezza antidrucciolo.

**Si deve evitare una messa in funzione involontaria. È necessario accertarsi che l'utensile elettrico sia spento prima di prelevarlo o trasportarlo.** Un avvio accidentale può causare infortuni.

**Tutti gli altri attrezzi devono essere allontanati prima di accendere l'utensile elettrico.** Un attrezzo che si trova in una componente mobile del prototipo può provocare lesioni.

**Lavorare sempre in una posizione di equilibrio.** In questo modo è possibile controllare meglio l'utensile nelle situazioni impreviste.

**È necessario indossare abbigliamento idoneo. Non devono essere indossati abiti larghi o monili. I capelli e i vestiti devono essere tenuti a distanza dalle parti in movimento.** I capelli, monili e vestiti possono rimanere impigliati nelle parti in movimento.

## **2.4 Utilizzo e trattamento**

**Il prototipo non deve essere sovraccaricato. Per svolgere i lavori devono essere usati utensili elettrici adatti allo scopo.** Usando gli utensili elettrici adatti è possibile lavorare meglio e in modo più sicuro.

**L'apparecchio deve essere spento e scollegato dall'alimentazione prima di procedere a regolazioni, prima di sostituire componenti o prima di ritirare il dispositivo.** Questa misura precauzionale impedisce un avvio involontario dell'utensile elettrico.

**Quando non viene utilizzato deve essere conservato in un luogo non accessibile a bambini. Questa apparecchiatura non deve essere utilizzata da persone che non hanno familiarità con il suo funzionamento o che non hanno letto le presenti istruzioni.** Le apparecchiature elettriche sono pericolose se vengono utilizzate da persone inesperte.

**La manutenzione e la cura dell'apparecchio devono essere eseguite scrupolosamente. È necessario controllare che le parti mobili funzionino in modo impeccabile e non si inceppino. Si deve anche verificare l'eventuale presenza di pezzi rotti o danneggiati che potrebbero pregiudicare il funzionamento. Le parti danneggiate devono essere riparate prima dell'impiego del dispositivo.** La causa di molti incidenti dipende dal cattivo funzionamento dell'apparecchio.

**Si deve utilizzare il prototipo conformemente alle presenti istruzioni, a tale riguardo è necessario tenere in considerazione le condizioni di lavoro.** L'utilizzo del dispositivo per applicazioni diverse da quelle previste può provocare situazioni di pericolo.

## **2.5 Avvertenze di sicurezza specifiche per la macchina**

### **2.5.1 Requisiti del personale di servizio**

Le persone di età **inferiore ai 16 anni** non possono usare questo prototipo.

Il personale addetto alla macchina deve sempre conoscere il contenuto del presente manuale di istruzioni per l'uso.

### **2.5.2 Sicurezza sul posto di lavoro**

**Lo spazio di lavoro deve essere protetto.** Gli spazi di lavoro non protetti possono comportare dei pericoli per l'operatore e per altre persone.

**Gli utensili elettrici non devono essere utilizzati nelle vicinanze di materiali combustibili.** Eventuali scintille potrebbero infiammare questi materiali.

**Evitare la presenza di punti dove le persone potrebbero inciampare.** Le cadute causate dalla presenza di intralci possono provocare lesioni gravi.

**La zona di test deve essere protetta.** È necessario che il prototipo venga bloccato con dispositivi di fissaggio piuttosto che con la propria mano.

**Si deve evitare la formazione di polvere sul posto di lavoro.** Le polveri sono facilmente infiammabili.

**Negli ambienti chiusi è necessario garantire un'aerazione e ventilazione sufficienti.** Pericolo derivante dalla formazione di polvere e dalla riduzione di visibilità.

**Le polveri di determinati materiali, come alcuni minerali, possono essere dannosi per la salute e possono provocare reazioni allergiche, malattie alle vie respiratorie e/o cancro.** Si deve assicurare una buona ventilazione del posto di lavoro e si raccomanda di utilizzare una maschera per la protezione delle vie respiratorie.

### **2.5.3 Sicurezza delle persone**

**Deve essere sempre indossato l'equipaggiamento per la protezione personale, si deve utilizzare quanto segue:**

**Guanti da lavoro di prima categoria;**

**Scarpe antinfortunistica.**

**Nel caso di presenza di persone oltre agli addetti è necessario che si tengano a distanza di 1m dall'area nella quale si stanno svolgendo i test.** Chiunque entri nell'area di lavoro o intervenga nella mobilitazione del prototipo deve indossare i dispositivi di protezione individuale.

**I cavi di alimentazione devono essere tenuti a distanza dalle parti taglienti o dalle parti in movimento.** La perdita di controllo dell'apparecchiatura può comportare lo strappo o la rottura del cavo di alimentazione della corrente oppure il cavo potrebbe rimanere impigliato.

**Il prototipo non deve essere mai rimosso dal banco di prova prima che le parti in movimento abbiano smesso di muoversi completamente.**

**Il prototipo non deve essere messo in funzione se non quando è stabilmente fissato al banco di prova.**

**L'apparecchio in funzione non deve mai essere rivolto verso parti del proprio corpo o verso le parti del corpo di qualcun altro.**

### **2.5.4 Pericoli correlati all'utilizzo**

**La sostituzione di parti deve essere eseguita con il massimo scrupolo e prima di iniziare la sostituzione è necessario scollegare il prototipo dall'alimentazione.**

**Prima di ogni test è consigliato controllare l'eventuale presenza di scheggiature o incrinature sul prototipo.**

**I componenti elettronici non devono essere sottoposti a temperature superiori a 40°C o inferiori a 5°C.** Operare a temperature estreme può causare malfunzionamenti o danni a parti meccaniche ed elettroniche.

**La piastra inferiore del sistema di sollevamento è dotata di 3 chiodi stabilizzanti affilati. Si raccomanda di mantenere il dispositivo in posizione verticale durante l'utilizzo e ben saldo al tavolo di prova tramite appositi vincoli e di utilizzare guanti da lavoro e scarpe antinfortunistica durante la movimentazione del prototipo dal banco di prova, mantenendo a distanza eventuali altri operatori.**

**La scarpa d'avanzamento è affilata quindi occorre prestare attenzione durante le operazioni di sostituzione della fustella e indossare guanti da lavoro.**

### 2.5.5 Manutenzione / Riparazioni

È necessario ispezionare il prototipo dopo un'eventuale caduta. Un utensile elettrico eventualmente danneggiato è pericoloso e non è più sicuro per il funzionamento. Prima di continuare il suo impiego deve essere ispezionato.

I lavori di riparazione e di manutenzione devono essere eseguiti da personale qualificato o autorizzato dal team DIANA. In caso contrario vengono a cadere tutti i diritti di responsabilità nei confronti del responsabile.

È consigliato sottoporre il prototipo a periodici controlli, indicativamente ogni 10 ore di lavoro. La causa di molti incidenti dipende dalla cattiva manutenzione degli utensili e funzionamento elettrico.

All'interno del sistema di percussione (tubo trasparente in policarbonato) è ben visibile un maglio in Piombo. **Data la tossicità del Piombo si raccomanda di non smontare il sistema di percussione e rimandare la Manutenzione al personale adibito del team DIANA**, che procederà a maneggiarlo tramite gli appositi dispositivi di sicurezza individuale (guanti e mascherina).

## 3 Caratteristiche tecniche

### 3.1 Dati tecnici

Prototipo di campionatore da equipaggiare su un Rover per l'esplorazione di Marte.

**Produttore:** team DIANA

**Potenza assorbita (W):** 25

**Dimensioni sistema in configurazione compatta:** 0.15x0.16x0.92 m

**Dimensioni sistema in configurazione estesa:** 0.15x0.16x1.5 m

**Colpi al minuto (spm) :** 15

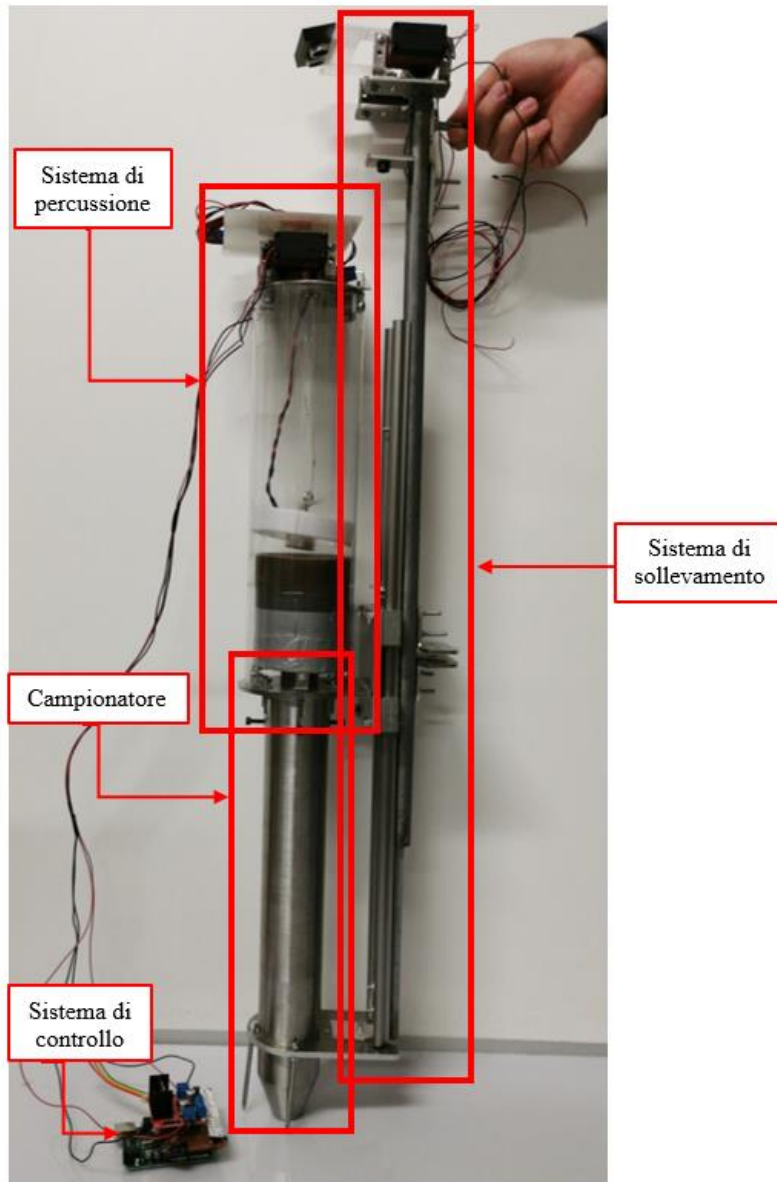
**Peso (kg):** 10

**Emissioni acustiche (dB):** lieve entità

### 3.2 Componenti della macchina ed elementi di comando

Il prototipo è composto da 4 principali sottosistemi:

- sistema di risalita;
- sistema di percussione;
- campionatore;
- sistema di controllo e alimentazione.



### Sistema di sollevamento:

- Nr. 2 guide lineari
- 1 carrello
- Piastra reggi motori
- Nr. 2 servomotori
- Rocchetto
- Corda di risalita
- Sensore di prossimità
- Piastra inferiore
- **Nr. 3 chiodi stabilizzanti**

### Sistema di percussione:

- Piastra di battuta
- Cilindro di battuta
- **Maglio in Piombo da 3 kg**
- Elettromagnete
- Centratore di corsa elettromagnete
- Cilindro di collegamento maglio-elettromagnete
- Tubo esterno trasparente in Policarbonato
- Piastra reggi motori
- Elettro serratura
- Nr. 2 servomotori
- Rocchetto
- Corda di risalita

### Campionatore:

- **Scarpa d'avanzamento**
- Tubo esterno
- Tubo interno trasparente
- Cestello
- Tappo di collegamento campionatore - sistema di percussione

### Sistema di controllo:

- Scheda Arduino
- Scheda di controllo con pulsante di emergenza
- Alimentatore



## **4 Prima di iniziare i test**

**Al fine di garantire un lavoro sicuro, prima di ogni test si raccomanda di prestare attenzione ai seguenti punti:**

**Tutte le avvertenze di sicurezza e di pericolo riportate nel presente manuale di istruzioni devono essere lette attentamente;**

**È necessario indossare i dispositivi di protezione individuale;**

**Prima di ogni utilizzo controllare che il sistema di sollevamento sia ben saldo al banco di prova, che i cavi elettrici siano ben collegati e funzionanti, che le parti non mobili del sistema siano ben salde e che tutti i componenti siano integri.**

## **5 Funzionamento e comandi**

### **5.1 Fissaggio prototipo al banco di prova**

Prima di iniziare i test di campionamento con il prototipo occorre fissare il sistema di sollevamento al banco di prova, tramite appositi morsetti e assicurandosi che il dispositivo sia del tutto vincolato al piano di appoggio ed ogni possibile movimento della struttura di sollevamento sia impedito.

### **5.2 Avvio operazioni di campionamento**

Effettuare i collegamenti del sistema di controllo alla fornitura di energia e al computer con il software Arduino tramite appositi cavi. Le operazioni di campionamento consistono nell'infissione del campionatore all'interno del campione di materiale opportunamente posizionato sotto al campionatore. Tali operazioni sono gestite dal sistema di controllo e vengono avviate attivando l'interruttore a bilanciere di accensione e spegnimento e l'apposito programma su software Arduino.

### **5.3 Termine operazioni di campionamento**

Raggiunto il termine delle operazioni di campionamento il sistema emette un segnale acustico, dopo il quale ogni alimentazione elettrica trasmessa al prototipo deve essere interrotta attraverso apposito interruttore a bilanciere di accensione e spegnimento.

### **5.4 Sostituzione fustella**

Terminato il test di campionamento la fustella (tubo in Policarbonato trasparente) risulterà piena di materiale, occorre sostituirla con una vuota, assicurandosi che ogni sistema di fissaggio sia opportunamente riposizionato al termine dell'operazione. Durante tale operazione il prototipo rimane fissato al banco di prova.

## **6 Pulitura**

Dopo avere eseguito i test ed aver scollegato il sistema di controllo dall'alimentazione, occorre pulire accuratamente quest'ultimo dalle polveri residue, eventualmente tramite soffiatura di aria compressa.

## **7 Manutenzione**

La manutenzione deve essere eseguita almeno una volta all'anno, inoltre è di volta in volta necessaria una manutenzione in base all'usura dei componenti. Per i lavori di manutenzione ordinaria e straordinaria sono incaricati esclusivamente membri del team DIANA.

## **8 Smaltimento**

Portare il dispositivo presso un centro di riciclaggio autorizzato ai sensi della normativa vigente nel luogo di utilizzo.

## 7 List of figures

Figure 1.1 Team DIANA’s lunar rover AMALIA .....	1
Figure 1.2 Team DIANA’s Martian rover TO-RO at European Rover Challenge 2018.....	2
Figure 1.3 Team DIANA’s Martian rover Trinity at European Rover Challenge 2019.....	2
Figure 1.4 Team DIANA’s Martian rover ARDITO at European Rover Challenge 2021.....	3
Figure 1.5 First design of DIANA’s soil sampling system for ARDITO rover .....	4
Figure 1.6 Team DIANA’s Martian rover ARDITO (design version presented at Indian Design Rover Challenge 2020).....	5
Figure 1.7 Team DIANA’s Martian rover ARDITO (ERC 2021) .....	6
Figure 2.1 ALTEC S.p.A. Mars soil simulant: grain size distribution with detail of D10 and D60 (Pizzamiglio, et al., 2018).....	8
Figure 2.2 ALTEC S.p.A. Mars soil simulant: Mohr Coulomb failure line (Pizzamiglio, et al., 2018) .....	8
Figure 2.3 Sample of Mars soil simulant from ALTEC S.p.A. ....	9
Figure 2.4 Cumulative number of rocks/m <sup>2</sup> greater than diameter D at the Pathfinder landing site (Golombek, et al., 2003).....	9
Figure 2.5 Sample of Mars soil simulant from Thales Alenia Space .....	10
Figure 2.6 a) Mechanical screening equipment, b) detail of biggest soil particles from Thales Alenia Space Mars soil simulant .....	10
Figure 2.7 Thales Alenia Space Mars soil simulant: grain size distribution with detail of D <sub>10</sub> and D <sub>60</sub> .....	11
Figure 2.8 a) Denison triple-tube core barrel (Johnson design 1940), b) Denison sampler (FHWA, 1997)...	14
Figure 2.9 Cable percussion drilling, view from different sides (image from Sub Surface Ltd) .....	15
Figure 2.10 Cable percussion drilling tools (image from DANDO company website) .....	16
Figure 2.11 Cable percussion drilling clack valve (image from DANDO company website) .....	16
Figure 2.12 Standard Penetration Test equipment (Schneider, et al., October 1999).....	17
Figure 2.13 Longitudinal cross-section of a Standard Penetration Test sampler without a provision for a liner, dimensions in mm (British Standard, 2007).....	18
Figure 2.14 NASA’s Perseverance rover and sample handling system detail (from “NASA Science Mars 2020 Mission Perseverance Rover - Sample handling” website).....	19
Figure 2.15 NASA’s Perseverance rover sampling and caching full system architecture (“Mars 2020 rover Sampling & Caching Subsystem” from Wikipedia commons) .....	20
Figure 2.16 NASA’s Perseverance Drill with Rock Core collected (“Sample Tube in Perseverance's Coring Drill” from NASA Science Mars Exploration Program website) .....	20
Figure 3.1 ARDITO rover mechanical structure with soil sampler prototype in closed configuration.....	23
Figure 3.2 ARDITO rover mechanical structure with soil sampler prototype in completely elongated configuration.....	23
Figure 3.3 Lateral view of DIANA’s sampling system with detail of lifting system.....	24
Figure 3.4 Detail of linear guide equipped with sliding roller thickness.....	24
Figure 3.5 DIANA’s sampling system: detail of electric lock and blocking plate.....	25
Figure 3.6 Front view of DIANA’s sampling system with detail of servomotors.....	26
Figure 3.7 Test: measure of extraction weight from Mars regolith.....	26
Figure 3.8 Sample characteristics .....	28
Figure 3.9 Sample Recovery Ratio.....	28
Figure 3.10 (left) Schematization of the triple core barrel Denison sampler with detail of the catcher - (right) catcher prototype developed by Geomarc S.r.l.....	29
Figure 3.11 Ashby logarithmic plot for strong and elastic beam (obtained with CES Edupack software).....	31
Figure 3.12 Experimental Wöhler plots (a) from generic literature and (b) from (de Jesus, et al., 2012).....	31
Figure 3.13 Ashby logarithmic plot for fatigue resistance of a beam element (obtained with CES Edupack software).....	32
Figure 3.14 DIANA’s harmonic steel catcher prototype.....	33
Figure 3.15 DIANA’s PLA catcher prototype (1 mm finger thickness): a) CAD model, b) 3D printed prototype .....	34
Figure 3.16 DIANA’s sampler assembly .....	34
Figure 3.17 Humidity and temperature soil sensor to be positioned inside the holder.....	35

Figure 3.18 DIANA’s advanced shoe and catcher .....	35
Figure 3.19 Quoted section of DIANA’s advanced shoe .....	36
Figure 3.20 Thales Alenia Space ROXY facility: internal view of test area (courtesy of Thales Group S.p.A.) .....	36
Figure 3.21 Thales Alenia Space ROXY facility: plan and tests position.....	37
Figure 3.22 DIANA’s test equipment for evaluation of weight and dropping height .....	38
Figure 3.23 Results of test campaign at ROXY facility of Thales Alenia Space .....	38
Figure 3.24 DIANA’s sampling system: mallet section.....	39
Figure 3.25 DIANA’s sampling system: mallet .....	40
Figure 3.26 DIANA’s sampling system: particular of (a) electromagnet, (b) endstop.....	40
Figure 3.27 DIANA’s sampler: detail of the percussion system .....	41
Figure 3.28 DIANA sampler: detail of the aluminium connection between sampler and percussion system.	41
Figure 3.29 DIANA’s sampler: electronic control (test configuration board) .....	43
Figure 4.1 Container for tests: a) lateral view, b) upper view with dimensions reference .....	45
Figure 4.2 Starting soils for sampling test.....	45
Figure 4.3 Soil classification modified from UNI EN ISO 14688-2 .....	46
Figure 4.4 Test soil: uniform sand.....	47
Figure 4.5 Test soil: uniform gravel .....	47
Figure 4.6 Mars soil simulant: reference grain size distribution from ALTEC S.p.A.....	48
Figure 4.7 DIANA’s simulant of Mars regolith: a) mixing procedure, b) resultant soil .....	48
Figure 4.8 Test soil: 50% sand - 50% gravel.....	49
Figure 4.9 Compaction hammer overall weight .....	51
Figure 4.10 Soil compaction sequence .....	52
Figure 4.11 Soil compaction procedure on test bench.....	52
Figure 4.12 Trend of compaction for one layer of 20 kg of soil.....	53
Figure 4.13 Length of soil entered in the holder L and height of penetration H .....	54
Figure 4.14 Holders involved in the test campaign .....	54
Figure 4.15 Variation of soil entrance length (a) and ratio (b) in the holder, changing the type of soil and diameter of the holder.....	55
Figure 4.16 “Pile effect” during sampling operations .....	56
Figure 4.17 “Arch effect” during sampling operations .....	57
Figure 4.18 “PLA 1 mm” catcher equipped on the holder: a) bottom view, b) lateral view, c) top view .....	58
Figure 4.19 “PLA 0.5 mm” catcher equipped on the holder: a) bottom view, b) lateral view, c) top view ....	59
Figure 4.20 “Harmonic steel” catcher equipped on the holder: a) bottom view, b) lateral view, c) top view.	59
Figure 4.21 “PMMA” catcher equipped on the holder: a) bottom view, b) lateral view, c) top view.....	59
Figure 4.22 Fingers made in different materials: a) harmonic steel, b) PLA 1 mm, c) PLA 0.5 mm, d) PMMA .....	60
Figure 4.23 Soil entrance for different catchers and soil tested (the first column “without catcher” is obtained from figure 4.15 for a diameter of the holder equal to 40 mm).....	61
Figure 4.24 Soil recovery for different catchers and soil tested .....	61
Figure 4.25 Entered soil length and recovered soil length with harmonic steel catcher equipped (holder internal diameter equal to 40 mm).....	63
Figure 4.26 Entered soil length and recovered soil length with PLA 1 mm catcher equipped (holder internal diameter equal to 40 mm).....	63
Figure 4.27 Entered soil length and recovered soil length with PLA 0.5 mm catcher equipped (holder internal diameter equal to 40 mm).....	64
Figure 4.28 Entered soil length and recovered soil length with PMMA catcher equipped (holder internal diameter equal to 40 mm).....	64
Figure 4.29 PLA 1 mm catcher failure during assembly .....	65
Figure 4.30 PLA 0.5 mm catcher failure after tests with uniform gravel.....	66
Figure 4.31 PMMA damaged after tests with uniform gravel.....	66
Figure 4.32 Recovered soil after tests with a) Mars regolith simulant, b) 50% sand - 50% gravel, c) uniform gravel. ....	67
Figure 4.33 Recovered soil after test with uniform sand.....	67

Figure 4.34 a) PLA 0.5 mm catcher equipped on the system composed by advanced shoe and holder, b) detail of the PLA 0.5 mm catcher.....	68
Figure 4.35 Beginning of sampling test with sampler prototype on loose uniform sand .....	69
Figure 4.36 End of sampling test with sampler prototype on loose uniform sand .....	69
Figure 4.37 Holder with sampled material of loose uniform sand .....	70
Figure 4.38 Beginning of sampling test with sampler prototype on Mars regolith simulant .....	71
Figure 4.39 End of sampling test with sampler prototype on Mars regolith simulant .....	71
Figure 4.40 Holder with sampled material of Mars regolith simulant.....	72
Figure 4.41 Detail of servomotors holding L-plates.....	72
Figure 4.42 Holder with sampled material of compacted uniform sand .....	73
Figure 4.43 Holder with sampled material of compacted Mars regolith simulant .....	73
Figure 4.44 Trace of sand passage inside the holder .....	74
Figure 4.45 Trace of sampled soil and reference heights for loss soil.....	75
Figure 4.46 Progressive distance measured at each blow performed by the soil sampler prototype .....	76
Figure 4.47 Comparison of results of sampling test.....	76

## 8 List of tables

Table 2.1 Physical properties of ALTEC S.p.A. Mars soil simulant (modified from Pizzamiglio et al., 2018)	9
Table 2.2 Quality Classes of soil samples (after EN 1997-2).....	12
Table 2.3 Quality classes of samples from different samplers (modified from AGI recommendations, 1977) .....	12
Table 2.4 Correlation between SPT-N values, friction angle and relative density (Meyerhof 1956) .....	18
Table 3.1 Sampler design parameters (modified from MachenLink web course).....	27
Table 4.1 Specific gravity $G_s$ for different types of soil particles .....	49
Table 4.2 Theoretical void ratio for each test soil .....	50
Table 4.3 Experimental void ratio for each test soil at loose condition.....	50
Table 4.4 Compaction parameters for the defined procedure.....	52
Table 4.5 Experimental void ratio for one layer with 20 kg of soil at compacted condition .....	53
Table 4.6 Compaction energy for four layers made with 20.0 kg of soil .....	53
Table 4.7 Main characteristics of the holders tested.....	54
Table 4.8 Recovery Ratio computed for the test campaign on different soils with holders characterised by different internal diameters.....	55
Table 4.9 Stiffness evaluation for different fingers .....	60
Table 4.10 Catchers main characteristics .....	60
Table 4.11 Evaluation of the recovery Ratios of entered soil (L) .....	61
Table 4.12 Evaluation of the recovery Ratios of recovered soil (R) .....	62

## 9 List of equations

(3.1) .....	27
(3.2) .....	27
(3.3) .....	27
(3.4) .....	28
(3.5) .....	29
(3.6) .....	30
(3.7) .....	30
(3.8) .....	30
(3.9) .....	30
(3.10) .....	30
(3.11) .....	30
(3.12) .....	32
(3.13) .....	32
(3.14) .....	32
(4.1) .....	49
(4.2) .....	50
(4.3) .....	57
(4.4) .....	57
(4.5) .....	58

## 10 References

- ACE wire and springs company. (n.d.). *Properties of common spring materials*. McKees Rocks Pennsylvania.
- Al-Khafaji, S. (2016). *Effect of the Different Energy of Compaction on Subset Course of Roads*. Saudi Journal of Engineering and Technology. **1** 3 86-91. DOI:10.21276/sjeat.2016.1.3.5.
- ASCE. (1999). *Technical Engineering and Design Guides as adapted from the US Army Corps of Engineers*. No. 30. Soil Sampling. ASCE Press.
- Ashby, M. (2003). *Material Selection in Mechanical Design*. Butterworth Heinemann. **03** C7 C7-1-C7-9. DOI <https://doi.org/10.1051/jp4:1993701>.
- Bond, Shuppener, & Scarpelli. (2013). *Eurocode 7: Geotechnical Design Worked Examples*. Dimova S., Nikolova B., Pinto V. A. **7** 51-52. DOI: 10.2788/3398.
- British Standard. (2007). British Standard (2007). *Geotechnical Investigation and Testing - Field Testing - Part 3: Standard Penetration Test*. Designation: EN ISO 22479-3:2005 + A1:2011.
- Cestari, F. (2009). *Prove geotecniche in sito*. Segrate: Edizioni Geo-Impianti.
- de Jesus, A., Matos, R., Fontoura, B., Rebelo, C., da Silva, L., & Veljkovic, M. (2012). *A comparison of the fatigue behaviour between S355 and S690 steel grades*. Journal of Constructional Steel Research. **79** 140-150.
- Fleck, N., Kang, K., & Ashby, M. (1994). The cyclic properties of engineering materials Overview No.112. Pergamon press Ltd.
- Golombek, M., Haldemann, A., Forsberg-Taylor, N., DiMaggio, E., Schroeder, R., Jakosky, B., Matijevic, J. (2003). Rock size-frequency distributions on Mars and implications for Mars Exploration Rover landing safety and operations. Journal of Geophysical Research: Planets. **E 12** 108.
- Hvorslev. (1949). *Subsurface exploration and sampling of soils for civil engineering purposes*. American Society of Civil Engineers, Committee on Sampling and Testing.
- Likos, W. J. (2010). *Site Investigation. Lecture notes*. Department of Civil and Environmental Engineering University of Wisconsin-Madison.
- Look, B. (2007). *Handbook of Geotechnical Investigation and Design Tables*. London, UK: Taylor & Francis.
- Maizza, G. (2019-2020). *Dispense del corso di Selezione e progettazione dei materiali per applicazioni ingegneristiche (SPMAI)*. Politecnico di Torino.
- Meyerhof, G. G. (1956). *Penetration tests and bearing capacity of cohesionless soils*, Journal of the soil mechanics and foundation division. ASCE, **82**, No. SM1, January, 1-19.
- Pizzamiglio, C., Genta, G., & Cofano, A. (2018). *3D Multibody-Discrete Element Co-Simulations of Flexible Wheel Performance for Small Planetary Rovers*. Ph.D. Thesis, Politecnico di Torino. 24-71.
- Schneider, J., & Mayne, P. (October 1999). *Soil Liquefaction Response in Mid-America Evaluated by Seismic Piezocone Tests*. Atlanta, GA 30332: Geosystems Program Civil & Environmental Engineering Georgia Institute of Technology. 00-03.
- Shuter, & Teasdale. (1989). *Techniques of Water-Resources Investigations of the United States Geological Survey*. U.S. Government Printing Office.
- Tanzini. (2011). *L'indagine geotecnica*. Dario Flaccovio Editore s.r.l.
- UNI EN 13286-2. (n.d.). *Unbound and hydraulically bound mixtures - Part 2: Test methods for laboratory reference density and water content - Proctor compaction*.
- UNI EN ISO 14688-2:2018. (n.d.). *Indagini e prove geotecniche - Identificazione e classificazione dei terreni - Parte 2: Principi per una classificazione*.

- W. T. Pike, U. S.-L. (2012). *Quantification of the dry history of the Martian soil inferred from in situ microscopy*. *Geophysical Research Letters*. **38** 24.
- Xi, B., Jiang, M., Cui, L., Liu, J., & Lei, H. (2019). Experimental verification on analytical models of lunar excavation. *Journal of Terramechanics*. **83** 1-13.

# 11 Acknowledgments

Il primo ringraziamento è per il team DIANA del Politecnico di Torino. Ringrazio tutti i colleghi, ormai divenuti amici, che hanno creduto in me e mi hanno affiancato in questi anni, senza mai dubitare della mia visione su questo progetto. Grazie a Carlo Tiozzo, per la costante e rassicurante presenza durante tutte le fasi di sviluppo e test del prototipo; a Leonardo Festa, per la fiducia professionale accordatami unita alla calorosa leadership; a Edoardo Vacchetto, per il supporto elettronico sempre accompagnato da un sorriso; a Lorenzo Caraccio, Tommaso Colamartino, Alessandro Dell'Atti e Gloria Nallo per i render e i modelli meccanici; a tutti gli altri membri del team che mi hanno affiancata durante questo lungo progetto.

Ringrazio i relatori, in primo luogo la professoressa Maria Rita Migliazza per avermi seguito sin dalla nascita di questo progetto con fiducia nel mio operato e caloroso supporto. Ringrazio poi il professor Daniele Costanzo e l'ing. Gianluca Bella per aver accuratamente seguito gli aspetti geotecnici della tesi e formulato le dettagliate revisioni.

Un ringraziamento speciale è dedicato alle imprese che hanno sponsorizzato economicamente questo progetto: a Giuggia costruzioni per il materiale inerte grazie al quale è stato possibile realizzare il simulante di regolite marziana e tutte le miscele per i test; a VetriAlba 2.0 per aver fornito il primo prototipo di banco di prova e a Vibel group per la produzione custom delle piastre in alluminio del prototipo.

Ringrazio poi le sponsorizzazioni tecniche fornite dal Laboratorio ufficiale Cismondi S.r.l., dall'impresa Sondeco S.r.l. nella figura del dottor geologo Enrico Mosso e lo RS Studio Associato di Ingegneria di Raina Marco & Sacco Paolo per l'opera di intermediazione con le imprese citate.

Ringrazio il personale del laboratorio MastrLAB del dipartimento DISEG del Politecnico di Torino. In particolare, ringrazio il responsabile tecnico Antonino Quattrone e i tecnici Davide Carello e Franco Grindatto per il supporto e la fornitura di materiale e attrezzature durante la campagna di test sul prototipo. Ringrazio inoltre il personale del Laboratorio di Geotecnica del dipartimento DISEG del Politecnico di Torino, nelle figure di Giovanni Bianchi e Oronzo Vito Pallara, per le consulenze tecniche, in particolare durante le operazioni di vagliatura meccanica.

Grazie al professor Giovanni Maizza per la disponibilità, l'abilitazione al corso di Selezione e Progettazione dei Materiali per Applicazioni Ingegneristiche (SPMAI) e all'utilizzo del software CES Edupack grazie al quale è stato possibile studiare i materiali idonei alla produzione del prototipo di cestello.

E infine un ringraziamento speciale alle persone che amo.

Ai miei genitori. Grazie per la straordinaria vita che mi avete donato, per i sacrifici, l'amore e l'incredibile forza con cui avete costruito la nostra famiglia e tutto ciò che abbiamo.

A mia sorella Chiara, perché sei sempre la mia risata più vera.

A Tommaso. Collega, amico, compagno di vita. Grazie per tutto l'amore che sai donare, per la tua eccezionale forza e la dolce pazienza.